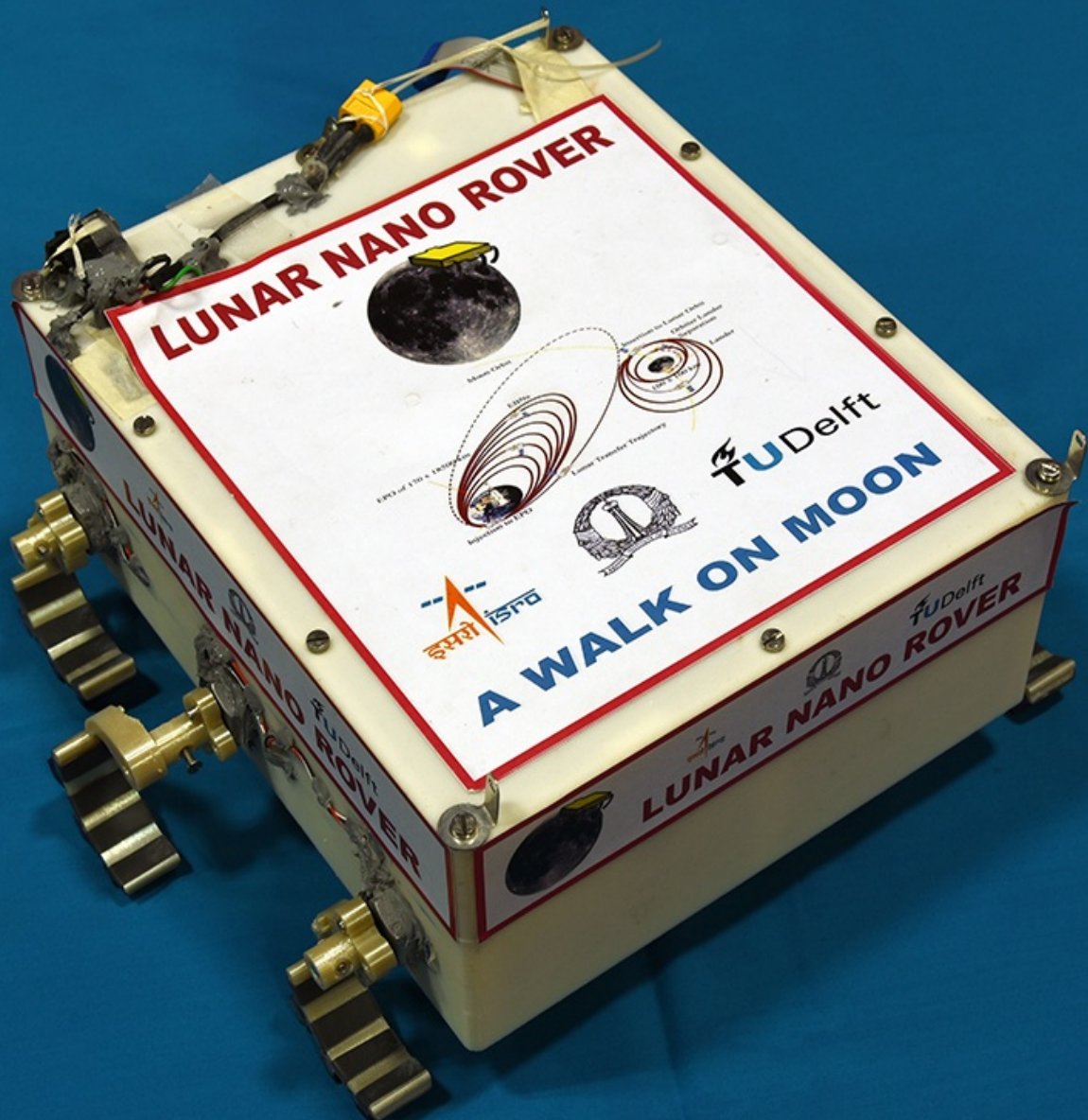


Adaptation Study of Zebro as Nano Rover for Lunar Exploration and Demonstration of Locomotion on Simulated Lunar Surface

Kiran Venkateswara Sharma

Master of Science Thesis



Adaptation Study of Zebro as Nano Rover for Lunar Exploration and Demonstration of Locomotion on Simulated Lunar Surface

Master of Science Thesis

For the degree of Master of Science in
Signals and Systems
at Delft University of Technology

By
Kiran Venkateswara Sharma

4507142

18-01-2018



Faculty of Electrical Engineering, Mathematics and Computer Science
Delft University of Technology
Mekelweg 4, 2628 CD Delft
The Netherlands

The work in this thesis was supported by Department of Microelectronics, TU Delft and Department of Electronics Systems Engineering, Indian Institute of Science (IISc), and was carried out at Indian Space Research Organization (ISRO). Their cooperation is hereby gratefully acknowledged.



Copyright © Kiran V. Sharma
All rights reserved.

Delft University of Technology
Department of
Circuits and Systems

The undersigned hereby certify that they have read and recommend to the Faculty of Electrical Engineering, Mathematics and Computer Science for the acceptance of a thesis entitled

ADAPTATION STUDY OF ZEBRO AS NANO ROVER
FOR LUNAR EXPLORATION AND DEMONSTRATION
OF LOCOMOTION ON SIMULATED LUNAR SURFACE :

by

KIRAN VENKATESWARA SHARMA

STUDENT NUMBER: 4507142

in partial fulfillment of the requirements for the degree of
MASTER OF SCIENCE SIGNALS AND SYSTEMS

Dated: 18-01-2018

Supervisor (TU Delft):

Dr. ir. Chris Verhoeven

Supervisor (ISRO):

Dr. M. Annadurai

Supervisor (IISc):

Prof. N. S. Dinesh

Abstract

The Moon is earth's only natural satellite, it has no atmosphere, no life. The days are nearly burning, the nights are freezing. It is old and cratered, smooth and young. Yet, curiosity and desire to explore the uncertainty has driven man to find scientific truth. Here comes a small "Nano rover" from TU Delft!

TU Delft, Netherlands and Indian Institute of Science, Bangalore, India are working towards an opportunity to land a space robot called "Nano Rover" on the Moon in collaboration with Indian Space Research Organisation (ISRO), Bangalore, India. The prime objective of the mission is that the rover should navigate on the Moon surface. The secondary objective is to capture photos intermittently and send the data to the earth. Considering the mass and time constraints, the existing terrestrial Zebro robot was proposed to be chosen for this purpose. However, Zebro is designed for terrestrial applications and it has to be adapted to the extreme environment conditions on the lunar surface and earth-moon transit orbit where the temperature can go as low as -180°C . Thus, it is quite challenging to modify the existing Zebro to suite the requirements for extra-terrestrial applications. Hence, a detailed study of lunar environment is necessary along with the extensive study on the adaptability of Zebro to be lunar compliant. This thesis presents (i) a literature study on the environment conditions on the Moon and during earth-moon transit orbit (ii) analysis of the existing Zebro and lists the requirements to adapt it to be lunar compliant (iii) conduct tests on materials, components and elements to enable usage of them for lunar and transit orbit environment (iv) design, develop and test the On Board Computer for lunar compatible Zebro and (v) demonstrate the locomotion of the robot on a simulated lunar terrain.

There are three major challenges in conceptualizing and realizing the Nano Rover - (i) stringent mission management (ii) adapting it to the hostile environment such as temperature, vacuum, radiation, vibration, shock (iii) strict product assurance needs. This thesis has comprehensively addressed these challenges and successfully adapted the existing terrestrial Zebro as Nano Rover. Highly reliable electronic components were chosen, tested, and used them in designing the locomotion system. A lunar compliant On Board Computer and a motor drive system were successfully realized meeting all the lunar mission needs. The prototype was tested successfully under extreme simulated lunar environment conditions and locomotion on a simulated lunar terrain was successfully demonstrated.

Table of Contents

Acknowledgements	ix
1 Introduction	2
1.1 Objectives of the Mission	3
1.1.1 The international educational objective	3
1.1.2 The international space collaboration objective	3
1.1.3 Technological development objective	4
1.2 Mission Challenges	4
1.3 Existing Terrestrial Zebro Versions	5
1.4 Thesis Problem Statement	6
1.5 Contributions	7
1.6 Thesis Outline	7
2 ISRO Lunar Mission and the Literature Study	8
2.1 Chandrayaan-2 Mission Management	8
2.1.1 Mission overview	8
2.1.2 Landing site	9
2.1.3 Summary of the outcome and actions based on mission management study:	11
2.1.4 Launch vehicle vibration and shocks	11
2.2 Temperature Specifications	11
2.3 Radiation Effects	12
2.3.1 Total Ionizing Dose (TID) effects	13
2.3.2 Single event effects	13
2.3.3 Radiation hardness assurance	13
2.4 Lunar Soil, Terrain and Gravity Conditions	14
2.4.1 Wheel/leg-soil interaction parameters	15
2.4.2 Mechanical soil properties	15
2.4.3 Terramechanics Dynamics Model	15
2.4.4 Experiments of Micro Zebro in lunar terrain test facility	16

3	Nano Rover Design Requirements	19
3.1	System Level Requirements	19
3.1.1	Structure subsystem requirements	20
3.1.2	Mechanisms subsystem requirements	20
3.1.3	Power subsystem requirements	20
3.1.4	Locomotion subsystem requirements	20
3.1.5	RF subsystem requirements	20
3.1.6	Assembly, Integration and Testing (AIT) requirements	20
3.1.7	Mission requirements	21
3.1.8	Product Quality Assurance requirements	21
3.2	Nano Rover Block Diagram	21
3.3	Materials, Components Selection and Qualification for the Nano Rover	22
3.3.1	Battery	22
3.3.2	Solar Cells	23
3.3.3	Passive and active components tests at cryogenic temperature	24
3.3.4	On Board Computer for the Nano Rover	24
3.3.5	Choice of motors	26
3.3.6	Choice of hall sensors	26
3.4	Brief introduction to all systems	27
3.5	Adaptation from Zebro to the Nano Rover	27
4	Hardware	29
4.1	Introduction	29
4.2	Introduction to FPGA architecture	30
4.3	Requirements of ISRO OBC card	30
4.3.1	Hardware Requirements	30
4.3.2	Mission requirements specification for Nano Rover	31
4.4	Block Diagram of the OBC Card	32
4.5	Hardware Design	32
4.5.1	AMBA Architecture	33
4.5.2	Core GPIO	34
4.5.3	Core AHB2APB bridge	34
4.5.4	Master Clock Generation	35
4.5.5	Power On Reset (POR) Generation	35
4.5.6	Power Generation	35
4.5.7	Control logic implementation	36
4.5.8	PWM generator	36
4.6	Motor Controller Card	36
4.6.1	Motor Drive Circuit	40
4.7	Printed Circuit Board Design	41
4.7.1	OBC card hardware	41
4.7.2	Motor Drive PCB	43
4.8	Summary	43

5	Software	45
5.1	Introduction	45
5.1.1	Why not Operating System(OS)?	45
5.2	Software requirements	46
5.2.1	Functional Requirement for VHDL	46
5.2.2	Functional Requirements for C	47
5.2.3	Mission Requirements	47
5.3	Data Mitigation Techniques	47
5.3.1	Error correcting codes	48
5.3.2	Triple Modular Redundancy (TMR)	48
5.4	Existing Zebro Locomotion Algorithm	49
5.5	Design for a novel, synchronous motor control in software	50
5.6	Locomotion software architecture	50
5.6.1	Application layer (Layer6)	52
5.6.2	Autonomy or Command Decoding Layer (Layer5)	52
5.6.3	Synchronization Layer (Layer4)	52
5.6.4	Individual Motor Control (Layer3)	52
5.6.5	PWM Generation Layer (Layer2)	52
5.6.6	Physical Layer (Layer1 - Motor Drive Electronics)	53
5.7	VHDL software design	53
5.7.1	OBC Scheduler	53
5.7.2	Locomotion software design	56
5.7.3	Operating sequence of the software	58
5.8	Software modules	58
5.8.1	Main module	58
5.8.2	Initialization module	58
5.8.3	Linear motion (forward and reverse) module	59
5.8.4	PWM generator module	59
5.8.5	Synchronization module	60
5.8.6	Switching between forward and reverse motion	60
5.8.7	Left rotation	62
5.8.8	Right rotation	62
5.9	Design Calculation for the Locomotion Algorithm	62
5.9.1	Friction analysis	62
5.9.2	Calculations for PWM generation	63
5.9.3	Calculations for PWM width adjustment of layer3 (Ring counter based lookup table)	65
5.9.4	Calculations for PWM frequency for the motors	66
5.10	Summary	67
6	Evaluation, Experimentation, and Demonstration of Locomotion	68
6.1	Experimental Setup	68
6.1.1	Structure	68
6.1.2	Motors	68
6.1.3	Legs	69
6.1.4	Hall effect sensor	70
6.1.5	OBC card and motor drive card	71
6.1.6	Power module	71
6.1.7	1/6 Gravity emulation	71
6.2	Locomotion Test on Flat Surface(Lab)	72
6.3	Locomotion Test on Lunar Terrain	72
6.4	Inference	73

7	Conclusion and Future work	80
7.1	Contributions of the thesis	81
7.2	Assembly, Testing and Recommendations	81
7.3	Future Work	82
7.4	Epilogue	83
A		86
A.1	Rovers for Interplanetary mission in the literature	86

List of Figures

1.1	Zebro Light	5
1.2	Micro Zebro	6
2.1	Chandrayaan-2 lander model	9
2.2	Chandrayaan-2 flight orbits	10
2.3	Wheel/leg-soil interaction model	15
2.4	Micro-Zebro on the simulated lunar terrain	17
2.5	Micro-Zebro on the simulated lunar terrain with 1/6th gravity emulation	17
2.6	Trails left by the Micro-Zebro on the simulated lunar surface	18
3.1	Block diagram of the Nano Rover subsystems	21
3.2	Battery specifications	22
3.3	Battery discharge characteristics at 20° C (–160° C soak for 240 hours)	23
3.4	Battery charge characteristics at 20° C (–160° C soak for 240 hours)	23
3.5	Battery pack under thermal test	24
3.6	Pre and post cold storage characteristics summary	24
3.7	Capacitors packages	25
3.8	Resistor packages	25
3.9	Passive components	25
3.10	Active components	26
3.11	Maxon motor with planetary gearhead under thermal test	27
4.1	Hardware block diagram	29
4.2	Block Diagram of the OBC	32
4.3	Cortex M1 core diagram	33
4.4	typical AMBA system	34
4.5	Single I/O Bit Block Diagram for Core GPIO	34
4.6	Core AHB2APB block diagram	35
4.7	100 MHz clock generation	35
4.8	POR generation	36
4.9	Power management	36
4.10	FPGA block diagram	37

4.11	Core PWM block diagram	37
4.12	DC motor schematics	38
4.13	PWM	38
4.14	PWM output	39
4.15	Three phase BLDC motor	39
4.16	Simplified construction of three phase BLDC motor	40
4.17	Timing diagram	40
4.18	Sensor states and motor drive states	41
4.19	Motor control	41
4.20	Motor drive schematics	42
4.21	PCB layout and top view of the populated PCB of the OBC	42
4.22	PCB layout and bottom view of the populated PCB of the OBC	43
4.23	PCB layout and top view of the motor card	44
4.24	PCB layout and bottom view of the motor card	44
5.1	Leg positions	46
5.2	Flow chart of existing algorithm	49
5.3	Software flow chart	51
5.4	VHDL design flow	54
5.5	hierarchy	54
5.6	Mode diagram	55
5.7	Top level abstraction	56
5.8	Medium level abstraction	57
5.9	Low level abstraction	57
5.10	Main module	59
5.11	Initialization routine	60
5.12	PWM waveforms	61
5.13	Synchronization	61
5.14	PWM Synchronization	62
5.15	Left rotation	63
5.16	Right rotation	64
5.17	Left rotation	65
5.18	Right rotation	65
5.19	Lookup table	66
6.1	3D structure	69
6.2	Motor assembly	69
6.3	Leg variants	70
6.4	Legs with different types and sizes	70
6.5	Hardware assembly	71
6.6	Wooden flat surface	72
6.7	Locomotion on wooden flat surface at lunar g	73
6.8	Locomotion on lunar terrain, flat surface	74
6.9	Time taken by the rover to cover 1 m on flat surface with normal g	74
6.10	Time taken by the rover to cover 1 m on flat surface with 1/6th g	78
6.11	Locomotion on lunar terrain, normal g with slope	78
6.12	Locomotion on lunar terrain, 1/6 g with slope	79
6.13	Time taken by the rover to cover 1 m on lunar surface with normal g	79
6.14	Time taken by the rover to cover 1 m on lunar surface with 1/6th g	79

Acknowledgements

The work presented in this thesis was carried out at Indian Space Research Organization (ISRO) and Indian Institute of Science (IISc). I would like to thank everybody involved with this project at both these institutions.

I would like to thank my supervisors Dr.ir Chris Verhoeven, Dr. Dinesh N.S and Dr. Venkatesha Prasad for their guidance.

This work would not have been possible without the love and affection from my family and friends. I would like to thank my father Dr.S.V.Sharma, my mother Mrs. Srividhya and my baby sister Chandni. I would also like to acknowledge Sujay Narayana for being my big brother and supporting me during the course of my thesis.

Delft, University of Technology
18-01-2018

Kiran Venkateswara Sharma

Chapter 1

Introduction

Since many decades, the space organizations such as NASA in the USA, ESA in Europe, JAXA in Japan, Roscosmos in Russia, and Indian Space Research Organisation (ISRO) in India, etc., have ventured into many interplanetary missions. These missions sometimes are flyby type and other times involve landing on the surfaces of the celestial bodies. Currently, TU Delft is working towards an opportunity to land a small six-legged robot called “Nano Rover” on the Earth’s moon. This is in association with Indian Institute of Science (IISc), and ISRO, India. The rover is planned to fly along with the *Chandrayaan-2* lunar mission of ISRO. The primary objective of this mission is that the Nano Rover should locomote on the Moon’s surface at least for about 200 m. The secondary objective is to capture photos and send the data intermittently to Earth over a direct link between the rover and the ground stations on Earth.

Rovers are broadly classified as macro rovers (>150 kg), mini rovers (30-150 kg), micro rovers (5-30 kg), and nano rovers (<5 kg) [1]. While the first three types are already popular, nano rovers have never been on an interplanetary mission. As there is no major apparent reason apart from carrying less payload, we conclude the reason seems to be more of a policy than technical for flying nano rovers. This is a major venture for either of the university students. Furthermore, very limited information is available in books or in the Internet from the available interplanetary space missions documents. Moreover, there is practically no or limited experience in the universities for this mission. Therefore, demonstration of this Nano Rover locomotion on the Moon by the students of TU Delft and IISc will be a unique feat. To take advantage of the opportunity provided by ISRO, TU Delft is working closely with ISRO and IISc to design and develop a lunar compliant nano rover.

With this background, we explicate some of the issues in this mission. The environment on the moon presents various challenges for the operation of a robot due to extreme conditions. These conditions that impact the robot’s operation on the moon can be characterized by seven major factors [2, 3] - dust, radiation, vacuum, temperature, terrain, Moon sand, and the Sun-Earth-Moon geometry. In particular, the Sun-Earth-Moon geometry will affect the duration of this mission as this determines the period of a Moon day. The impact of the other factors will be further explained in Chapter 2.

It is apparent from the mission that the locomotion subsystem is one of the important modules in this nano rover. Mobility can be achieved by different methods such as wheels, tracks, legs, hybrids, hoppers, and ballistics [1]. All these concepts can be conceived for a lunar exploration scenario. It is necessary to select a particular method after having carefully considered advantages and disadvantages. Wheels are most commonly used for many terrestrial and planetary robotic vehicles. While wheels are capable of achieving higher speeds than trackers and walkers on a flat terrain, it is relatively less capable of negotiating obstacles as compared to legged robots [1]. With this unique advantage for legged robots that seems to be more ideal for the moon’s environment, advancement in technology, experience in matured designs and demonstrated performance of the legged robots, TU

Delft has developed a hexapod robot called “Zebro” [4, 5] which is considered as the baseline product for developing our Nano Rover.

Any such space mission will have a few major mission requirements. This has been determined by ISRO adhering to mass, power and volume [6]:

1. **Mass:** The mass budget provided is limited to a maximum of 1.5 kg which imposes a ceiling on the total mass available to each subsystem and to the Nano Rover as a whole. The constraints levied on structural strength and stiffness, thermal conductivity and grounding need to be met.
2. **Power:** The power budget of about 24 Wh imposes a limitation on the power available to each subsystem. The use of simple power electronics, high efficiency motors, high efficiency power scheduling along with shared computational and storage resources operating on nominal power are to be taken into consideration.
3. **Volume:** The volume constraints provided by ISRO is 220x160x60 mm. This imposes a stringent limitation on the volume available to each subsystem and the payloads. The use of multi layered cards, components/electronic devices with high density packing and small footprint area are to be taken into consideration in addition to sharing of the available subsystem resources such as memory, processor, FPGAs etc.

Apart from the above requirements, all the parts and materials to be used on the Nano Rover must necessarily meet the space qualification requirements [7, 8], which are explained later in this thesis.

In this thesis, we focus and explain the relevant details of the complete mission that are necessary for this thesis. The work in this thesis mainly involves building an engineering model of the rover that can walk on lunar terrain. The work involves building an on-board computer and motor driver, assembling the rover using available motors (in our case, we used a DC motor which is far more challenging compared to brushless DC motors or stepper motors), developing algorithms for locomotion and lastly, testing and recording the inferences. Now, we briefly provide mission objectives, problem formulation and contribution of the thesis.

1.1 Objectives of the Mission

At the outset, this mission comprises of three main objectives: international educational objective, international space collaboration objective and the technological development objective.

1.1.1 The international educational objective

This mission is part of a larger understanding between two prominent universities, TU Delft and IISc, and is a major educational joint venture. Therefore, the first objective is educational, between geographically and culturally different institutions. Since the Nano Rover is developed by students, it gives an opportunity to the students from TU Delft and IISc to work on a large research and engineering project where the goal is to develop an interplanetary mobile system. Working on such a project will improve their skills on various kinds of aspects and give the students a unique experience and training for working in the space industry.

1.1.2 The international space collaboration objective

This mission between TU Delft and IISc is supported by ISRO which is one of the major space organization in the world. Students collaborating with such organizations get to understand the dynamics of the space program and learn to work professionally in realising a system for space. The students will also experience the unique culture of the organisation which may help them to be trained to work in multi-dimensional activities.

1.1.3 Technological development objective

The third objective is technology demonstration and qualification. The Nano Rover provides a way to demonstrate and/or qualify technologies developed by students for interplanetary applications. With the Nano Rover mission, TU Delft is aiming to bring the rover platform to a higher level and enable new applications for high reliability applications and scale newer heights in the development of the space technology, specifically for interplanetary mission.

The above objectives for Nano Rover mission can be summarized as follows with three goals:

1. The primary goal is to perform mobility activities on low gravity terrain of the Moon surface. This also includes semi-autonomous navigation and hazard avoidance capability.
2. The secondary goal is to communicate with specific ground stations on the Earth directly. This includes receiving telecommanding signals from ground stations and send health status, payload data back to the Earth.
3. The final aim comprises of payload operations which includes camera and a few measurement using available sensors.

Nano Rover need to be designed, developed and realized to work reliably on the lunar surface. The rover need to be dropped at a suitable site on the lunar surface identified by Chandrayaan-2 mission team of ISRO. There will be main and some redundant subsystems to ensure reliability. Nano Rover need to successfully demonstrate locomotion on the lunar terrain, communicate to earth directly, carry out feasible scientific experiments, and survive for one lunar day [1].

1.2 Mission Challenges

This Nano Rover mission has many challenges that need to be addressed before initiating the design. The main challenges are as follows.

1. **Thermal and Vacuum:** The lunar Nano Rover is expected to be mounted outside the spacecraft and is likely to face extreme temperature swings in deep vacuum of 10^{-6} torr. The operating temperatures on the moon surface are likely to be around -20°C and $+70^{\circ}\text{C}$. The biggest challenge is the lower end of the temperature extremes during the transit of the Nano Rover from the Earth to the Moon which is likely to be around -186°C . However, the rover electronics will be turned off at this stage and is termed as storage temperature. The electrical, mechanical, and thermal design of the Nano Rover must take these challenges into consideration for reliable functioning of the Nano Rover on the Moon surface.
2. **Radiation:** The earth-moon transient orbit and the Moon's surface is exposed to hazardous ionizing radiation. The sources include solar wind, solar flares and galactic cosmic rays. All the elements, materials and the components used in the rover must be capable of withstanding these radiations without degradation in its performance. Generally, the interplanetary missions are realized using high reliability materials and components. Those items which do not meet these requirements must be identified and appropriate mitigation techniques must be adopted to meet the mission requirements.
3. **Legs:** The lunar terrain surface is likely to be composed of fine granular loose soil/dust which can be as thick as 30 mm with a slope of about 15° , containing boulders of about 30 mm. The dust may seriously damage the bearings used in the moving elements and the motors used in legs. Hence, the challenge is to design a locomotion system for the Nano Rover consisting of motors and legs to successfully walk on the Moon, overcome the obstacles, and climb the boulders to cross over.

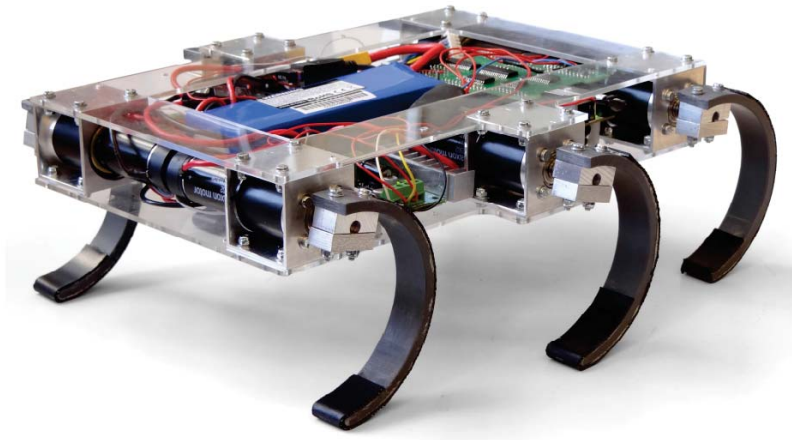


Figure 1.1: Zebro Light

- Vibration:** As the Nano Rover is likely to be piggybacked on a spacecraft in Chandrayaan-2 mission that is launched using Geo Synchronous Launch Vehicle(GSLV), the rover will experience substantial vibration and shocks as high as 20 g and 12 dB/octave respectively during various phases of the launch. The system design of the Nano Rover must be robust enough to meet all these requirements.

Considering the time constraint of launch preparedness and aforementioned challenges, it is quite challenging to modify the existing Zebro to suit the requirements of the mission. Before outlining the problems tackled in this thesis, we provide a brief history of Zebro versions for the sake of completeness.

1.3 Existing Terrestrial Zebro Versions

Zebro is a hexapod robot developed at the TU Delft. Zebro, is one of the most important robots within the swarm theme of the TU Delft Robotics Institute. Probably, the most distinguishing feature of Zebro is that it does not have wheels or human like limbs. Instead, it has six rotating legs. These legs allow Zebro to move over a wide variety of terrains, many of which are not negotiable by the conventional wheeled robots. Over the years, there have been many versions of Zebro. Much effort has been made by TU Delft students to design and develop these Zebros that vary in size and mass.

In 2012, it was decided by TU Delft that research needed to be done on swarm robotics, and Zebro was chosen as the favored platform. This choice was made based on the similarities between Zebro and many insects. Having no wheels, it walks just like many insects do. Insects are one of the main sources of inspiration for the field of swarm robotics, and hence the two were combined.

The first Zebro [4] was developed by Gabriel Lopez, Professor at Delft Center for Systems and Control (DCSC) department, TU Delft, based on the RHex robot designed by Boston Dynamics. This Zebro weighs 7 kg and is intended to be a research tool. After the first Zebro was constructed, new and improved designs were made recently.

The second Zebro is the Zebro light [9] which is approximately half the size of the previous Zebro. The dimensions of the Zebro light is 300x200x60 mm and weighs around 3.5 kg and is shown in Figure 1.1. It is designed to retain the robustness and versatility of the Zebro while making it lighter and smaller. This model of the Zebro is intended to be a platform for implementing swarming. Zebro light has a

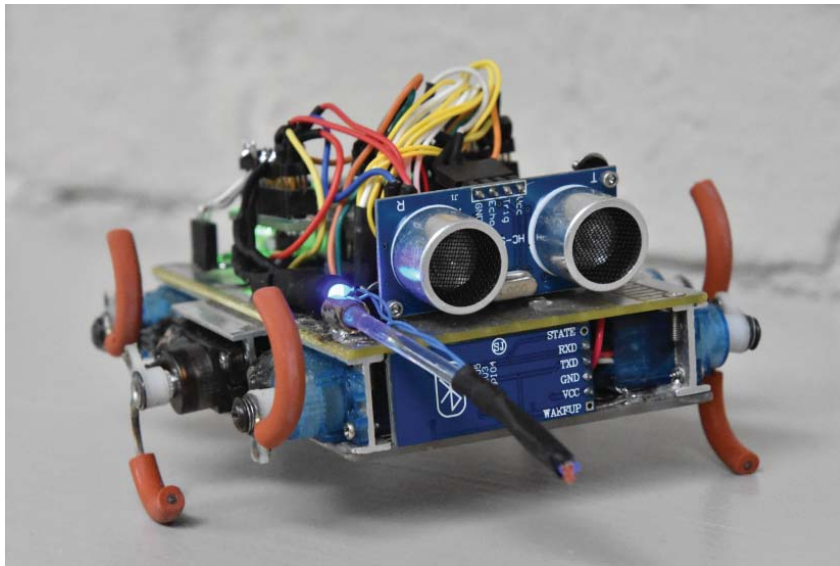


Figure 1.2: Micro Zebro

Beaglebone processor module, running on the linux operating system. This Zebro implements a PID controller for the controlled locomotion of each leg using DC motors.

Micro Zebro, shown in Figure 1.2, is another version of Zebro, built by Dr. Chris Verhoeven and his students, which fits comfortably on your palm. Micro Zebro's electronics is built around Atmel's ATMEGA microcontroller and the locomotion system includes servomotors. The legs are made using simple bent thick wires as wheels. It has also got ultrasonic direction sensors to detect obstacles.

The Pico Zebro is the smallest Zebro yet. It is 50x40x15 mm in size. The Pico Zebro has an ATMEGA microcontroller as Central Processing Unit. The Pico Zebro can be controlled using Bluetooth, mass producible, and can be easily assembled.

Looking into the literature, Zebro light nearly matches the mission requirements in terms of mass and size. Hence, Zebro light, is taken as the baseline version, and is modified to adapt to the lunar environment and mission requirements. We also use Micro Zebro for testing the locomotion on simulated lunar terrain because of its immediate availability, which can give inputs to design the Nano Rover.

1.4 Thesis Problem Statement

This is a maiden attempt at TU Delft to conceptualize a challenging task of the realization of a Nano Rover for interplanetary missions. This leads to a research question - "Is it possible to adapt the existing terrestrial Zebro as the Nano Rover for lunar mission and demonstrate locomotion on a simulated lunar surface?". Since there is a limited knowledge on such interplanetary space missions, there is a necessity to perform adaptability study of Zebro for the lunar environment, and indigenously design and develop the Nano Rover. This thesis is mainly aimed at:

1. Studying the environmental conditions on the Moon landing site and in Earth-Moon transit orbit to enable comprehensive realization of the Nano Rover to perform locomotion on the lunar surface.
2. Analyzing the existing Zebro and sketch the requirements to adapt it to the lunar and transit environment. Further, conduct environmental tests on selected electronic components and modules to certify them for lunar and transit orbit environment requirements.

3. Considering all the interplanetary mission requirements for effective functioning and locomotion on the Moon - design, develop and realize the “On Board Computer” with required “Motor drive” for the Nano Rover.
4. Locomotion of the Nano Rover is one of the key research requirements in this lunar mission. It is necessary to design, develop and evaluate the implemented locomotion algorithms for the Nano Rover.
5. Testing and demonstrating the locomotion of the rover on a simulated lunar terrain.

1.5 Contributions

Noting the above problems and challenges, we built a Zebro model and implemented all the requirements. We also tested the same. Specifically, the following are the contributions of the thesis in the sequel.

1. First and foremost task was to carryout the adaptability study for the design of the engineering model of the rover. We have recorded extensively the requirements, terrain information, and all the important mission related data.
2. Locomotion algorithm was specifically developed and tested for DC motors. We have provided implementation details of all the algorithms.
3. Design of Hardware and Software has been explicated along with its implementation.
4. Finally, we tested the implemented model on the specifically designed lunar terrain in ISRO facility. The soil characteristics match with the data from other lunar missions.

1.6 Thesis Outline

The rest of this article is structured as follows. In Chapter 2, the important literatures for the realization of the Nano Rover such as Chandrayaan-2 mission management, study on environmental conditions during different mission phases, and brief information on the lunar terrain is presented. The systems requirements that need to be considered while designing the Nano Rover for reliable locomotion on the lunar terrain are listed in Chapter 3. Chapter 4 is dedicated for hardware conceptualization, design and realization. In this Chapter, information on the development of On Board Computer and motor drive is presented. In Chapter 5, we describe the different software layers implemented on the chosen hardware, and algorithms for the locomotion of the Nano Rover is proposed. In Chapter 6, we present the test and evaluation results of the designed Nano Rover prototype and the observations from the experiments carried on the simulated lunar terrain. Finally, we conclude in Chapter 7 by listing the possible recommendations and future work.

ISRO Lunar Mission and the Literature Study

The task of realization of the Nano Rover for lunar mission is challenging and needs understanding of the various conditions and environments that the Nano Rover is likely to go through. Some of these must be addressed during the entire mission: temperature extremities, radiation effects, lunar soil interaction with legs, lunar gravity effect, moon dust, static charging effect on the Moon surface, Moon day conditions, sun angle for power maintenance, and vibration/shock requirements. Therefore, for the sake of completeness, the following topics are considered for detailed study for designing the Nano Rover.

1. Chandrayaan-2 Mission Management
2. Temperature and other environmental specifications for Nano Rover
3. Radiation effects
4. Lunar soil, terrain and gravity conditions on the lunar surface
5. Experiments with locomotion of Micro Zebro in Lunar terrain test facility
6. Adaptation of terrestrial Zebro as Nano Rover

2.1 Chandrayaan-2 Mission Management

As the Nano Rover is slated to be landed on lunar surface in Chandrayaan-2 mission, it is essential to study the mission management first before we design the rover. The primary objective of this mission management study is to understand the electrical, mechanical and environmental specifications that would be part of the system design of the Nano Rover.

2.1.1 Mission overview

Chandrayaan-2 is the second spacecraft in its series of lunar exploration from ISRO. The mission involves launching of orbiter, lander and a rover to the Moon where the orbiter revolves around the lunar orbit at 100 km altitude and the lander performs a soft landing on the lunar surface. The rover which is indigenously developed at ISRO performs mobility and certain scientific measurements on the Moon surface. While this primary rover resides inside the lander, the Nano Rover is planned to



Figure 2.1: Chandrayaan-2 lander model

be mounted on the outer surface of the ramp of the lander, acting as the secondary rover. Figure 2.1 shows the 3D model of the lander. The mission is scheduled to be launched by Geo Synchronous Launch Vehicle (GSLV)-Mk II from Sathish Dhavan Space Center (SHAR), Sriharikota, India in the first quarter of 2018 [10].

2.1.2 Landing site

The landing site analysis has been performed using the 1 m and 0.45 m resolution Lunar Reconnaissance Orbiter, and the data obtained from the Chandrayaan-1 mission. The hazard maps have been created [2]. The constraints used to select the landing site are - terrain slopes less than 15° , boulders less than 0.3 m, craters and boulders distribution, availability of sunlight for at least 14 days, visibility of the Earth for radio communication (i.e., on the near side) and local terrain features such that they do not shadow the site for long durations. The prime site is designated as “SLS54” which is at latitude -70.9074° and longitude 22.7680° .

The Chandrayaan-2 mission carries an orbiter and a lander as composite until Moon Bound Orbit of 100×100 km is reached. After reaching a 100 km circular orbit, lander and orbiter gets separated, followed by the descent and landing of the lander at the pre-defined landing site.

The various mission phases are classified as Pre-launch Phase, Earth Centric Phase, Lunar Transfer phase, and the Moon centric phase [10]. The overall flight orbits are shown in Figure 2.2.

1. Pre-launch Phase: This phase begins 60 days before the launch day and it involves transportation of the spacecraft, ground tests and orbit-lander-rover interface. It consists of the implementation of all ground softwares, establishing the links, and communication with the ground networks, test and evaluation of all ground software and hardware elements, performing the end to end testing using the spacecraft data and simulator data.
2. Earth Centric Phase: This is the second phase and is split into two sub-phases - Launch Ascent Phase, and Earth-bound Maneuver Phase.
 - (a) Launch Ascent phase: In this phase, the exact launch scenario will be displayed. The ascent phase constitutes the visualization of launch pad at SHAR, launch vehicle model (GSLV), launch trajectory, ignition and shutoff of all stages, stage separation, heat shield separation, satellite injection, initial attitude acquisition, and solar panel deployment. All

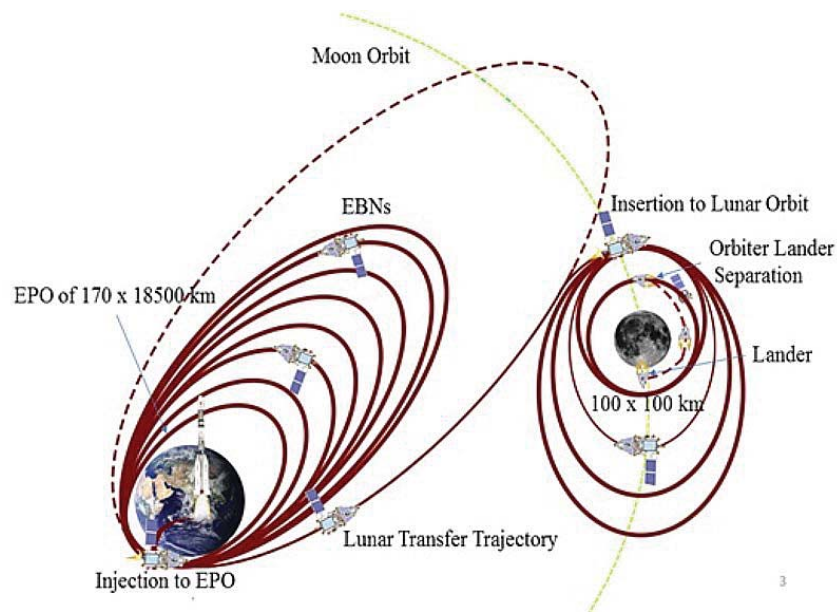


Figure 2.2: Chandrayaan-2 flight orbits

the launch related events will be configured based on the planned pre-flight trajectory as provided by the vehicle project team. There is no real-time interface during ascent phase and all the events are pre-programmed. After satellite separation, the solar panel deployment and initial attitude acquisition for satellite are displayed based on the ground received telemetry data [10].

- (b) Earth-bound Maneuver phase: During this phase of the mission, a series of apogee raising maneuvers will be conducted to raise the apogee from about 23601 km to about 374116 km. As a part of these operations, the spacecraft will be rotated from its nominal orientation to maneuver orientation (known as forward rotation) and back to its nominal orientation (known as reverse rotation) after the maneuver. Also, during the maneuver, the spacecraft is expected to hold the engine nozzle aligned with the anti-velocity direction. The attitude display system greatly simplifies the verification of these events in a visually intuitive manner. Also, the graphical display of the of the 440 N Longitude Apogee Motor engine firing and the 22 N thrusters for attitude control will also be displayed.
3. Lunar transfer phase: After the Transfer Lunar Injection (TLI) on April 15th 2018, the spacecraft is in Lunar Transfer Trajectory (LTT). It enters the Moon's Sphere of Influence (SOI) at a distance of about 66000 km from Moon's center. The time taken to reach Moon's SOI is about 5 days from TLI burn end and the spacecraft enters Moon's SOI in a hyperbolic arrival trajectory on Apr 20, 2018. This is shown in Figure 2.2.
 4. Moon centric phase: This phase has four sub-phases: Lunar Insertion Phase (LOI), Moon-bound Maneuver Phase (MMP), Moon-Centric Normal Phase (MCP), Orbiter-Lander Separation Phase (OSP), Descent and Landing Phase for Lander, and Lander normal phase.
 - (a) Lunar Insertion phase: In LOI operation, satellite's angular momentum is adjusted in such a way that the spacecraft enters into a stable orbit around the Moon. The trajectory part will be pre-programmed based on the nominal plan. Real-time interface will be available for attitude and thruster firing.
 - (b) Moon-bound Maneuvers phase: The attitude and orbit visualization during the Moon bound phase will be made similar to Earth Parking Orbit phase. Major focus during the Moon bound phase will be as follows: attitude control, imaging feasibility and lunar bound maneuvers.

- (c) Orbiter-Lander Separation phase: This is the significant step prior to landing on the Moon. The orbiter lander separation happens over far side of the Moon, which implies there will be no real time telemetry available during the separation initially. The trajectory, separation event, and maneuver will be preprogrammed as per nominal scenario and will be displayed in simulation Mode until telemetry is received.
- (d) Descent and Landing phase: During descent phase, real time attitude and trajectory information will be available from telemetry. With Systems Tool Kit's (STK) real time interface, the complete visualization of descent trajectory and landing will be done. The terrain model of the Moon for landing site will be loaded during pre-reconfiguration. After landing, the separation of rover from lander will be displayed with respect to the telemetry data.

2.1.3 Summary of the outcome and actions based on mission management study:

The Nano Rover undergoes various environmental conditions during different phases in the mission as explained before. Based on the mission profile, all the requirements and specifications for dynamic loads and temperature extremes on the Nano Rover are described in the subsequent sections. These need to be addressed while realizing and qualifying the Nano Rover for lunar flight and landing.

2.1.4 Launch vehicle vibration and shocks

During the launch, the Nano Rover mounted on the lander would experience vibration and shock from the launch vehicle. The vibration and shock levels on the various systems during the launch are listed in Table 2.1 and Table 2.2 respectively [11, 12, 13].

Table 2.1: Quasi-static loads of GSLV Mk-II: The longitudinal and lateral acceleration

Flight Event	Longitudinal(g)			Lateral(g)		
	Static	Dynamic	Combined	Static	Dynamic	Combined
Max Dynamic Pressure	-2.42	0	-2.42	0.2	+/-0.9	1.1
GS1 peak acceleration	-4.1	0	-4.1	0.2	+/-0.3	0.5
GS1 shut off	-1.6	+/-2.4	-4.0	0	+/-0.6	0.6
GS2 peak	-3.41	0	-3.41	0.6	+/-0.2	0.8

Table 2.2: Level of shock

Frequency(Hz)	SRS
100-1000	12 dB/oct
1000-5000	1500 g
5000-10000	6 dB/oct
No. of pulses	2

Based on the GSLV launch and the lander landing dynamic load conditions, the expected worst case vibration on the Nano Rover is 20g out of plane and 20g in plane.

2.2 Temperature Specifications

Nano Rover is slated to be mounted on the outer surface of the ramp of the lander, exposing to vulnerable extremes of temperatures. The temperature levels during various phases of the mission are as follows [10, 14].

1. Earth Centric,Launch and Ascent Phase and Pre-Launch Phase: +25° C

2. Earth-bound Maneuver Phase: -186°C
3. Lunar Transfer phase: 18days, at -186°C
4. Transfer Trajectory Phase: -186°C
5. Lunar Insertion Phase (LOI): -186°C
6. Moon-bound Maneuver Phase: -186°C
7. Moon-Centric Normal Phase: -186°C
8. Orbiter-Lander Separation Phase: -186°C
9. Descent and Landing Phase for Lander: 0°C
10. Lander normal phase: 0°C to 70°C

The above profiles give us the temperature specifications for the Nano Rover with -186°C as storage temperature and -40 to $+70^{\circ}\text{C}$ as operating temperature.

2.3 Radiation Effects

The objective of this section is to review the basic physics and theory of the definition of the radiation environment present the available models, and define the limits of the applicability of the models to the real environment [8].

Since the Sun is a gas, its solar magnetic field is convoluted and highly variable. Both the long term variation in the magnetic field that occurs in a 22-year cycle and the short term variations in the form of intense, short lived storms are responsible for observable changes in the interplanetary and near-Earth radiation levels. The two storm phenomena occurring on the Sun that affect particle levels are solar flares and Coronal Mass Ejections (CMEs). Solar flares are seen as sudden brightening in the photosphere near sunspots. Flares are intense releases of energy involving tearing and reconnection of strong magnetic field lines. In fact, they are the solar systems largest explosive events. Large increases in the solar wind density in interplanetary space are measured after solar flare occurrence because the energy released from the flare accelerates particles in the solar plasma to high energies.

The high temperature of the corona inputs sufficient energy to allow electrons to escape the gravitational pull of the sun. The effect of the electron ejections is a charge imbalance resulting in the ejection of protons and heavier ions from the corona. The ejected gas is so hot that the particles are homogenized into dilute plasma. While the solar wind is millions of metric tons of matter moving at a million kilometers per hour, its density is so low that the physics is that of a vacuum. The energies of the particles range from approximately 0.5 to 2.0 keV/nuc. The average density of the solar wind is 1 to 30 particles/cm³. we could be interested in the final effect induced by exposition, without caring about the microscopic modifications inside the device. Similar failures are known as Single Event Upset (SEU). Another common kind of transient effect is the Single Event Latch-up (SEL), in which a more severe failure happens, leading the device outside its operating range and thus damaging it. The common way of classifying radiation effects from a physical point of view is based on the distinction between displacement damage and ionization damage. Actually displacement is due to neutrons (heavy and neutral) and charged particles when very energetic, while ionization is mainly due to protons, electrons and photons. The main difference between neutrons and charged particles is that neutron damage takes place by mean of nuclear interactions, while ionization damage is related to atomic interactions, i.e., electromagnetic ones. So neutrons are more penetrating than charged particles, and act mainly on the bulk of the device (i.e., on Silicon). On the other side ionizing radiation often cannot overcome the Silicon Dioxide layer, so the effect is referred also as surface damage.

2.3.1 Total Ionizing Dose (TID) effects

The most common ionizing radiation effects in the oxide are: (i) charge trapping, i.e., charge freezing in the oxide, leading to recombination centers formation and field effects (ii) Si-SiO₂ interface modification with strong direct effects on the bulk semiconductor. Total Ionizing Dose (TID) is due to energetic light particles such as electrons, photons, and ions impinging on materials, where they generate electron/hole pairs [8]. Some fraction of these pairs will recombine, but a fraction will remain trapped as charges in parts layers. These charges are likely to cause progressive TID damage. Degradation leads to irreversible parametric drifts, and eventually functional failures at device level.

2.3.2 Single event effects

Radiation damage to on-board electronics can be due to single event effects. Single event effects (SEEs) are individual events which occur when a single incident ionizing particle deposits enough energy to cause an effect in a device [8]. There are many device conditions and failure modes due to SEE, depending on the incident particle and the specific device. It may be convenient to think of two types of SEEs: soft errors and hard errors. Soft errors are nondestructive to the device and may appear as a bit flip in a memory cell or latch, or as transients occurring on the output of an I/O, logic, or other support circuit. Also included are conditions that cause a device to interrupt normal operations and either perform incorrectly or halt. Hard errors may be (but are not necessarily) physically destructive to the device, but are permanent functional effects. Different device effects, hard or soft, may or may not be acceptable for a given design application. Unlike TID degradation, SEE rates are not evaluated in terms of a time or dose until failure, where the stopwatch begins at launch, but a probability that an SEE will occur within a known span of time. Devices are tested in ground test facilities to characterize the device in a radiation environment. Calculations are also performed to predict the radiation environment for a particular mission orbit. Environment predictions are used with the experimental device data to calculate the probability of occurrence of SEEs in the device for the mission.

SEU or Soft error: Heavy ion LET threshold should be greater than 40 MeVcm²/mg [8]. Devices with large LET threshold and small cross-section are preferred. If the LET thresholds are smaller than 40 MeV-cm²/mg, SEU rate should be calculated and suitable mitigation technique is to be adopted.

Single Event Latch-up (SEL): Since SEL leads to permanent failure, all components should be immune to latch-up (tested up to 80 MeV-cm²/mg) [8].

SEGR / SEB: Single event gate rupture and single event burnout effects occur only in power transistors where the biasing voltages are high [8]. These effects are sensitive to biasing voltages (VGS, VDS) and the LET of heavy ions. The biasing voltages of power devices should be below VGS versus VDS curve for an ion of LET 60 MeVcm²/mg.

2.3.3 Radiation hardness assurance

Radiation accelerates the aging of the electronic parts and material and can lead to a degradation of electrical performance; it can also create transient phenomena on parts. Such damage at the part level can induce damage or functional failure at electronic box, subsystem, and system levels. A rigorous methodology is needed to ensure that the radiation environment does not compromise the functionality and performance of the electronics during the system life. This methodology is called hardness assurance. Radiation hardness assurance process starts first with top-level estimations of the radiation environment, then the radiation levels are refined and the electronic designs analyzed in order to validate the most sensitive parts. The mitigation techniques for TID and SEE are as follows [10, 14].

Table 2.3: Electronic components and their radiation design margin

Device	Package Style	Device Radiation Hardness krad(Si)	TID Transfer orbit krad(Si)	TID Moon Phase krad(Si)	Total TID krad (Si)	Radiation Design Margin(RDM)
Linear ICs	DIP	20	1.14	1.63	2.77	7.2
	TO5,TO39,TO99,SMT	20	2.92	2.2	5.12	3.9
	TO3	20	1.43	1.61	3.04	6.6
MOS/CMOS ICs	DIP,SMT	100	1.14	1.63	2.77	36.1
	CQFP,FP etc	100	1	1.49	2.49	40.2
MOSFET	TO,SMT	100	2.92	2.2	5.12	19.5
	TO3,SMT	100	1.43	1.61	3.04	32.9
BJT	TO18,TO5,TO72,SMT	50	2.92	2.2	5.12	9.8
	TO66	50	2.76	2.1	4.86	10.3
	TO3	50	1.43	1.61	3.04	16.4
Zener diodes	DO7,DO35,SMT	100	2	2.06	4.06	24.6

Requirements for radiation shielding

Total Ionizing Dose (TID) level at device level can be reduced by local shielding [8]. However, the SEE are caused by high energy particles and local shielding is not an effective mitigation technique. SEE effects can be managed by selecting the right components and implementing the proper mitigation techniques by design.

The shielding calculations were made using software (DOSEMAP, a ray tracing software developed at ISRO), based on (i) spacecraft structure which includes main cuboids, load cylinder, fuel tanks, shear web, dimensions, thickness, and density (ii) electronics package dimensions, thickness, and density (iii) The number of PCBs and PCB dimensions, thickness, and density. A total of 24.5 transfer orbit details are considered for Chandrayaan 2 mission to calculate the radiation shielding material thickness. Considering the location of the Nano Rover in the lander, Table 2.3 provides the summary of the components proposed to be used in the Nano Rover, their radiation hardness capability after effective shielding. As it can be observed in the table, positive margins ensure that the Nano Rover will meet the TID radiation requirements.

Mitigation for Single Event Effects (SEE)

We enumerate the SEE mitigation techniques here.

1. MOSFETS used are radiation hardened from IR 100 KRad TID and 40 Mev SEE. No additional protection is required.
2. FPGAs used are radiation hardened from Actel 20 KRad TID and 40 Mev SEE. No additional protection required
3. Memories and SRAMs - 20 KRad TID. This needs protection from bit upsets. Triple modular redundancy is planned as the solution.

2.4 Lunar Soil, Terrain and Gravity Conditions

The soil properties play an important role in the rover mobility. Since the lunar soil is not homogenous, these properties must be predicted online. The Sojourner rover [15] had used a bevameter type method

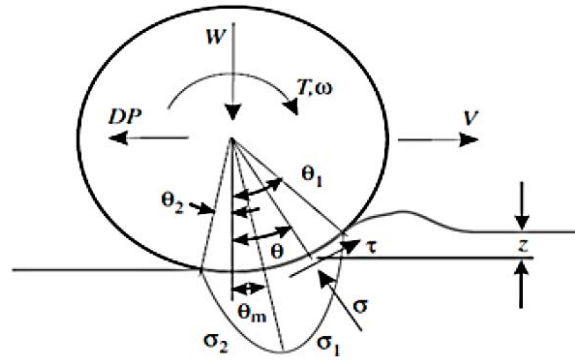


Figure 2.3: Wheel/leg-soil interaction model

to estimate the cohesion and internal friction. The prediction of these soil properties are done by comparing the mobility of the computational and experimental model.

2.4.1 Wheel/leg-soil interaction parameters

The parameters that would affect the mobility of the rover due to terramechanics include sinkage, drawbar pull, slip, torque, etc.

2.4.2 Mechanical soil properties

In addition to the wheel/leg-soil interaction parameters, the knowledge of mechanical soil properties must be known in advance for rovers mobility prediction. Lack of knowledge of these properties would result in inaccurate estimation of rover wheel/leg/leg-soil interaction parameters such as slip, torque, etc.

2.4.3 Terramechanics Dynamics Model

A mathematical model to develop the dynamics of the rover must involve the wheel/leg-soil interaction as the rover moves on the lunar regolith. For this, the terra mechanics of the soil must be considered to know how the wheel/leg behaves as it moves over an uneven surface covered with loose soil. The wheel/leg-soil interaction was first formulated by Bekker [15] and the equation by Wong [16, 17, 18] is used. Figure 2.3 shows the wheel/leg-soil interaction model where θ_1 and θ_2 are the entry and exit angles respectively, θ_m is the point of maximum stress, σ and τ are the normal and shear stress acting between the wheel/leg and soil, z is the sinkage, W is the weight.

Since the rover will travel on uneven surface, the slope of the terrain must be taken into account to compute the slip. The weight acting on the wheel/leg for the sinkage computation will have a cosine component of the weight with respect to the slope of the terrain, thus the equation of sinkage will be

$$z = \left[\frac{3w \cos(\text{slope})}{b(3-n) \left(\frac{k_c}{b} + k_\phi \right) \sqrt{2r}} \right]^{\frac{2}{2n+1}}$$

where, n is the sinkage exponent, b is the rover wheel/leg width, k_c and k_ϕ are the pressure sinkage module and r is the radius of the rover wheel/leg.

There are various other terramechanics properties that must be considered further for the analysis which are tabulated in Table 2.4 as per the study conducted by Genya ???. In the table, 'c' is the

Table 2.4: Lunar soil properties

Parameter	Value	Unit
c	0.8	kPa
ϕ	37.2	deg
$k(eq)(k_c/b + k_\phi)$	831125	$N/m^{(n+2)}$
n	1	-
k	0.036	m

cohesion, ϕ is the internal friction angle, and ' k ' is the soil deformation module. The weight obtained from kinematics is based on the link lengths of the rover but has no relation with the mechanical soil properties of the soil. The entry angle of the wheel/leg is a function of the weight and also the terramechanics properties.

The Moon's surface and environment characteristics pose various challenges for the selection and design of a particular robotic vehicle. The Moon's surface is essentially a smooth, soft surface with shallow undulations. Wheeled rovers show considerable difficulties while climbing slopes over 15° since the slip ratio drops suddenly. Legged rovers have better slope climbing and obstacle traversing capabilities than wheeled rovers.

Not many legged walking robots developed for space applications exist today, although a few vehicles are currently being developed in US and Europe. Walkers are highly stable while moving over obstacles and have better mobility during downhill motion due to better center of mass position. However, it has the disadvantage of high power consumption, since it needs power for both lifting of legs and forward motion. Conversely, a wheeled rover is energy efficient. The information on the rovers used for interplanetary mission till date and their designs are discussed in Appendix A.1.

The operational speed of a lunar vehicle is usually limited in the range of 10 cm/s due to safety concerns. It is limited by the type of gears used in the motor and power availability. The size of the vehicle is also a crucial factor while considering the mission scenario. It can be said that a rover in the mass range of 30 – 100 kg is capable of accomplishing many science tasks by accommodating more integrated instruments and payloads. Also small rovers are capable of generating enough power for surviving the entire mission. Micro-rovers (5 – 30 kg) and Nano-rovers (<5 kg) can be better suited for accomplishing specific mission objectives within limited range and power availability. These rovers are not capable of accomplishing a wide range of objectives like big rovers. However, in the case of small rovers, there are various flexibilities possible in choosing a mission. Nano rovers may not be independent in operation and deployed either from lander through tethers.

A swarm of small, low-cost rovers is a potential option for a mission. A swarm of low-cost robots would ensure lower risks. The safety concern can still be compromised if rover egress occurs inside the crater floor.

2.4.4 Experiments of Micro Zebro in lunar terrain test facility

From the literature study, it is clear that the Moon surface has loose soils, there are boulders, and there can be slope up to 15° . Nano Rover is likely to experience all these conditions. Even though there are theoretical explanations about soil interaction with wheels, there is no literature available in public domain about the functioning of legged rover on the Moon surface to draw an analogy and take forward the design. It is opined that many experiments need to be conducted with the terrestrial Micro Zebro so as to incorporate observations appropriately in the Nano Rover design. It is essential to perform experiments in order to have practical experience of the Nano Rover functioning on the Moon in order to effectively address all the possible requirements for the Nano Rover.

In all the experiments for locomotion study on simulated lunar terrain, Micro Zebro is used as the test vehicle as shown in Figure 2.4. Lunar gravity is simulated using a spring connected to the body of the Micro Zebro as shown in Figure 2.5. The test conditions, tests and observations are as follows.

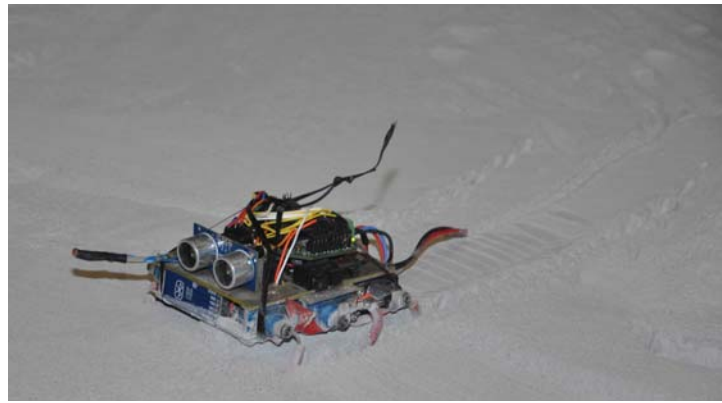


Figure 2.4: Micro-Zebro on the simulated lunar terrain

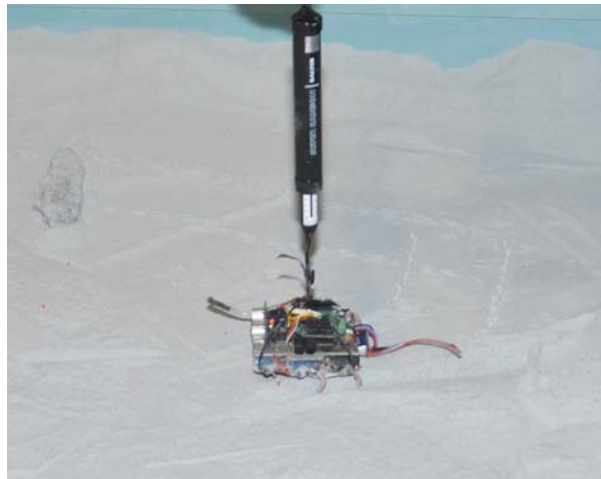


Figure 2.5: Micro-Zebro on the simulated lunar terrain with 1/6th gravity emulation

1. The time taken by the Zebro to cover 1 m is given in Table 2.5
2. Flat and best lunar terrain: Micro Zebro is able to perform normally similar to the hard terrestrial surface both under normal and 1/6th gravity.
3. Loose and disturbed soil: With the loose soil of about 20 mm, Micro Zebro is able to walk normally similar to the hard terrestrial surface both under normal gravity and 1/6th gravity. The trails left by the Micro-Zebro on the simulated terrain is shown in Figure 2.6.
4. Locomotion on slope: Under normal gravity, Micro Zebro is able to climb 15°, slope with difficulty and drags towards left or right due to thinner legs and inadequate frictional force. Under 1/6th gravity, Micro Zebro struggles much more than the locomotion at normal gravity confirming the need for wider legs and higher friction between legs and soil.
5. Obstacles: The size of the legs is about 25 mm from the centre to the edge. In normal gravity and 1/6th gravity emulation, Micro Zebro is able to negotiate the rock of about 30mm to 40 mm

Table 2.5: Average time taken to cover 1 m

Sl.no	Lunar Surface	Normal g	Lunar g
1	plain lunar surface	60 seconds	55 seconds
2	upward lunar slope	108 seconds	90 seconds
3	downward lunar slope	50 seconds	45 seconds

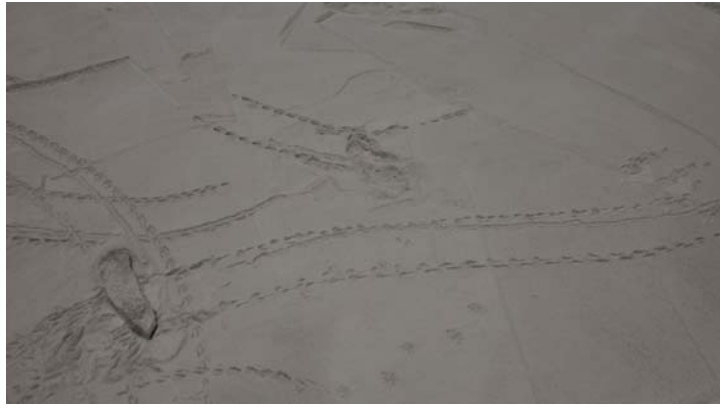


Figure 2.6: Trails left by the Micro-Zebro on the simulated lunar surface

size. This is due to the fact that the rubber in the leg is providing adequate friction and also leg size is adequate to climb the above rock size.

In summary, while lunar gravity helps locomotion on the plain lunar terrain, it greatly affects climbing up/down and negotiating obstacles. Nano Rover must be designed with the motor that can provide sufficient running torque to overcome obstacles on the Moon and maneuver on loose soil. The design of the legs must be carefully done so as to ensure that the Nano Rover is able to climb up/down expected slope of about 15° without slipping. This would need legs to be sufficiently wide along with powerful motor and enough high holding torque.

Nano Rover Design Requirements

In this chapter, we provide the mission and subsystem requirements for the Nano Rover development. We consolidate all the requirements for the design and development of the rover. Since space systems are designed to meet the highest reliability and lowest failure rates, Chandrayaan-2 mission profiles is considered for the design and realization of the locomotion system of the Nano Rover.

Considering the mission requirements and environmental specifications presented in the previous chapter, we deduce the main design requirements for the locomotion module of the Nano Rover which are as follows.

1. The Nano Rover shall be realized by adopting most reliable proven methodologies for interplanetary mission. Power system management, On Board Computer (OBC), motor drive electronics and the locomotion software and hardware shall demonstrate the highest reliability.
2. All the systems shall be designed using Military/European Space agency (ESA)/NASA/ISRO qualified parts and materials with established reliability. All the materials shall have the heritage of usage in previous space programs. These items shall be screened and accepted for usage in the Nano Rover. All the elements used shall meet the reliability requirements in terms of design margins, derating and redundancy.
3. Space Radiation requirements need to be complied for both Total Ionising Dose (TID) and Single Even Effects (SEE). Elements and the electronics used shall meet the radiation requirements of earth orbit, transit orbit, Moon orbit and on the Moon radiation. Mitigation techniques such as radiation shielding for TID, triple modular redundancy for memories, current sense, and shut down circuit for SEE mitigation is mandatory. Demonstration of compliance to radiation through analysis and/or experiments is mandatory.
4. Design of the layouts and PCBs shall be compliant to ISRO satellite design standards. Every element, parts and sub assemblies shall demonstrate the quality requirements. Product assurance guidelines of ISRO shall be strictly adhered to.
5. All the subsystems of the rover shall meet the working temperature of -40 to $+70$ °C and storage temperature of -186 °C. It should also sustain the vibration requirements as mentioned in the previous chapter, and should be functional in vacuum. This is applicable for all the elements used in building the Nano Rover.

3.1 System Level Requirements

The requirements in system level areas are as follows.

3.1.1 Structure subsystem requirements

The Nano Rover structure shall be within the envelope design constraints specified to provide adequate strength and stiffness to the structural members, the mechanical support, and for mounting of the components, assemblies and packages. Since solar cells are used as energy source in the Nano Rover, solar panel substrate for mounting solar cells shall be provided. The structure shall meet the the vibration and shock specifications as given by the mission team for the Nano Rover. The rover chassis is to be made of aluminum, carbon material or any suitable materials such as Ultem that can withstand the required environment requirements.

3.1.2 Mechanisms subsystem requirements

Mechanisms shall provide the mobility and steering capability for the Nano Rover on the unstructured terrain. Mechanisms shall ensure the stable Nano Rover chassis platform that can move over slopes and obstacles. They shall also endure the launch loads and landing loads with hold down and release mechanism. The mechanism shall provide solar panel hold down and release mechanism.

3.1.3 Power subsystem requirements

The solar array shall be used as the primary source for power generation. The power systems shall provide battery as a secondary source for power distribution to subsystems. Necessary charging and maintenance scheme for battery shall be incorporated. The power distribution (either raw bus power or DC/DC power) to all the Nano Rover subsystems including payloads (either continuous or in duty cycle mode) for their functioning shall also be provided. The power system shall provide a sleep circuit and wake-up circuit consuming almost no power. Provision to operate the Nano Rover in a minimum mission mode with solar array power without battery backup has to be envisaged during the design of power systems. Wake-up circuit closes the emergency switch connecting battery to the subsystems to switch ON the critical systems upon charging of the battery to the threshold level. It shall have the provision to operate the Nano Rover in a minimum mission mode with solar array power without battery backup.

3.1.4 Locomotion subsystem requirements

Being the heart of the Nano Rover, locomotion shall be controlled by the OBC designed using microprocessors, FPGAs, memories and other supporting circuits with highest reliability and proven flight heritage. The motor drive electronics shall be able to control the motors independently and demonstrate fault free locomotion under lunar environment.

3.1.5 RF subsystem requirements

RF systems provide two-way communication ensuring adequate link margins and gains between the Nano Rover and ground station. A detailed configuration for Forward Link Antenna and Return Link Antenna has to be developed.

3.1.6 Assembly, Integration and Testing (AIT) requirements

The AIT subsystem team shall accommodate all the subsystem deliverables and provide layout design within the envelope constraints specified for the Nano Rover in order to meet their functional, thermal, structural and assembly / disassembly requirements. It shall also ensure ideal location of packages, cards and components - both inside and outside the Nano Rover structure in order to survive the launcher and the lander loads. The team is also responsible for the integration and testing of all the subsystems based on approved test procedures and providing interfaces between lander and the Nano Rover to meet the overall requirements.

3.1.7 Mission requirements

The Mission team shall plan the Nano Rover mission operations for the upcoming lunar mission. The team shall also plan the sequencing of Nano Rover commissioning and landing. The team provides procedures to carry out the day-to-day operations of Nano Rover in view of its movement and payload operation within the power budget.

3.1.8 Product Quality Assurance requirements

The Quality Assurance team shall generate the product qualification guidelines for the cards, components, processes, packages and the total Nano Rover mobility system during storage, handling, development, operations, testing, and launch. The team shall generate the precautions (electrical and mechanical) required to be taken during various phases of the Nano Rover subsystems fabrication, assembly, test and launch. The team shall also generate the test philosophy of engineering model and flight model for both hardware and software. The team shall generate the subsystems test philosophy of the Nano Rover during tests carried out at terrain test facility and including environmental tests of Nano Rover during assembled mode and integrated testing with lander. The team shall also generate the environmental and radiation qualification levels for the Nano Rover during launch and on the lunar terrain.

All the requirements shall be generated by the respective teams and ensure that the Nano Rover design shall strictly adhere to all the requirements and procedures. The expertise of ISRO personnel shall be taken and the guidelines followed for space systems shall be followed by the respective teams for the realization.

3.2 Nano Rover Block Diagram

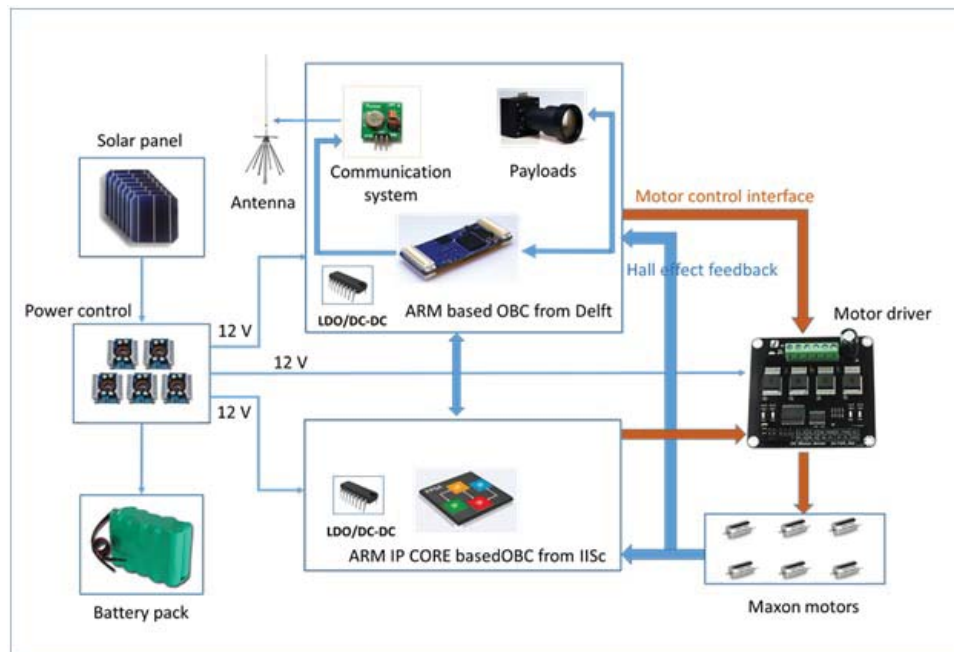


Figure 3.1: Block diagram of the Nano Rover subsystems

Considering all the aforementioned system requirements, the overall block diagram of the nano rover is shown in Figure 3.1. The connectivity between various subsystems are also shown. The solar panel is the main source of power generation. There is a battery which gets charged and shall be used

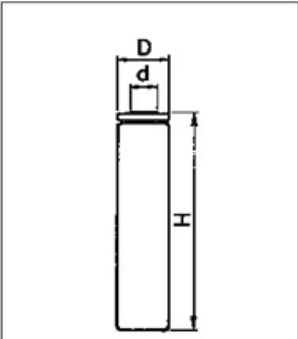
during eclipse. The heart of the rover is the OBC card. Two OBCs, one from ISRO and one from TU Delft are being developed for redundancy. The communication between the OBCs are through dedicated IO lines. The communication to ground and the payload designs will be developed by TU Delft. This thesis mainly concentrates on the design of the OBC card (from ISRO), the motor drive electronics and the locomotion algorithm.

3.3 Materials, Components Selection and Qualification for the Nano Rover

The Nano Rover is conceptualized to demonstrate the functioning with highest reliability under challenging space environments such as -186°C storage temperature, hard vacuum and radiation environment. Hence the choice of the battery, electronic components and materials need to be compliant to meet these challenging requirements. These components are MIL/ESA/NASA high reliability grade with operating temperature of -55°C to $+125^{\circ}\text{C}$ with no specific note on the storage temperature. However, for the proposed Nano Rover, these elements need to meet cryogenic temperatures. Hence these components have also been specially and specifically tested to meet the mission requirements.

Cell Type NCR18650B		
Specifications		
Rated Capacity	*at 20deg.C	Min.3200mAh *at 20deg.C
Nominal Capacity	*at 25deg.C	Min.3250mAh *at 25deg.C
		Typ.3350mAh
Nominal Voltage		3.6V
Charging Method		Constant Current -Constant Voltage
Charging Voltage		4.2V
Charging Current		Std.975mA
Charging Time		4.0hrs.
Ambient Temperature	Charge	$0\sim+45^{\circ}\text{C}$
	Discharge	$-20\sim+60^{\circ}\text{C}$
	Storage	$-20\sim+50^{\circ}\text{C}$
Weight(Max)		47.5g
Dimensions (Max.)*	(D)	18.25mm *without tube
		18.50mm *with tube
	(H)	65.10mm *without tube
		65.30mm *with tube
Volumetric Energy Density		676Wh/l
Gravimetric Energy Density		243Wh/kg

Discharged State after Assembling		
Dimensions(Typ.) of Bare Cell	H	64.93mm
	D	18.2mm
	d	7.9mm



*Maximum size without tube

Figure 3.2: Battery specifications

3.3.1 Battery

The batteries provide a backup source of energy in the absence of solar energy due to the orientation of the space subsystems with respect to pointing the Sun. When the space systems are in eclipse and when they do not receive solar energy, batteries provide power to the systems. The choice of the Nano Rover battery primarily depends upon its capability to withstand cryogenic temperatures for the full mission period and also charge, store and deliver the required energy to the load. There is only one choice for this battery which has been custom made one for ISRO, type based on NCR18650B by M/S LG, Japan. The battery specifications are shown in Figure 3.2. These cells have to be characterized for cryogenic temperatures. The characteristics of the cell after 240 hours of storage in cryogenic temperatures are shown in Figure 3.3 and Figure 3.4 respectively. The batteries under test at cryogenic temperature is shown in Figure 3.5 Figure 3.6 is the summary of the study of the LG battery proposed to be used in the Nano Rover.

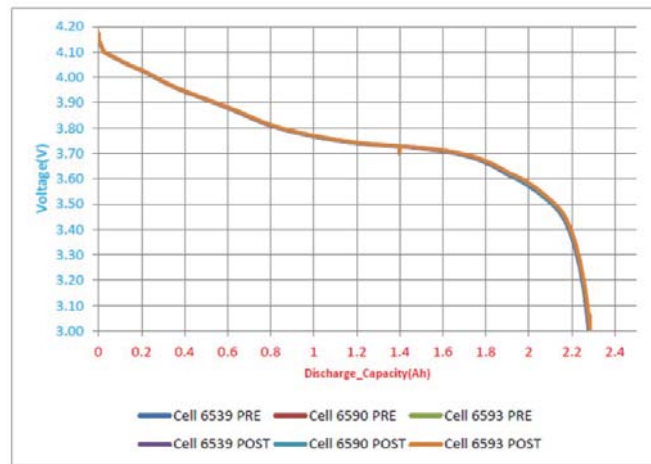


Figure 3.3: Battery discharge characteristics at 20° C (–160° C soak for 240 hours)

Comparative charge voltage characteristics during standard capacity test at 20 °C for LG 3.5 Ah cells (–160°C soak for 240hours).

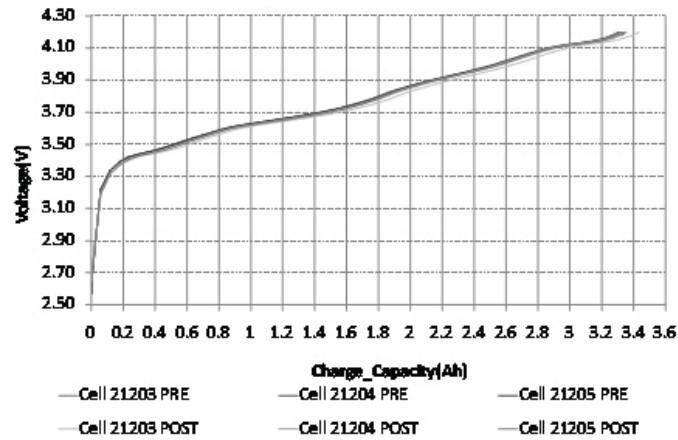


Figure 3.4: Battery charge characteristics at 20° C (–160° C soak for 240 hours)

3.3.2 Solar Cells

The main source of power generation for the Nano Rover is the solar cell. A solar cell (also called a photovoltaic cell) is an electrical device that converts the light energy directly into electric energy utilizing the photovoltaic effect. Solar cells are often encapsulated as a module. These modules often have a sheet of glass on the sun-facing side, allowing light to pass while protecting the semiconductor wafers. Solar cells are usually connected in series in modules, creating an additive voltage. Connecting cells in parallel yields a higher current; however, problems such as shadow effects can shut down the weaker (less illuminated) parallel string (a number of series connected cells) causing substantial power loss and possible damage because of the reverse bias applied to the shadowed cells by their illuminated partners. Strings of series cells are usually handled independently and not connected in parallel, though individual power boxes are often supplied for each module, and are connected in parallel. In the case of the Nano Rover, it has been decided to use solar cells which are capable of providing 12V, 1.2A using a combination of series and parallel solar cells. The solar cells chosen are from Azur Space, where each cell can deliver 2.0V, 0.2A. A set of solar arrays with 6 cells in series are connected in parallel to generate 12V, 1.0A power.

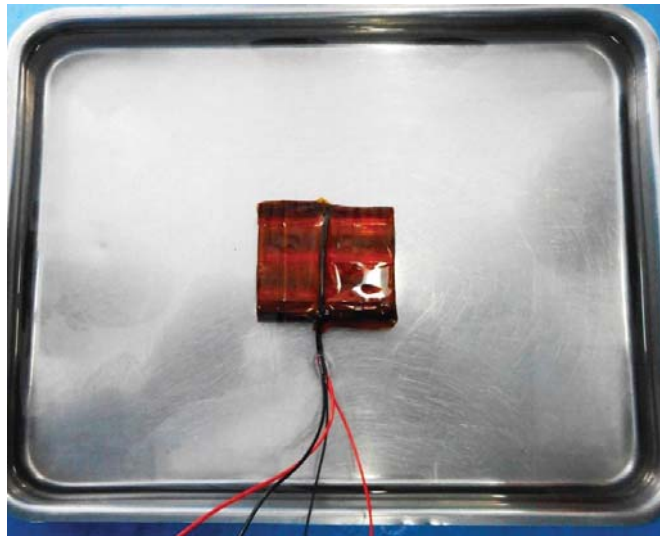


Figure 3.5: Battery pack under thermal test

Cell No.	SOC (%)	EOCr (m Ω)		EODr (m Ω)		Dynamic (m Ω)		AhIn (Ah)		PDC (Ah) post test	AhOut (Ah)		
		Pre	Post	Pre	Post	Pre	Post	Pre	Post		Pre	Post	
-160$^{\circ}$C soak for 240 hours													
Panasonic 3.4 Ah cells	15704	0	63	63	251	258	58	54	3.2499	3.2694	0.055	3.2111	3.2011
	15705	50	61	60	255	276	54	52	3.2481	3.2273	1.654	3.2112	3.2024
	15706	100	61	60	249	282	52	52	3.2489	3.2220	3.214	3.2365	3.2289
LG 3.5 Ah cells	21203	0	45	46	234	234	36	38	3.329	3.435	0.084	3.316	3.361
	21204	50	46	46	238	224	38	39	3.306	3.335	1.709	3.338	3.369
	21205	100	44	45	229	231	40	39	3.335	3.355	3.306	3.322	3.335

Figure 3.6: Pre and post cold storage characteristics summary

3.3.3 Passive and active components tests at cryogenic temperature

The passive components recommended for usage in the Nano Rover are: capacitor types CKR, CLR, CNC, CDR, CWR and CTC metal poly propylene type, resistors types RNR, RCR, RWR and RM series. The passive component types and their package styles are shown in Figure 3.7 and Figure 3.8 respectively. These have been exclusively procured for high reliability applications. Based on the requirement, the devices have been tested at cryogenic temperatures before usage in the Nano Rover. Similarly, based on the successful completion of tests, buffers, LDOs, diodes, transistors, and other active and passive components are selected for usage in the Nano Rover as per bill of materials.

A few of the passive and active component types used in the rover are represented in Figure 3.9 and Figure 3.10 respectively.

3.3.4 On Board Computer for the Nano Rover

The recommended devices for interplanetary mission that are available for this application are Leon3 32-bit Processor, FPGA RTX2000 and Pro ASIC3 from M/S Micro semi USA. It is decided to consider

S.NO	TYPE	STYLE
1	CERAMIC	CKR06
2	CERAMIC	CKR06
3	WET TANTALUM	CLR79
4	CERAMIC	CNC58
5	CERAMIC	CDR33
6	SOLID TANTALUM	CWR06
7	SOLID TANTALUM	CWR06
8	METAL POLY PROPYLENE	PM90

Figure 3.7: Capacitors packages

S.NO	TYPE	STYLE
1	Metal Film	RNR60
2	Metal Film	RNR55
3	Carbon Composition	RCR07
4	Carbon Composition	RCR05
5	Wire Wound	RWR80
6	Film: Thick/Thin	RM1206
7	Film: Thick/Thin	RM1206

Figure 3.8: Resistor packages

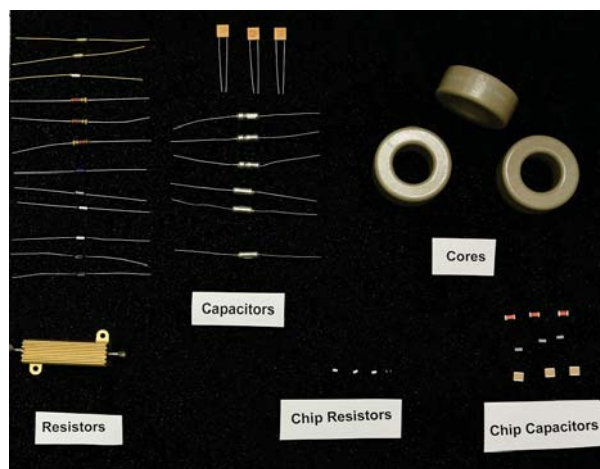


Figure 3.9: Passive components

the latest chip ProASIC3 series of FPGAs as the heart of the OBC as it offers a breakthrough in performance, density, and features for today's most demanding lunar mission applications. It offers significant weight reduction, board space savings, lower cost and highest reliability. ProASIC3 devices support the ARM - Cortex-M1 soft processor IP core, offering the benefits of programmability. The ProASIC3 families are based on non-volatile flash technology and support 100 to 35K LEs and up to

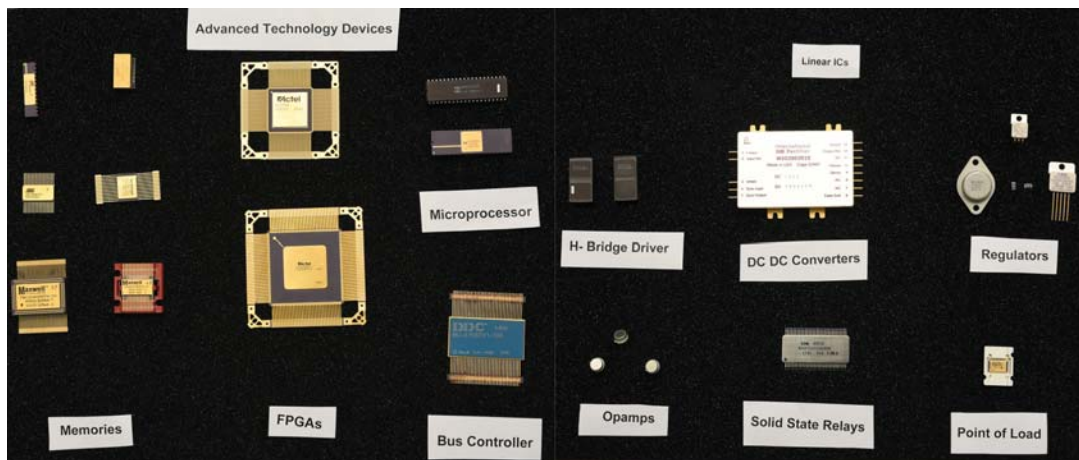


Figure 3.10: Active components

620 I/Os. ProASIC3 offers military grade devices with temperate range of -55 to 125°C and support 3K to 35K logic elements. Compared to other options of FPGAs and processors, Pro ASIC3 also has key feature of relatively higher dynamic power savings, static power savings, single-voltage operation, optimized for high performance, reprogrammable, non-volatile, 1.2V to 1.5V core voltage support and wide range of I/O voltage support from 1.2V. On top of all this this device meets the storage temperature of -186°C . It is also available in a small 208 pin Ceramic Quad Flat Package (CQFP) and space qualified product. Hence, it is an ideal choice for realisation of the OBC functionalities and other glue logic for the Nano Rover.

3.3.5 Choice of motors

The motor assembly is the combination of a motor and a gearbox. The two classes of DC motors mostly used are Brush Less DC motors (BLDC) and Brushed DC (BDC) motors. Both the motors have their own advantages and disadvantages. For example, the brushes of a brushed DC motor cause friction. This friction will result in wear and heat. On the other hand, the control of a BLDC motor is much harder and it is much more expensive. Compared with a BDC motor, the BLDC motor has many advantages such as higher efficiency and reliability, lower acoustic noise, smaller and lighter, greater dynamic response, better speed versus torque characteristics, higher speed range and longer life. Additionally, only BLDC motors are available for the interplanetary mission - from M/S Maxon, Switzerland, and M/S Faulhaber, Germany. We choose EC series BLDC motors from Maxon, for the final flight model of the Nano Rover as they are specially made for interplanetary missions. The selected Maxon motor dipped in liquid Nitrogen for cryogenic testing is shown in Figure 3.11

3.3.6 Choice of hall sensors

The locomotion controller must always know the position of the legs in order to coordinate the six legs into specific gait pattern. Bipolar hall sensor is used to detect the position of the legs in the Nano Rover The Hall-effect devices contain a monolithic integrated circuit which incorporates a hall element, a linear amplifier, a threshold amplifier, and a schmitt trigger on a single hall logic silicon chip. The hall effect sensor also includes a on-chip bandgap voltage regulator that allows operation with a wide range of supply voltage from 4.5 to 24 volts. The output amplitude is constant at switching frequencies from DC to over 200 kHz. The unipolar hall effect turns on with a (logic level 0) after a sufficient magnetic field from the south pole of a magnet approaches the symbolized face of the device (operating point) and turns off (logic level 1) after the magnetic field reaches a minimum value. The bipolar device turns on (logic level 0) in the presence of a magnetic south pole and turns off (logic level 1) when subjected to a magnetic north pole. Both magnetic poles are necessary for operation



Figure 3.11: Maxon motor with planetary gearhead under thermal test

for bipolar devices. The hall effect sensors used in the Nano Rover are of space grade, from OPTEK. This product has passed radiation hardness testing up to 350 Krad (si).

3.4 Brief introduction to all systems

The Nano Rover is a battery powered 6 legged rover. Six electric motors of BLDC type are used for the rover movement. Semi-circular ‘C’ shaped legs made of molded high density enhanced plastic are employed on all six BLDC motors. These legs help the rover to move over the rough surfaces, navigate on obstacles, climb gradients and even on the fine dusty soil of the Moon. A hall sensor is placed on each the outer surface of the mounting area of each motor. The legs carry a powerful magnet which outputs a digital signal when they come to the vicinity of the hall sensor. This signal is used to control the legs for the favorable movement. The power source for the motors are batteries. As solar panel cannot deliver the current required to move all 6 motors at a time, locomotion is carried only when battery is charged satisfactorily. The On Board Computer is designed to generate the gate driven PWM signals for running the 6 BLDC motors in a synchronized way via a hall sensor feedback mechanism so that the nano rover performs desired locomotive maneuvers. Signals from the OBC are fed to 6 MOSFET gates in the motor drive circuit which in-turn switches on and off the motors in a controlled fashion. Importantly, this module is involved in waveform shaping and timing generation which completely characterizes the motor operation and behavior.

3.5 Adaptation from Zebro to the Nano Rover

Considering the mission requirements, experiments and adaptation study, the Zebro light is modified as the Nano Rover and the systems adapted are listed in Table 3.1.

Table 3.1: Adaptation of Zebro Light to the Nano Rover

Sl.no	Element	Existing Zebro	Nano rover-proposed options	Remarks
1	Leg	Plastic	Aluminum,Polymide,Polyemide, etc	Chassis, Legs and body to be conductive, light weight, meet structural needs, withstand mission environment
2	Chassis	Acrylic	Aluminum, Carbon-carbon	
3	Solar panel	None	Honey comb structure	
4	Landing mechanism	None	Ejection System for safe landing from 1m,	

Table 3.2: Electronics

Sl.no	Element	Existing Zebro	Nano rover-proposed options	Remarks
1	OBC & Motor Drive Electronics	All Commercial Components, & Processor Atmel 328	Soft Core in FPGA ACTEL 2000 & Core ARM/8086	All Components are Space Grade Qualified to,Mil / GSFC / ESCC / ISRO/ MIL QML V/ Class S/ Class K/ ESCC 5000 specifications
2	Battery	Commercial	LG or MIMO, Size dia=18mm length=65 mm, 4V/1Ah 40gms each	Space Grade by ISRO
3	Solar panel	None	Multi junction,efficiency 30%, power 1.1 W Voc=2.7 V,Is=0.5 A, size 80x40 mm	
4	Motors	Commercial,multi vendor	Maxon	
5	Magnet	Semerium cobalt	Semerium cobalt	
6	Communication System	commercial blue-tooth	Space System,UHF/VHF/S-band	
7	PCB	FR4	Glass epoxy with,specialized treatment for low temp	
8	Other components	commercial	Capacitor:.,CDR,CKR,CSR, Resistor: RER, RWR	

Hardware

4.1 Introduction

This chapter deals with the hardware design of Nano Rover. The electronic hardware design revolves around the OBC, the motor drive card, power card, solar cells, and the corresponding software. The TU Delft team will also develop an OBC and the payload unit. The system developed by TU Delft is termed as the Payload Data Management Unit (PDU). The two pieces of hardware shall communicate with each other through a protocol, which shall be decided by the teams. The motor drive shall be driven by the selected OBC at a time. The power for the OBC shall be derived from the common power electronics. Power generated by the solar cells or the batteries shall be used based on the availability of the sunlight on the lunar surface.

The locomotion algorithm could have been demonstrated on any off-the-shelf available microprocessor kits. However, most of these kits will not adhere to the mission requirements of mass, power and volume as mentioned in Chapter 1. Hence, it was decided to design and realize an OBC card which meets the aforementioned requirements. This chapter emphasizes on the design and realization of the OBC card from ISRO. The overall hardware block diagram is shown in Figure 4.1. The locomotion algorithm resides in the PROM. The integrated system logic resides in the FPGA. The level converters are mainly for conversion of voltage levels between TTL logic and other subsystems.

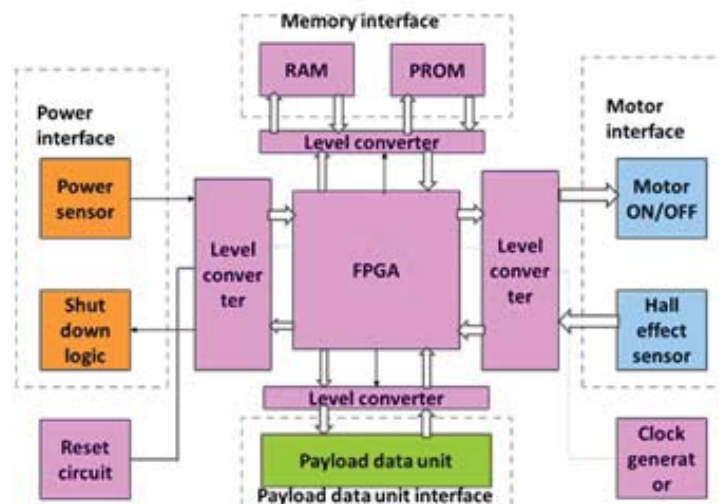


Figure 4.1: Hardware block diagram

The ISRO OBC card has interfaces with the Payload Data Unit (housing both the TUD OBC and the payloads) as shown in Figure 4.1. It also has interface with the power card¹ and motor controller card. The overall design is realized using three Printed Circuit Boards (PCB). The OBC functionalities are realized using the OBC card. All motor functionalities are realized using the motor control card. The power logics are realized using the power card. The power good signal from the power card is detected and then the OBC card logics are enabled. The OBC generates the PWM signals for the motor control card. The hall sensor inputs are read by the OBC card. The software resides on the PROM mounted in the OBC card. An SRAM is included in the OBC card to store the variables and the look up tables. Level convertor buffers are used to translate data to and from the I/O devices. Separate control signals are given for controlling the cards from the OBC card. Interface signals are provided for smooth transition from the ISRO OBC card to the TU Delft PDU card.

4.2 Introduction to FPGA architecture

The latest chip from ProASIC3 series of FPGAs [27] is used to implement the OBC logic as it offers a breakthrough in performance, density, and features for the most demanding lunar mission applications. It also offers significant weight reduction, board space savings, lower cost, and highest reliability needed for a space system. ProASIC3 devices support the ARM - Cortex-M1 soft processor IP core, offering the benefits of programmability and quicker realization time. The ProASIC3 families are based on non-volatile flash technology. They support 100 to 35k LEs, and up to 620 I/Os. ProASIC3 (M1A3P1000) FPGA is available in military grade with an operating temperature range of -55 to 125° C. The military grade devices support 3k to 35k logic elements along with 32-bit Cortex M1 soft processor implemented in the FPGA. Additionally, ProASIC3 FPGAs offer the following key features.

1. Relatively higher dynamic and static power savings.
2. Single-chip, single-voltage operation and instant-ON.
3. Optimized for high performance, reprogrammable, and non-volatile flash.
4. Low core voltage support between 1.2 V to 1.5 V.
5. Wide range of I/O voltage support from 1.2 V.
6. Innovative flash freeze technology for instantaneous switching from active to static mode.
7. In-system programming (ISP) with optional on-chip AES decryption.
8. Immune to configuration loss due to atmospheric neutrons (firm errors).
9. The device meets the required storage temperature of -186° C.

4.3 Requirements of ISRO OBC card

4.3.1 Hardware Requirements

The hardware requirements of ISRO OBC card are as follows.

1. **Power on reset:** A pulse of 64 milliseconds (minimum required for FPGA) shall be issued as a master reset to bring all the hardware to a known state. Reset qualifier is required inside the FPGA to validate this reset pulse.

¹We use 'card' and 'module' interchangeably.

2. **Clock requirements:** Clock frequency will be 100 MHz, all the glue logic inside the FPGA shall use clocks derived from this master clock. A PLL derives the system clock of 25 MHz from the master clock.
3. **Motor control:** The locomotion of the motors shall be achieved by a combination of hardware and software. The locomotion shall be enabled only when the power is available. There shall be an independent control for each phase of the motor. Independent bits shall be made available for reading the hall effect sensors.
4. **I/O decoding:** There shall be a total of 32 IO registers which can be read from or written into. Each bit of the register shall be programmable. Provision shall be made to have one extra read and write register for future expansion.
5. **Memory decoding:** There shall be a $32k \times 16$ PROM where the code resides and the control signals for the PROM like chip select and read shall be generated by the hardware. RAM is used for the storage of temporary variables and shall be of $8k \times 16$ size.
6. **Mitigation techniques:** The RAM variables shall be suitably mitigated using triple modular redundancy to prevent single event upsets. The memory address decoding and the corresponding bidirectional buffer control signals shall be generated by the hardware.
7. **Subsystem handshake techniques:** Software shall be modular to accommodate algorithms for navigation or payload management with minimum modification.
8. **Supply voltage:** Supply of 12 V, 5V, 3.3V and 1.5V shall be available on the board.

4.3.2 Mission requirements specification for Nano Rover

Following are the mission requirements for the Nano Rover software and locomotion.

1. On getting release command, switch closure to give power to OBC.
2. Power On Reset (POR) to the OBC to begin executing the code.
3. Detect Power Good (P_G) i.e., wait for power to be available.
4. Initialize all subsystems.
5. Autonomous event management and/or programmability of various events.
6. Run Scheduler for systematic service of all subsystem tasks.
7. Move Rover: Generate motor actuation signals and receive input from the hall effect sensors in the given direction
8. On P_G failure, enable battery recharging.

These steps translate into the following sequence of operations for the OBC.

1. On getting release command from the lander, there will be power ON to the OBC.
2. The OBC shall take reset pulse from reset generator circuit and generate appropriate reset signals to bring all modules to a default condition.
3. The OBC shall take clock input and generate suitable timing signals for each of the module.
4. The OBC generates control signals to read power good, hall sensors and Payload Data Unit (PDU).

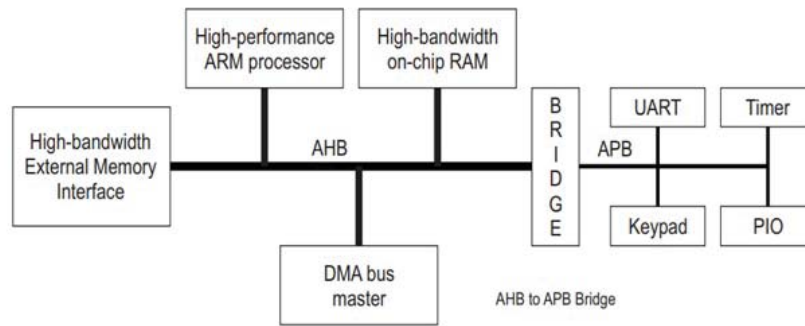


Figure 4.4: typical AMBA system

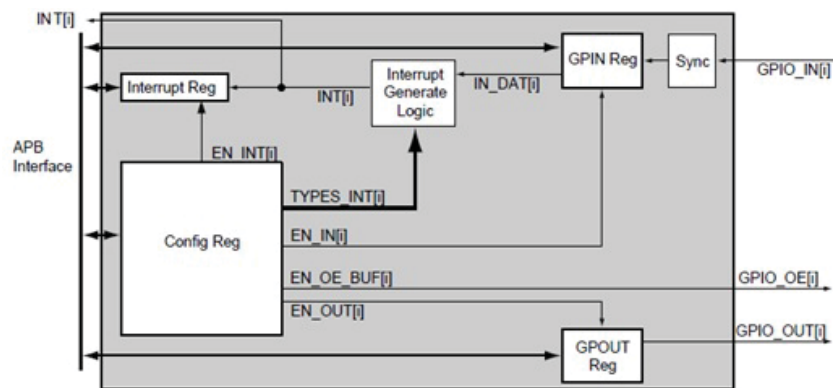


Figure 4.5: Single I/O Bit Block Diagram for Core GPIO

4.5.2 Core GPIO

Core GPIO [22] provides an APB register-based interface with up to 32 general purpose inputs and 32 general purpose outputs. The input logic contains a simple three-stage synchronization circuit, and the output is also set synchronously. Each bit can be set to either fixed configuration or register-based configuration via top-level parameters, including input type, interrupt type/enable, and output enable.

The key features of Core GPIO are

1. AMBA 2 APB support, forward compatibility with AMBA 3 APB
2. 8, 16, or 32-bit APB data width
3. 1 to 32 bits of I/O, for all APB-width configurations
4. Fixed or configurable interrupt generation
5. Parameter-configurable for single-interrupt signal or up to 32-bit-wide interrupt bus
6. Fixed or configurable I/O type (input, output, or both)
7. Configurable output enable (internal or external implementation)

4.5.3 Core AHB2APB bridge

Core AHB2APB [21] (AMBA Bridge) is an AHB slave that links the AHB bus to the APB bus and acts as the master on the APB bus. Address decoding for the APB bus is carried out within Core

AHB2APB and this provides select signals for up to 16 APB slave slots. Read and write transfers on the AHB bus are converted to corresponding transfers on the APB bus. High bandwidth peripherals such as memory controllers are typically connected to the AHB, whereas the APB bus is used for less demanding peripherals such as watchdogs. Unlike the AHB bus, transfers on the APB bus are not pipelined. Figure 4.6 shows the CoreAHB2APB block diagram.

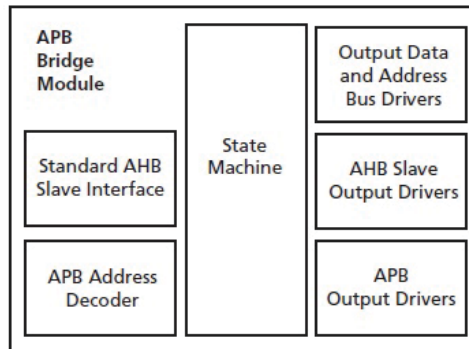


Figure 4.6: Core AHB2APB block diagram

4.5.4 Master Clock Generation

The master clock is generated using a 100 MHz Crystal Oscillator MCM2799 as shown in Figure 4.7 which is fed to the FPGA. Within FPGA, the 100 MHz clock is routed through a global clock net to ensure low clock skew. This clock drives the HCLK input of the Cortex-M1 core through a CLKINT buffer. The CLKINT buffer is used to ensure low skew routing for the HCLK signal. HCLK is the main clock input that clocks the majority of the logic in the processor core and other cores in the system.

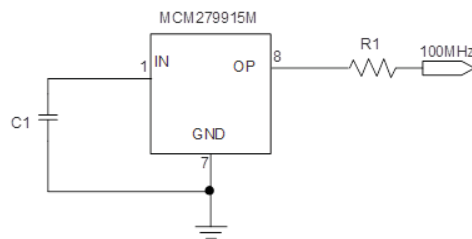


Figure 4.7: 100 MHz clock generation

4.5.5 Power On Reset (POR) Generation

A pulse of 64 millisecond (minimum required for FPGA) is generated using the circuit shown in Figure 4.8. The POR signal is fed to the FPGA where it internally drives a reset synchronization block within the Cortex-M1 core to generate a synchronized reset signal HRESETn. The synchronization block ensures that resets which may assert asynchronously are deasserted synchronous to the HCLK. HRESETn internally drives the SYSRESETn input of the processor core and is also an output from the top level of Cortex-M1 core for use as a synchronized reset to other components in the design clocked by HCLK.

4.5.6 Power Generation

An input voltage of 12V for the OBC is provided from the power card through a connector. Necessary internal supplies of 5V, 3.3V and 1.5V are generated from 12V using the circuits shown in Figure 4.9.

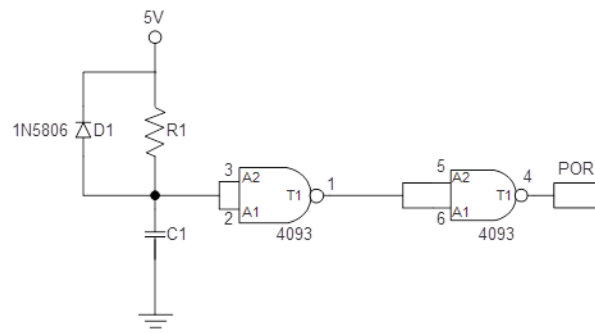


Figure 4.8: POR generation

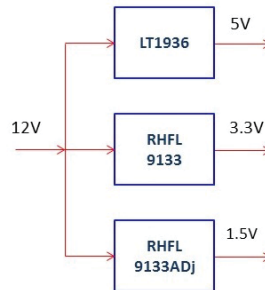


Figure 4.9: Power management

4.5.7 Control logic implementation

The control logic of the OBC Card is the heart of the locomotion system and implemented in a ProASIC3 FPGA. The control logic is designed to give the gate driving PWM signals for running the six motors in a synchronized way via a hall sensor feedback mechanism so that the rover performs desired locomotive maneuvers. This logic is implemented by configuring Cortex M1 core, AHB, Advanced Peripheral Bus (APB), SRAM and the CORE GPIO controller as shown in the block diagram in Figure 4.10.

4.5.8 PWM generator

The PWM generator IP core is capable of generating up to 16 PWM signals which are independently controllable. The block diagram of the PWM IP core is shown in Figure 4.11. The IP core receives the duty cycle as a count from the software through the APB interface and the PWM pulses generator are output to the motor drive card through the GPIO pins to the motor controller card. This IP core is capable of generation of 16 PWM pulses. In the Nano Rover, 6 PWM pulses are used to control the 6 motors which are in turn connected to the legs. The BLDC motor need 6 control pulses. The sequence of operating the BLDC motors is explained in the motor controller card. A truth table is provided by the manufacturer (see Figure 4.18) indicates the way the coils have to be energized for the motor operation. The corresponding truth table has been converted into combinational logic inside the FPGA and the corresponding levels are transferred to the motor card.

4.6 Motor Controller Card

The PWM pulses generated in the OBC card are transferred through the motor controller card through a connector. The gate is controlled by the PWM circuit. A brief explanation of the BLDC motor and the truth table for the coil energization as mentioned .

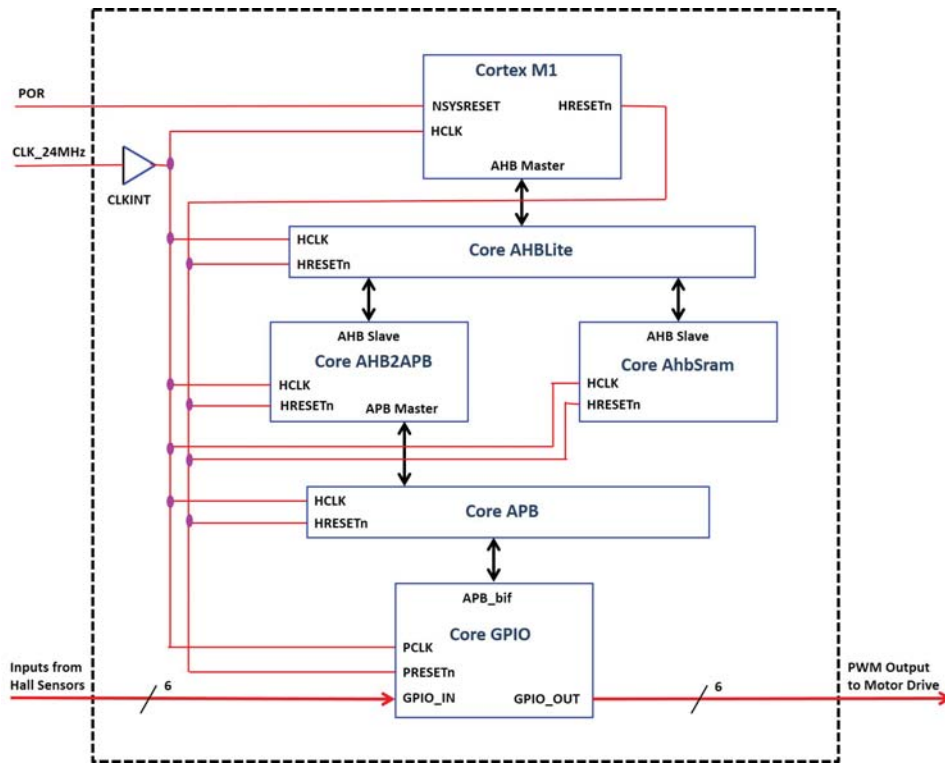


Figure 4.10: FPGA block diagram

Figure 4.12 shows a schematic diagram of DC motor. A standard mathematical model describing the relationship between motor current and supply voltage neglecting inductive effects is given by

$$i_a = \frac{1}{R_a}(V - K_b \dot{\theta})$$

Where R_a = armature resistance (ohms), V = input voltage, K_b = back-emf constant, $\dot{\theta}$ = leg speed (radian/second), i_a = armature current (A).

The motor will draw current based on the difference between the supplied voltage and the back emf which is directly proportional to the motor speed. For a given supply voltage, the motor will accelerate until the back emf balances the supply voltage such that the torque produced by the current draw matches the load torque. The relationship between current and torque is

$$\tau = K_t i_a$$

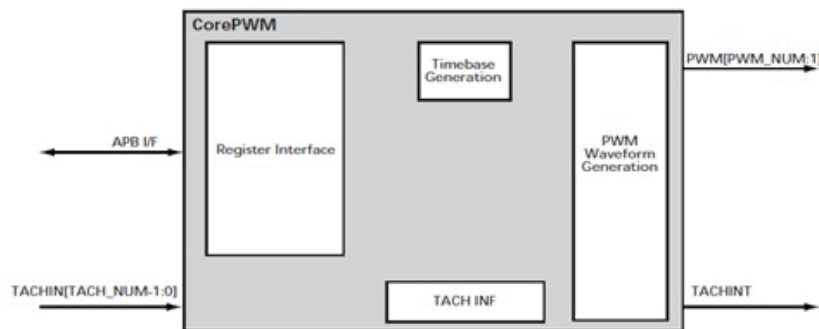


Figure 4.11: Core PWM block diagram

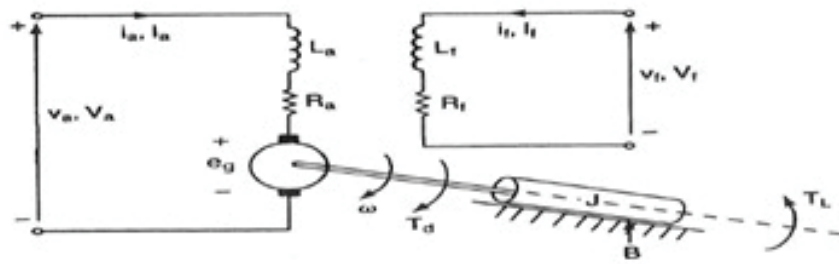


Figure 4.12: DC motor schematics

Where K_t = torque constant, i_a = armature current, τ = motor torque applied to each leg.

To control the motor, we use Pulse-Width-Modulation (PWM) to generate the output voltage. The basic technique involves generating a series of square waves of varying duty cycles. Figure 4.13 shows a PWM. Because the period of the square waves is small compared to the electrical dynamics of the motor, the motor behaves as if it was connected to a source voltage equal to the average voltage of the square wave input. By varying the duty cycle, the apparent output voltage can be made to vary from 0 volts to almost the full voltage of the supply.

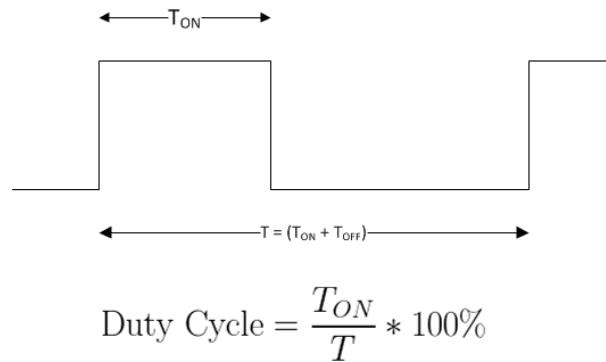


Figure 4.13: PWM

PWM, as it applies to motor control, is a way of delivering energy through a succession of pulses rather than a continuously varying (analog) signal. By increasing or decreasing the pulse width, the controller regulates energy flow to the motor. A simple comparator with a sawtooth carrier (chopping signal) can turn a sinusoidal command into a pulse-width modulated output. In general, the larger the command signals, the wider the pulse. Figure 4.14 shows the PWM output for a typical commanded signal. The output of a PWM amplifier is either zero or tied to the supply voltage, as the duty cycle changes to deliver more or less power, efficiency remains essentially constant.

Unlike a brushed DC motor where commutation happens in hardware, BLDC motor accomplishes commutation electronically using rotor position feedback to determine when to switch the current. Feedback usually entails an attached hall sensor or a rotary encoder. The stator windings work in conjunction with permanent magnets on the rotor to generate a nearly uniform flux density in the air gap. This permits the stator coils to be driven by a constant DC voltage (hence the name brushless DC), which simply switches from one stator coil to the next to generate an AC voltage waveform with a trapezoidal shape. Brushless DC motors use electric switches to realize current commutation, and thus continuously rotate the motor. These electric switches are usually connected in an H-bridge structure for a single-phase BLDC motor, and a three-phase bridge structure for a three-phase BLDC motor shown in Figure 4.15. Usually, the high-side switches are controlled using pulse-width modulation (PWM), which converts a DC voltage into a modulated voltage, which easily and efficiently limits the startup current, control speed and torque. Generally, raising the switching frequency increases PWM losses, though lowering the switching frequency limits the systems bandwidth and can raise the ripple current pulses to the points where they become destructive or shut down the BLDC motor driver.

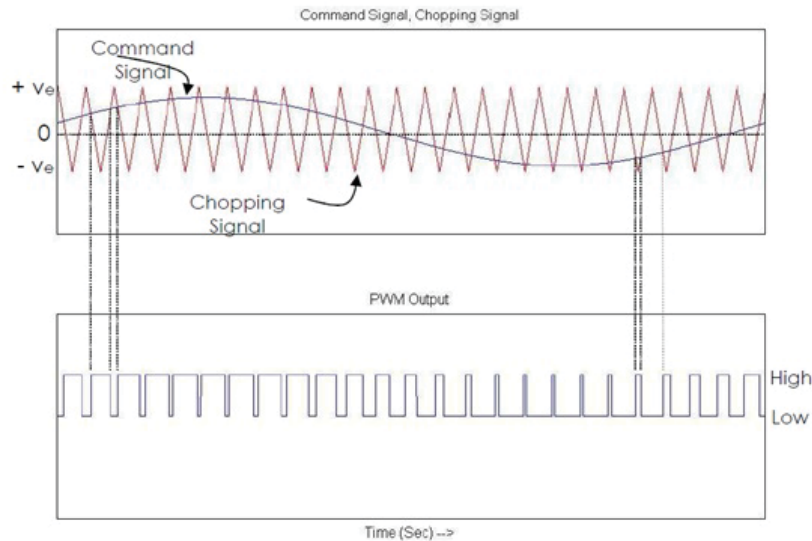


Figure 4.14: PWM output

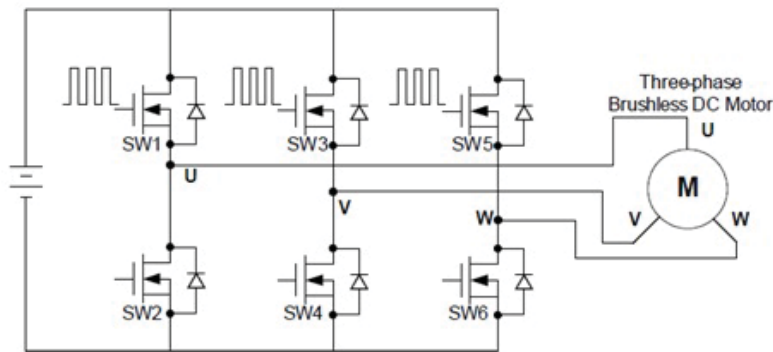


Figure 4.15: Three phase BLDC motor

Figure 4.16 is a simplified illustration of BLDC motor construction. A brushless motor is constructed with a permanent magnet rotor and wire wound stator poles. Electrical energy is converted to mechanical energy by the magnetic attractive forces between the permanent magnet rotor and a rotating magnetic field induced in the wound stator poles.

Here, three electromagnetic circuits are connected at a common point. Each electromagnetic circuit is split in the center, thereby permitting the permanent magnet rotor to move in the middle of the induced magnetic field. Most BLDC motors have a three-phase winding topology with star connection. A motor with this topology is driven by energizing two phases at a time. The static alignment shown in Figure 4.16, is that which would be realized by creating an electric current flow from terminal A to B, noted as path 1 on the schematic in Figure 4.15. The rotor can be made to rotate clockwise 60° from the A to B alignment by changing the current path to flow from terminal C to B, noted as path 2 on the schematic. The suggested magnetic alignment is used only for illustration purposes because it is easy to visualize. In practice, maximum torque is obtained when the permanent magnet rotor is 90° away from alignment with the stator magnetic field. The key to BLDC commutation is to sense the rotor position, then energize the phases that will produce the most amount of torque. The rotor travels 60° per commutation step. The appropriate stator current path is activated when the rotor is 120° from the alignment with the corresponding stator magnetic field, and then deactivated when the rotor is 60° from the alignment, at which time the next circuit is activated and the process repeats. Commutation for the rotor position, shown in Figure 4.16, would be at the completion of current path 2 and the beginning of current path 3 for clockwise rotation. Commutating the

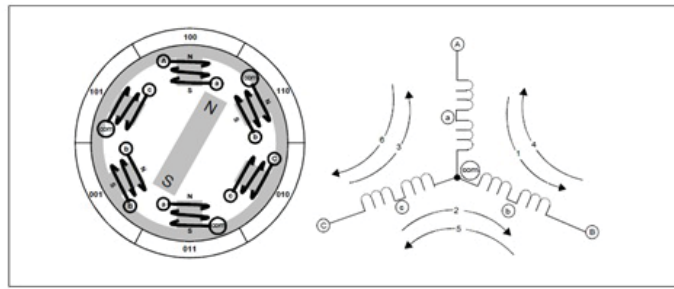


Figure 4.16: Simplified construction of three phase BLDC motor

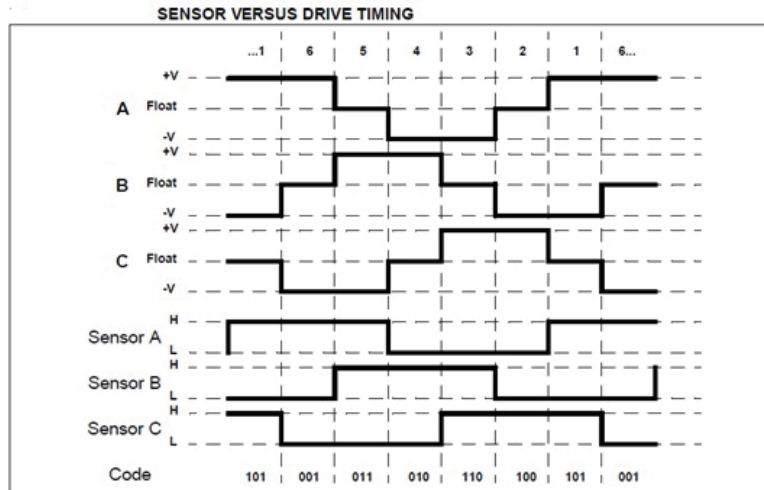


Figure 4.17: Timing diagram

electrical connections through the six possible combinations, numbered 1 through 6, at precisely the right moments will pull the rotor through one electrical revolution. In the simplified motor of Figure 4.16, one electrical revolution is the same as one mechanical revolution. In actual practice, BLDC motors have more than one of the electrical circuits shown, wired in parallel to each other, and a corresponding multi-pole permanent magnetic rotor. For two circuits there are two electrical revolutions per mechanical revolution, so for a two-circuit motor, each electrical commutation phase would cover 30° of mechanical rotation.

Each driver requires two pins, one for high drive and one for low drive, so six pins of PORTC will be used to control the six motor drive MOSFETS. Each sensor requires one pin, so three pins of PORTE will be used to read the current state of the motors three-output sensor. The sensor state will be linked to the drive state by using the sensor input code as a binary offset to the drive table index. The sensor states and motor drive states are derived from Figure 4.17 and Figure 4.18 respectively. Based on these, the direction of rotation can be specified. Figure 4.19 shows the motor control drive for a three phase BLDC motor.

Figure 4.16 provides the basic block diagram of BLDC motor driver. Control signals to the driver are generated based on the hall effect sensor input. Hall effect sensors outputs are continuously monitored during rotation. Motor current will be monitored through a current sense circuit.

4.6.1 Motor Drive Circuit

The functional requirements of this card is to give the necessary drive for the BLDC motors. The supply for the card is transferred from the OBC card through a connector. The PWM pulses generated for the independent motors are also transferred from the OBC card through a connector. Since the

CW SENSOR AND DRIVE BITS BY PHASE ORDER									
Pin	RE2	RE1	RE0	RC5	RC4	RC3	RC2	RC1	RC0
Phase	Sensor C	Sensor B	Sensor A	C High Drive	C Low Drive	B High Drive	B Low Drive	A High Drive	A Low Drive
1	1	0	1	0	0	0	1	1	0
2	1	0	0	1	0	0	1	0	0
3	1	1	0	1	0	0	0	0	1
4	0	1	0	0	0	1	0	0	1
5	0	1	1	0	1	1	0	0	0
6	0	0	1	0	1	0	0	1	0

Figure 4.18: Sensor states and motor drive states

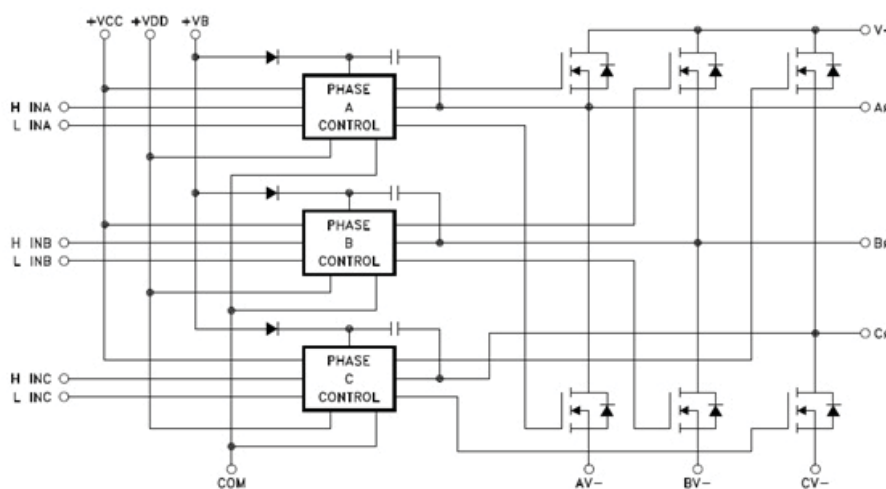


Figure 4.19: Motor control

card shall be controlled by both the PDU unit also, the PWM inputs are connected through buffers. At any given time, only one of the cards, either OBC or PDU card can control the legs of the rover. The necessary precaution of both the cards not controlling the motor movement have to be ensured. The schematics for controlling one phase of a BLDC motor is shown in Figure 4.20. the same is replicated for other two phases of the motor. The PWM lines from OBC are connected to the MOSFET gate. The current sense resistor is sensed using a $1\ \Omega$ resistor. When the motor current is more than 0.6A , the comparator output goes high. This circuit is used as the current limiter. A freewheeling diode is also provided to take care of the current spikes. Six such circuits are required to drive each motor in the rover. With BLDC motors, 3 such circuits are required by each motor, since these BLDC motors are of 3 phase. Current through MOSFET is sensed and fed back to the comparator which turns OFF these MOSFETS in case of excessive current.

4.7 Printed Circuit Board Design

Hardware is implemented using the guidelines for space onboard specifications including derating for reliability. Component placement and routing shall comply to space onboard PCB guidelines. Hardware shall be realized on a minimum space grade six layer PCB, shall consist of four signal layers, one power layer and one ground layer.

4.7.1 OBC card hardware

OBC Card is realized as a six layer MLB using High Tg FR4 (glass epoxy) material with board dimension of $130\text{mm}\times 120\text{mm}$. The overall thickness of the PCB is $2.0 \pm 0.15\text{mm}$. The design

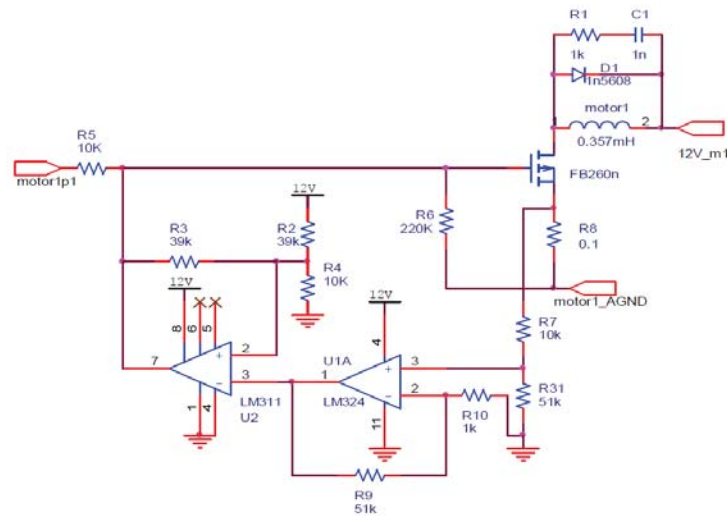


Figure 4.20: Motor drive schematics

comprises around 100 components of both actives and passives mounted on both the sides of the board. Component placement and routing have been carried out in compliance with space onboard PCB guidelines. All the ICs have been provided with decoupling capacitors as recommended for onboard design. The PCB layer stack-up definition is as follows.

1. Layer-1: Top component placement and signal routing
2. Layer-2: Ground plane
3. Layer-3: Signal routing
4. Layer-4: Signal routing
5. Layer-5: Split Power plane for 5V, 3.3V, 1.5V
6. Layer-6: Bottom component placement and signal routing

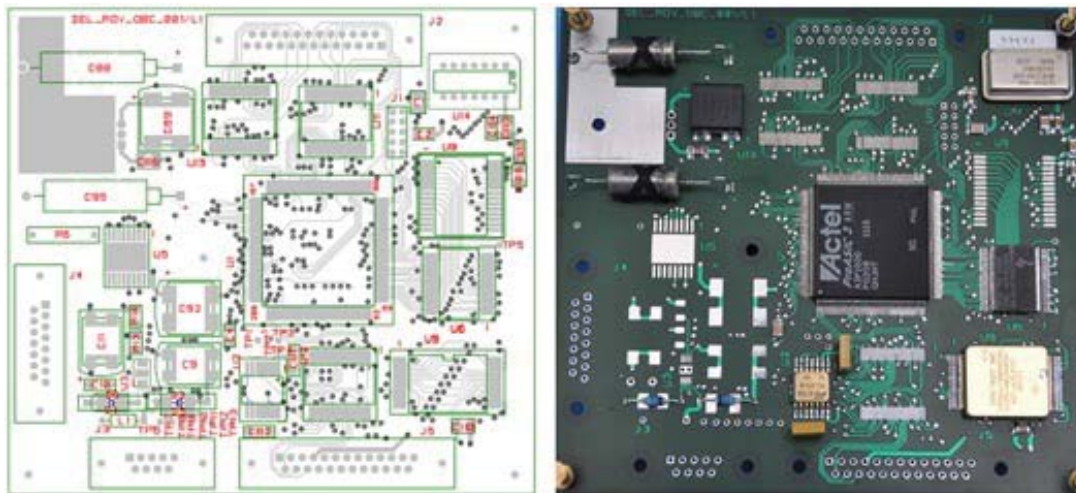


Figure 4.21: PCB layout and top view of the populated PCB of the OBC

The placement and routing can handle around 600 interconnections grouped as 10 bus channels of various widths. The routing topologies like orthogonal routing, memory routing, Daisy chain routing

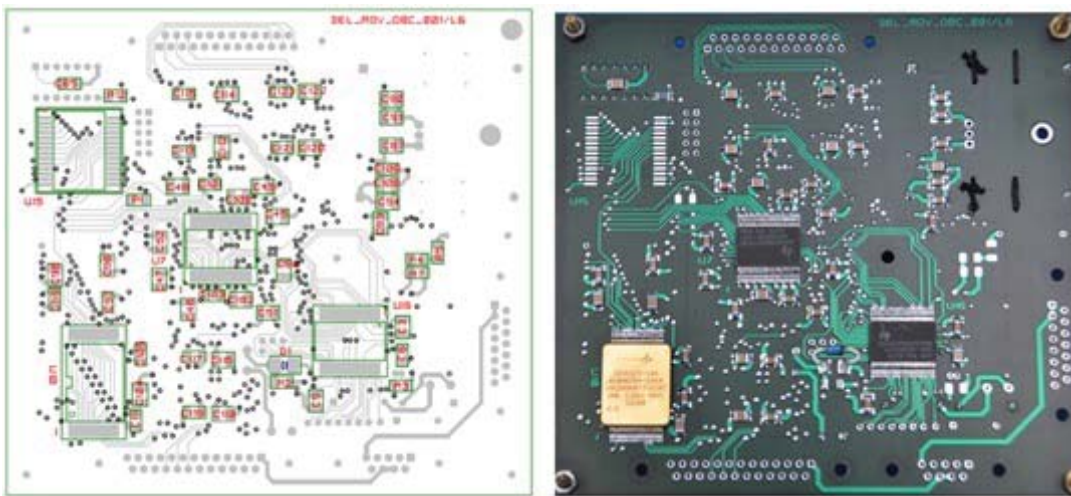


Figure 4.22: PCB layout and bottom view of the populated PCB of the OBC

for bus channels and Point to Point routing were implemented on the board for routing completion and for Signal/Power Integrity compliance. The ground plane and split power planes are designed for optimal power distribution and EMI/EMC compliance. The PCB layout, and top and bottom views of the OBC are shown in Figure 4.21 and Figure 4.22 respectively.

4.7.2 Motor Drive PCB

The motor card is realized using a 4-layer PCB. There are two signal layers and two power layers. This card also has connections from the OBC card for receiving the PWM pulses. There is a dedicated connector to send the hall effect pulses back to the OBC card. The layer stack-up definition is as follows.

1. Layer-1 Top component placement and signal routing
2. Layer-2 Ground plane
3. Layer-3 Power plane
4. Layer-4 Signal routing

The PCB layout, and top and bottom views of the motor driver are shown in Figure 4.23 and Figure 4.24 respectively.

4.8 Summary

This chapter dealt with designing and realizing the hardware (OBC and motor controller) for Nano Rover. The hardware has to be compliant with the mission and space qualification requirements. Therefore, we could not use any off-the-shelf available microprocessor kits.

This chapter began with specifying the hardware and mission requirements. The hardware design, specifically the ProASIC3 FPGA architecture and design were discussed in detail. The motor controller card for the brushed and brushless DC (BLDC) motors were design. The truth table for BLDC motors that specify how to operate the motors were also discussed. The PCB realization details of the OBC and motor controller card were explained. Particularly, we chose 6 layer card for the OBC card and 4 layer board for the motor controller card. This chapter followed the standard procedure for design any space qualified hardware beginning from the requirement gathering phase to the realization phase.

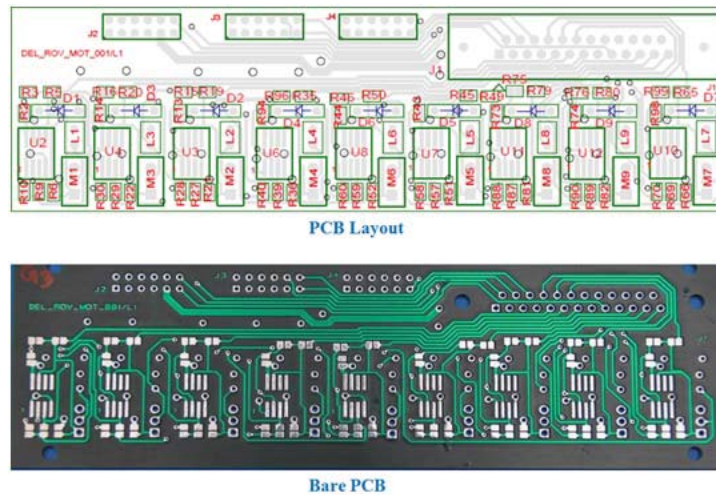


Figure 4.23: PCB layout and top view of the motor card

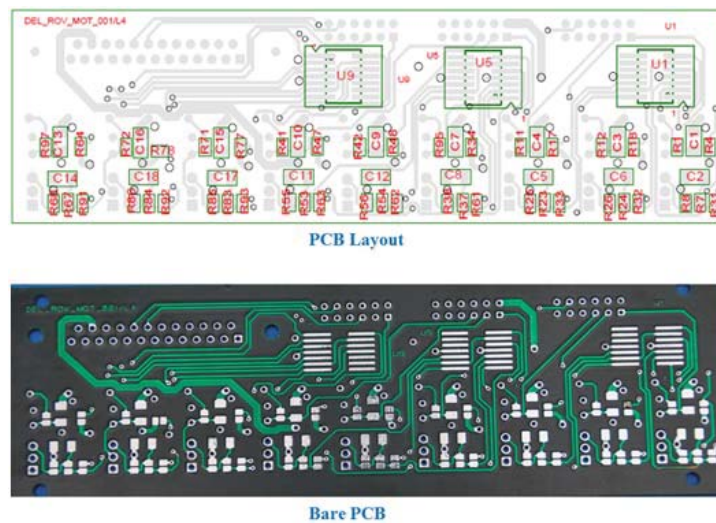


Figure 4.24: PCB layout and bottom view of the motor card

5.1 Introduction

In the previous chapter, we designed and developed a space-qualified OBC and motor controller card. The software and algorithms for the mission goals, i.e., OBC scheduler and locomotion, need to be designed and developed. This chapter caters to this need. To begin with, we analyzed the existing Zebro locomotion algorithm. A major limitation of this algorithm is the synchronization of the individual motors as this causes a jerky movement of the rover. Therefore, we overcame this limitation through a novel ring-counter based algorithm. The design and implementation of this algorithm are discussed here.

The overall software for the OBC card is written in VHDL and C. The glue logic and the IP core modules are connected using a hierarchical structure. The tool used for implementation of the VHDL coding is the Libero SoC Design Suite [20]. This tool has been recommended by the FPGA manufacturer as it offers high productivity with its comprehensive, easy-to-learn, easy-to-adopt development tools for designing with M1 ProASIC FPGA. The suite integrates the industry standard Synopsys Synplify Pro synthesis and Mentor Graphics ModelSim simulation with the best-in-class constraints management, power analysis, timing analysis, and push button design flow. An integrated development environment from IAR Systems for compiling and debugging embedded ARM applications using assembly, C and C++ is used for development of hardware.

5.1.1 Why not Operating System(OS)?

The entire system has been developed using a combination of hardware and software. An operating system like linux could have been used. OS does not guarantee real time operations, the speed of the motor is around 27000 rpm [28], it is very difficult to count the hall sensor pulses at this rate in a real time without the help of hardware. Hence, the reading of hall sensor pulses are counted using a hardware counter in VHDL language. Since the rpm of the leg is very low compared to the motor the outer envelop is controlled by software.

The scheduler software and the locomotion algorithm has been developed in C. MicroSemi offers a utility called Soft Console which has been used for downloading the executable into the PROM inside the OBC card. The software is a scheduler based design where each function is serviced systematically. The primary function of the locomotion software is to move the legs of Nano Rover. The leg position for Nano Rover is shown in Figure 5.1.

The legs are connected to the motors. The legs of M1, M3, M5 move together and legs of M2, M4, M6 move together. For forward movement, motors M1, M3, M5 are turned ON and after a delay

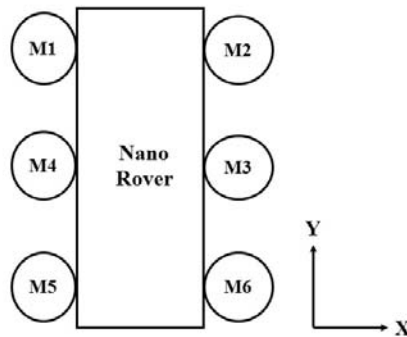


Figure 5.1: Leg positions

the motors M2, M4 and M6 are turned ON. The actual movement happens when all the motors are moving. Hence the overlap between the motors determines the distance travelled by the rover. The design is PWM based pulse control for controlling the movement of the individual motors. Locomotion module of the flight software ensures proper pulse shaping of the waveform which is fed to the motors to perform desired locomotive maneuvers. Switching on and off of the motors and synchronization among all the legs is done by referring to a hall effect sensor feedback mechanism. Control parameters for the locomotion software are the PWM duty ratios to control the speed of different motors, and the delay counter values which decide for how long the motors continue to run.

5.2 Software requirements

We follow the ISRO's standard practices for software development, which is similar to the standard software development lifecycle [26]. The mandatory requirements for the software are listed below. The locomotion algorithm is a module and shall be called by the main function of the OBC software whenever a need arises for locomotion. The requirements are listed for the FPGA design using VHDL as well as the software for OBC in C.

5.2.1 Functional Requirement for VHDL

1. Cortex M1 IP core shall be used as the main ARM processor [25].
2. The design shall be modular.
3. Provision for expandability shall be provided in the design.
4. Decoding logic and control signal generation for RAM and ROM.
5. IO Decoding Logic for control of peripherals which include power ON/OFF, motor ON/OFF, Payload Data Unit(PDU) ON/OFF.
6. Generation of control signals to read power good, hall sensors and PDU units. Generation of direction and output enable for bidirectional buffers/level translator.
7. Shall take clock input and generate suitable timing signals for each of the module.
8. Shall take reset pulse from reset generator circuit and generate a reset signal to bring all modules to a default condition.
9. Timing signals shall be generated suited to the locomotive algorithm to coordinate the movement of all legs.

10. Generate appropriate control signals to hand over control to the PDU and gain control from PDU.

5.2.2 Functional Requirements for C

1. Shall be modular.
2. Shall be layered architecture.
3. Software shall be written using C language.
4. The compiled hex file shall reside in the PROM.
5. Care shall be taken to maintain data integrity in the SRAM area using proper mitigation techniques like TMR or error correction.
6. The software shall be mode based.
7. The software shall be cyclometric. There shall be a determined number of linear independent paths.
8. All the events shall be time multiplexed onboard coding guidelines shall be followed.
9. The timing for the events shall be generated by the hardware. Care shall be taken to complete each event within a stipulated time.
10. Care shall be taken to avoid event collision.
11. All the events shall be serviced periodically.
12. There shall be a clear entry and exit point for each module.
13. Care shall be taken that the software should never enter into an endless loop or hang state.
14. Watch Dog Timer (WDT) functionality shall be implemented to ensure that the system comes to a known default state in case of any software hang ups.

5.2.3 Mission Requirements

1. The Nano Rover shall have a mechanism to descend down from the lander.
2. The software shall have independent telecommand and telemetry requirements and in the absence of TC and TM, autonomy features for the mission operations shall be available.
3. The Nano Rover shall be operated based on the power availability.
4. The minimum mission life is one lunar day which is approximately 15 earth days.

5.3 Data Mitigation Techniques

Since the space environment comprises of high energy charged particles which might bombard onto any spacecraft thereby creating single event upsets and in severe cases even burnouts, it is prudent to have redundant variables for important parameters which are stored in different regions of the memory onboard. The data shall be protected with suitable mitigation techniques. Two techniques are practiced in the space systems for data protection.

1. Error Correction Codes
2. Triple Modular Redundancy

5.3.1 Error correcting codes

Error correcting codes are block codes in which parity bits are appended after the information bits while storing the data in the memory. The written data is read back and suitable decoding is done to read the data back. Hamming codes are the most popular error correcting code used. This code has an error correcting single bit errors and detecting two bit errors. Hamming codes are a family of linear error-correcting codes. Hamming codes can detect up to two-bit errors or correct one-bit errors without detection of uncorrected errors. By contrast, the simple parity code cannot correct errors, and can detect only an odd number of bits in error. Hamming codes are perfect codes, that is, they achieve the highest possible rate for codes with their block length and minimum distance of 3. In mathematical terms, Hamming codes are a class of binary linear codes. For each integer there is a code with block length $n = 2r - 1$ and message length $k = 2r - r - 1$. Hence the rate of Hamming codes is $R = k/n = 1 - r/(2r - 1)$, which is highest possible for codes with minimum distance 3 (i.e. the minimal number of bit changes needed to go from any code word to any other code word is 3) and block length $2r - 1$. Due to the limited redundancy that Hamming codes add to the data, they can only detect and correct errors when the error rate is low. This is the case in computer memory, where bit errors are extremely rare and Hamming codes are widely used. In this context, an extended Hamming code having one extra parity bit is often used. Extended Hamming codes achieve a Hamming distance of 4, which allows the decoder to distinguish between when at most one-bit error occurred and when two bit errors occurred. In this sense, extended Hamming codes are single-error correcting and double-error detecting, abbreviated as SECDED. Parity adds a single bit that indicates whether the number of 1 bits in the preceding data was even or odd. If an odd number of bits is changed in transmission, the message will change parity and the error can be detected at this point. The most common convention is that a parity value of 1 indicates that there is an odd number of ones in the data, and a parity value of 0 indicates that there is an even number of ones. If the number of bits changed is even, the check bit will be valid and the error will not be detected. Moreover, parity does not indicate which bit contained the error, even when it can detect it. The data must be discarded entirely and re-transmitted from scratch. On a noisy transmission medium, a successful transmission could take a long time or may never occur. However, while the quality of parity checking is poor, since it uses only a single bit, this method results in the least overhead.

5.3.2 Triple Modular Redundancy (TMR)

TMR logic is used as primarily for protecting data. The concept of TMR is to store each data in different locations. For memory write operations, the data is written into 3 different locations. For memory read operations, the data is read from all the 3 different locations. Majority Voting Logic is applied to these read variables and then the value is updated again in the specified 3 locations. Normally in the absence of any error, all the 3 values shall be the same. In case of any data corruption, the values will differ. Any 2 values if matched shall be taken as the valid data. The third location which has error shall be updated with the corrected data. This is explained below: The variables are assigned to 3 locations. If the data read is X,Y,Y, then the actual variable is assigned the value of Y. If the data is read as X,X,Y or X,Y,X, then the variable is assigned as X. If the data is read as X,Y,Z, then it indicates that the entire data is corrupted and an error is reported. TMR is implemented in the Nano Rover by assigning all the variables in the form of a 3-element array, ideally all of which should be identical. All variables are stored or read back from 3 arrays. Majority Voting Logic (MVL) is applied to take the value of variables of which at least 2 are identical. The third variable (which should have been the same but has been corrupted due to SEU) is stored with the correct variable. Whenever a variable is to be used, the value stored in at least two of the array locations is used and in case of SEUs, the third location is overwritten with the correct value. Data scrubbing is an error correction technique which uses a background task that periodically inspects memory for errors, and then corrects the error using a copy of the data. It reduces the likelihood that single correctable errors will accumulate; thus, reducing the risk of uncorrectable errors. Due to the high integration density of contemporary computer memory chips, the individual memory cell structures became small enough to

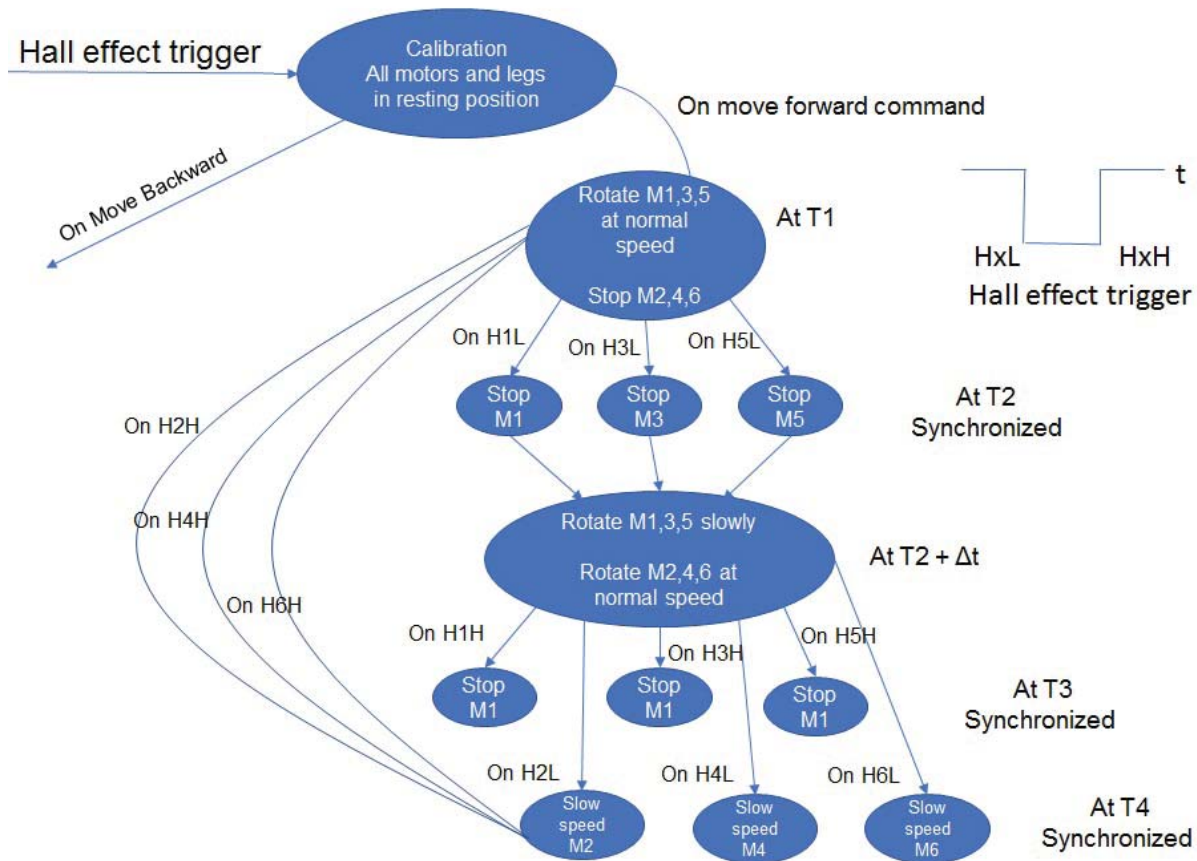


Figure 5.2: Flow chart of existing algorithm

be vulnerable to cosmic rays and/or alpha particle emission. The errors caused by these phenomena are called soft errors. This can be a problem for DRAM and SRAM based memories. Also, memory marching is scheduled periodically to ensure the repetitive reads and writes in the memory locations prevent them from any form of degradation. This is called SCRUBBING and is done periodically for all the variables. Memory scrubbing does error-detection and correction of bit errors in RAM. Since there is a single RAM used, the Hamming code for error correction is not used. Only TMR and regular scrubbing of the SRAM variables have been used in this Nano Rover. The look up tables are stored in 3 different arrays with an offset of 256 location search. While writing data to memory, the base address pointer stores the variable in the first array. The offset of 256 is added to the base address and this becomes the pointer for the storing of the variable in the second array. The base address is then added with an offset of 512 and the variable is stored in the 3rd array. While reading back, the first array is read. The second array is read with an offset of 256 and the 3rd array is read with an offset of 512. Majority voting Logic is then applied to the read variables and the variable is then used for the operations. In addition to this, the OBC scheduler periodically does the data scrubbing for the entire RAM area.

5.4 Existing Zebro Locomotion Algorithm

The state diagram of the existing Zebro locomotion [9] is shown in Figure 5.2. The initial position is calibrated for all the legs in resting position. On getting the command, the motors start running. Two motors on one side and one motor on the centre of the opposite side are moved together. In the existing design HxH and HxL indicate the leading edge and falling edge of the hall pulses. As the magnet comes into the vicinity of the hall effect sensor the low edge trigger is observed, when the

magnet leaves the hall effect sensor the signal goes high indicating one revolution. The motor number is indicated by x. 6 such pulses will be observed for the individual motors. In the existing design when HxL goes low for one set of motors the other set of motors are initiated. The rover moves during the overlap period. When HxH is reached the first set of motors are stopped and the cycle repeats till the intended distance is reached. In case of one of the motors in a set arrives later or sooner there will be a jerk in the rover movement. This is due to the non synchronization among the motors of the set. This is overcome in the new algorithm presented in the following sections.

The existing design in the Zebro Lite is based on synchronization of the 3 motors at a time. Provision does not exist to change the single motor control within the 3 motors. For example, if legs 1,3,5 move synchronized and legs 2,4,6 move synchronized, and for some reason the leg 3 is slower than leg 1 and 5, the algorithm does not have a way to speed up leg 3 by extending the drive to leg 3 to move in tandem along with its group of 1 and 5. This might cause a jerk in the movement of the rover. The proposed algorithm which has been implemented takes care of this and provides independent control of the legs to provide smoother movement amongst the legs.

In the rest of the chapter, we describe our novel ring-counter based Nano Rover locomotion algorithm.

5.5 Design for a novel, synchronous motor control in software

The new synchronized motor control algorithm for the Nano Rover is shown in Figure 5.3. The algorithm is modular in nature. The detailed design is explained later in this chapter. The motors M1, M3, M5 are moved together and motors M2, M4, M6 are moved together. The earlier algorithm does not have provision to synchronize among the motors of the same group. The modified algorithm has implemented a ring counter based hall sensing detector module wherein any motor of a group which is lagging or leading among themselves can also be individually controlled by controlling the PWM pulses of the independent motors thereby maintaining the movements less jerky. This algorithm has been successfully tested on the lunar terrain also and the results are presented in the next chapter. Figure 5.3 can be explained with the help of the following points:

1. Initially, motors 1,3,5 (the first set) are operated till they finish one rotation each.
2. The legs are stopped as soon as the hall pulse for corresponding legs is triggered.
3. The program waits for the last hall sensor pulse from this set to move on to the next phase of operation.
4. On receiving the last pulse of the set, all six legs are operated which constitutes the overlap region where the linear motion of the rover happens.
5. The time for this overlap interval is set by a counter value in a delay variable. The value is decremented in every loop and finally the movement is stopped when the variable becomes 0.
6. After this, the first set of motors is stopped (1,3,5) and the other set continues on with its full rotation and similar steps are repeated over time till the master counter becomes 0 signaling end of locomotion.

5.6 Locomotion software architecture

The software is defined as individual modules. A layered structural design is used for the design implementation. Each module takes an input, processes the input and passes as parameters to the next module. The advantage of this design is that change of one parameter in any module does not have an impact in the overall software design and is restricted to that particular module alone.

- Depending on the required torque and distance to be travelled, speed 's' is calculated.
- During rotation, motors rotate at speed 's' and during movement, 3 motors rotate at speed 's/k'
- In every loop, values of $\Delta Vx1$, $\Delta Vx2$ may change depending on motor speed

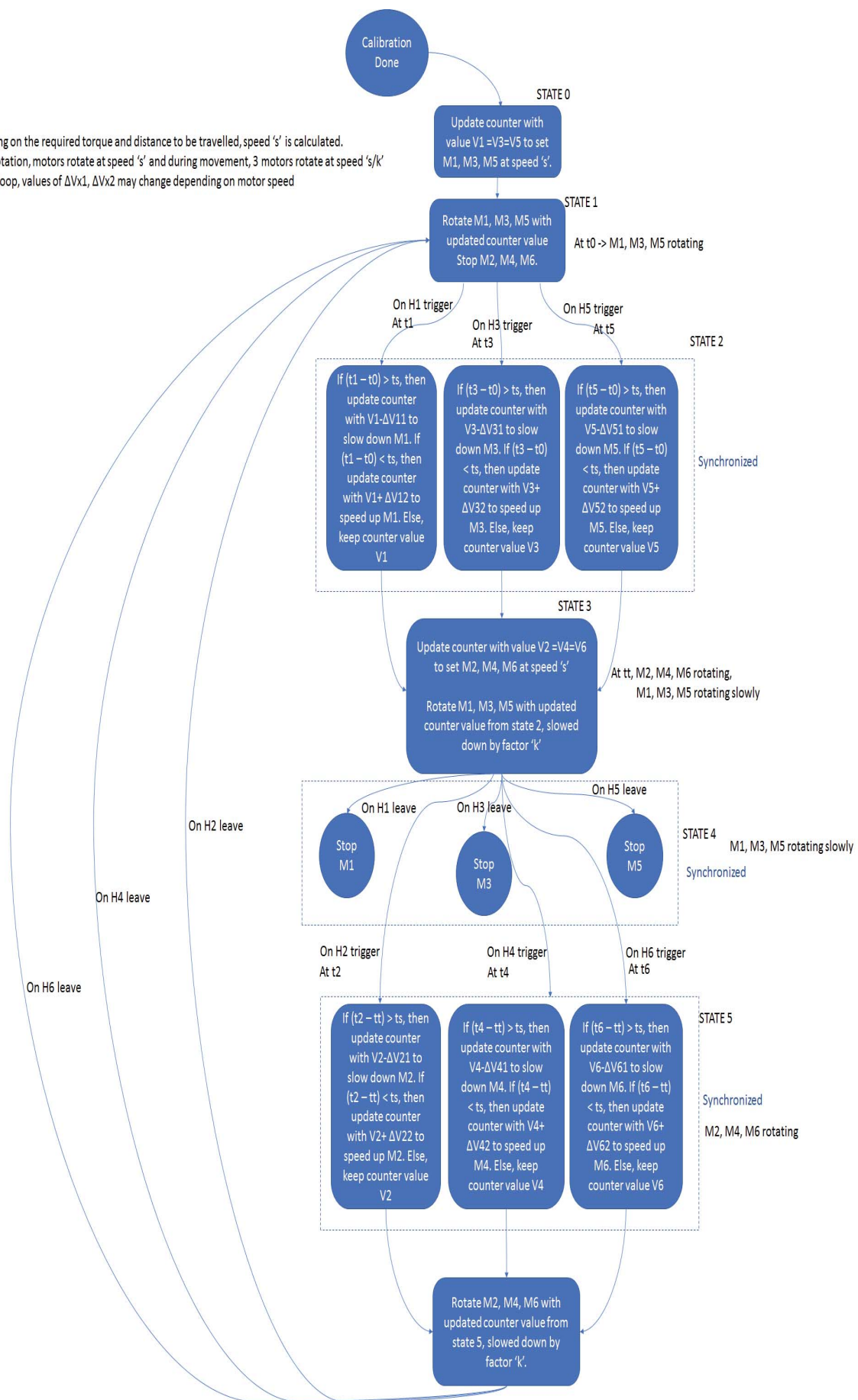


Figure 5.3: Software flow chart

5.6.1 Application layer (Layer6)

Selecting motor and leg is done in this module. The choice of motors is limited to DC motors and BLDC motors. The different types of leg diameter and shapes are also taken as inputs. The choice can also be hardcoded in the viable area and can be made as design specific. The selection of legs decides the proportionality constant between the motor rpm and translational speed of the rover. The choice of motors influences the VHDL scheme and the hardware architecture implementation. The number of hall sensor inputs and the number of output PWM lines is determined by the motor selection. The BLDC motors require 24 hall sensor input lines and 18 PWM output lines, compared to 6 inputs and 6 outputs required in the case of DC motors.

5.6.2 Autonomy or Command Decoding Layer (Layer5)

The choice in this layer decides whether the locomotion is fully based on autonomy or whether any commands are expected from ground. The current Nano rover software does not expect any command from ground. The locomotion algorithm is invoked based on the availability of the power good signal. If the power is available, the sequence of operation which is described in the next section shall be followed. This layer accepts the commands for the locomotion algorithm to function and derives required parameters like the rpm of legs and duty ratio of the PWM. The commands expected in this layer are: 1. Direction of movement, i.e. forward, reverse, left and right. 2. Speed of motion 3. Distance to be covered

5.6.3 Synchronization Layer (Layer4)

The synchronization of the group of motors is addressed in this layer. Motors M1, M3, M5 move together and the motors M2, M4, M6 move together. The distance moved by the rover is determined by the amount of overlap in the motor sets. This module adjusts the overlap timing of the motor sets. This layer is for synchronizing the wheels to ensure proper stability and movement of the rover. This layer includes both the initial synchronization which is carried out in the very beginning after the rover starts operating after the first power good signal and the synchronization which happens between the legs of the same set 1,3,5 or 2,4,6 during the movement of rover.

5.6.4 Individual Motor Control (Layer3)

This layer takes care of the synchronization of the individual motors within a set. This layer comprises of a PD controller to set the duty ratio of legs among a set to ensure that 3 legs moving at a time are always synchronised. This synchronization might get disturbed due to external imbalances like loose soil or boulders in the way of the rover. The PD controller ensures that in case the legs go out of sync, the adjustment of rotations per minute(rpm) via duty ratio of the PWM brings back all the legs of a set to an identical position. The normal arrival of a motor in the set is monitored as a counter value. If all the motors move in synchronism, the hall sensors will arrive at the same count value. In case of lag or lead of any motor, the count at which the hall pulses arrive shall vary. If the count is less, then it means that the particular motor has moved faster and the width of the PWM is decreased. If the count value of the motor is more than the expected value that indicates that the motor has moved slower than expected and the corresponding PWM value is increased.

5.6.5 PWM Generation Layer (Layer2)

This layer generates the envelope for the leg movement. The values are stored in an array as a look up table. The array contains 128 elements. TMR is provided for all the variables. The nominal speed is taken as the centre element of the array. The arrival of the pulses in the estimated speed is stored as the centre of the array. The read count is used as the pointer to the array. Depending upon the

count at which each motor has arrived, the array pointer is used to either increase or decrease the PWM width of the motor. Each motor has an independent array. This layer deals with generating the pulse width modulated signal for running the motors. The commands obtained in layer 5 are used to derive the duty ratios and timing signals to generate the required PWMs to run the motors. Also, the time for which the PWM is expected to be generated is calculated from the commands received.

5.6.6 Physical Layer (Layer1 - Motor Drive Electronics)

This layer has the actual hardware call routine where the count is translated as a PWM signal and is output to the individual motor. This layer is also responsible for reading the hall sensor output of the motors which goes as a corresponding count value to the synchronization layer. This layer is programmed in VHDL and decides the configuration of the OBC card including the number of input and output pins, the number of timers, counters and I2C and UART interfaces defined. A detailed description of this is made earlier in Chapter 4.

5.7 VHDL software design

The software for connecting the various IP cores are written using the VHDL code. Figure 5.4 illustrates the overall system design flow, including both hardware and software development. The following are the tasks carried out in Libero SoC.

1. Generate HDL and testbench files using create smart design.
2. Simulate VHDL behavioral, post-synthesis and post-layout designs with ModelSim.
3. Assign IO ports, package pins and view package layout using IO editor.
4. Apply timing constraints like clock, set-up and hold.
5. Synthesize and optimize the HDL using Synplify Pro.
6. Perform place and route and timing analysis.

The top module design encompasses all the IP cores. The connectivity is given by proper signal assignment across the modules. The timing analysis and logical verification has been performed. The design file is downloaded into the ProAsic FPGA. The registers inside the FPGA are also provided with TMR logic.

5.7.1 OBC Scheduler

The OBC scheduler software is written in C. The fundamental objective of the OBC software is to allocate time periodically to all the functionalities. It shall take care of the smooth change over of the OBC to the PDU. The scheduler shall start only after the detection of the power good signal. This signal ensures that adequate power is available for the Rover operations. The software is mode based and is invoked only after the verification of the power good signal. There are 4 modes of operation envisaged for the mission.

- Mode1: Locomotion
- Mode2: PDU Operations
- Mode3: Communication
- Mode4: Battery Charge Enable mode.

The modes will be active only if power good is available. The mode diagram is shown in Figure 5.6. The total duration is limited to 5 minutes.

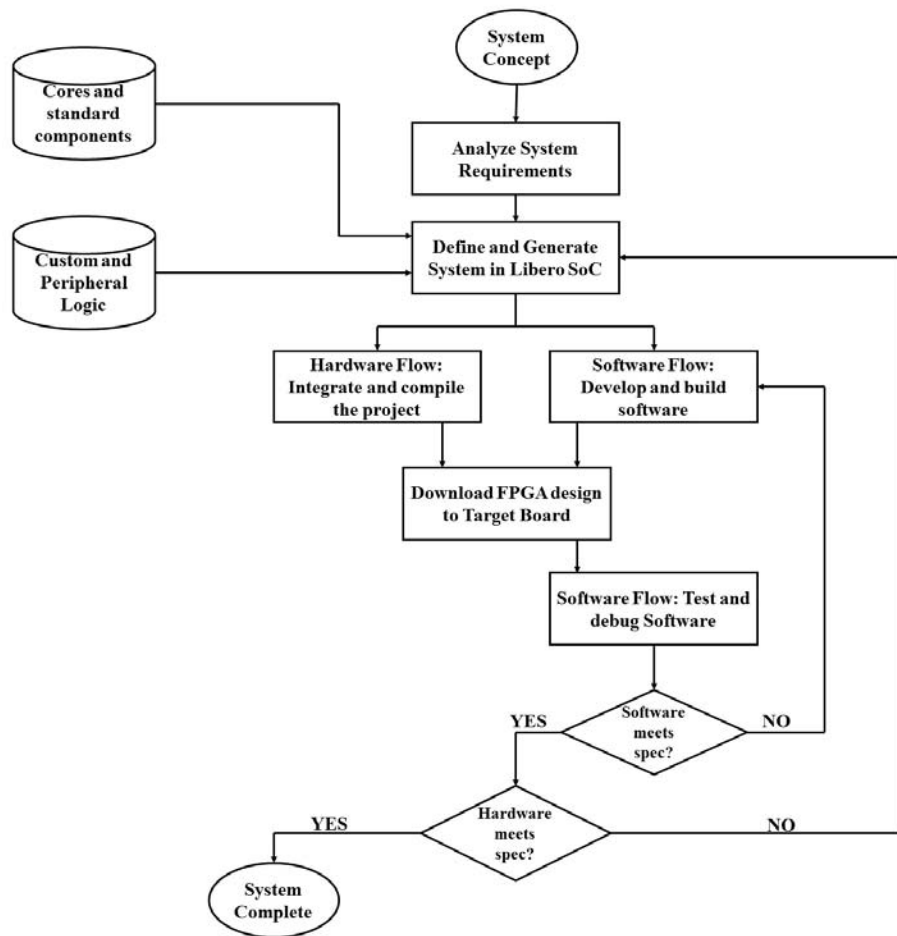


Figure 5.4: VHDL design flow

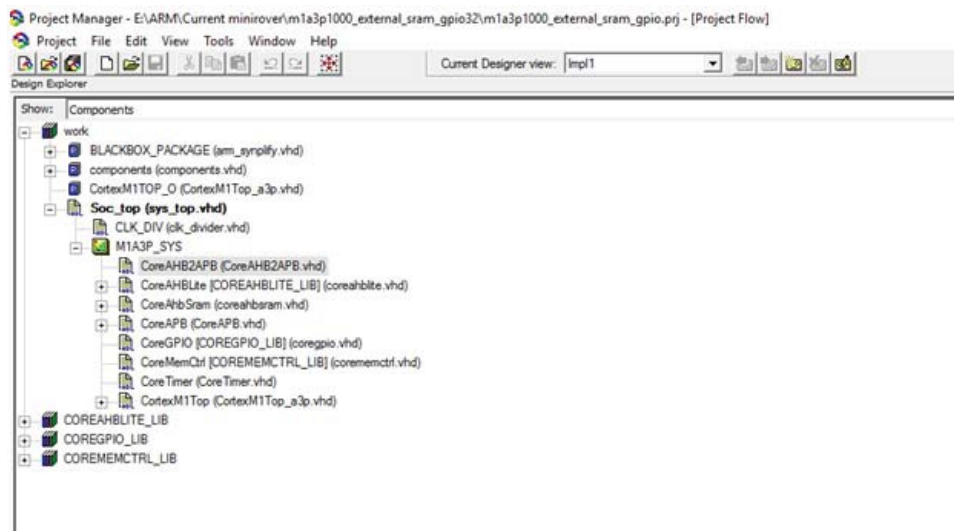


Figure 5.5: hierarchy

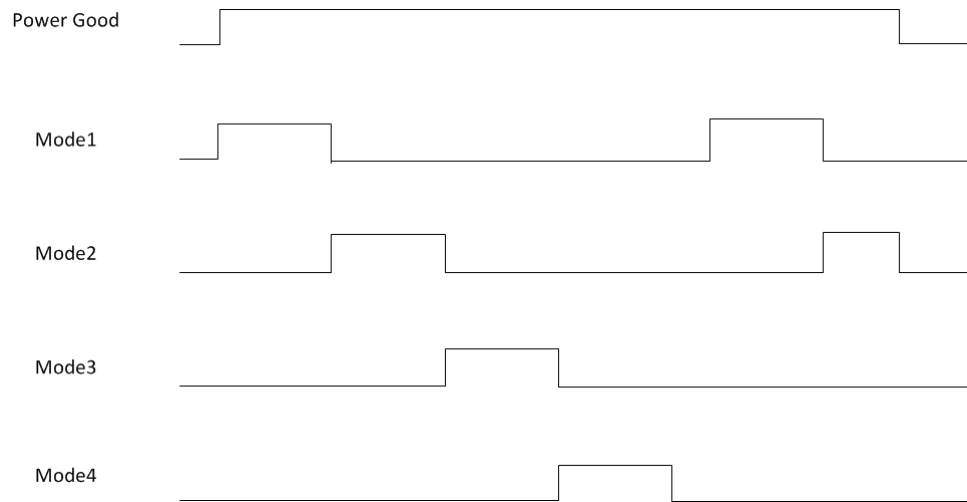


Figure 5.6: Mode diagram

Algorithm 1 OBC Scheduler

```

Function main()
loop
  while not  $P_G$  do
    nop
  end while
  if  $P_G$  then
    call mode ( $m$ )
  end if
end loop

```

Algorithm 2 Modes

```

Function mode (Mode  $m$ )
if  $m == \text{Mode1}$  then
  call locomotion ()
else if  $m == \text{Mode2}$  then
  call PDUOperations ()
else if  $m == \text{Mode3}$  then
  call communicate ()
else if  $m == \text{Mode4}$  then
  call recharge_battery ()
end if

```

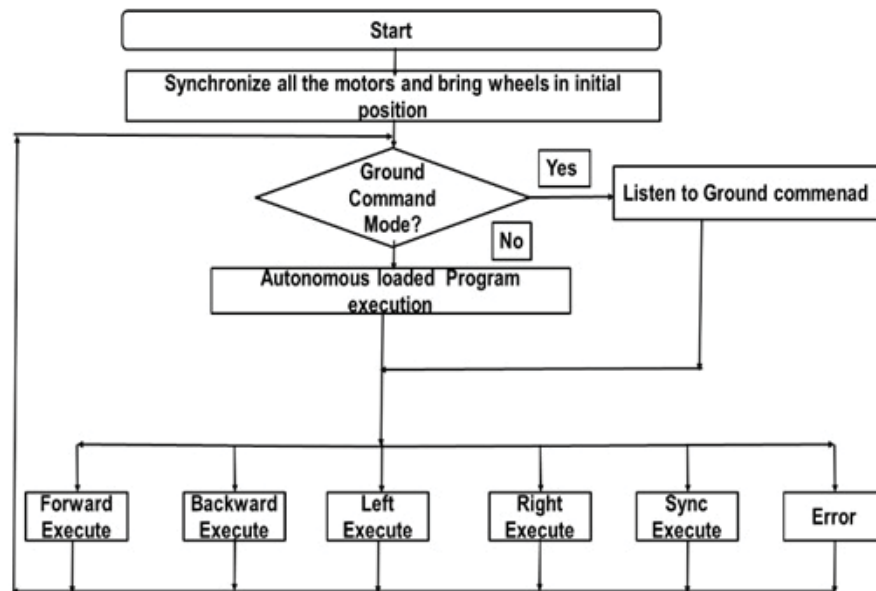


Figure 5.7: Top level abstraction

5.7.2 Locomotion software design

The software runs an initialization routine to bring all the legs to a predetermined position. Then it derives the speed and the execution time values either from the ground command or autonomous program execution. An outer counter is loaded with a fixed count value based on the distance or time. Based on the speed and time the required number of revolution per minute (rpm) is computed and accordingly PWM envelope is generated to control the speed of motors. The locomotion algorithm dynamically controls the PWM envelope and phase lags to ensure stability of the rover on different types of moon terrains. The hardware software interactions shall be tightly coupled. The address and control signals for reading and writing into the memory and IO area shall be provided by the hardware.

Top Level Abstraction

The direction of movement and the speed or the distance to be covered are the parameters derived in this module. The inputs might be either from the autonomy which is decided by the OBC Scheduler or from the ground commands received from the OBC.

Medium level abstraction

The overlap duration which determines the speed at which the legs shall move is calculated. The initial duty ratio at which all the legs shall be moved is also calculated. A look up table is generated based on the minimum value which can be updated for the synchronization of the individual motor group.

Low level abstraction

The generation of the PWM envelop is generated in his layer. This is the layer that interacts with the hardware. The motor is controlled by the PWM pulses through the GPIOs. The hall effect pulses are also read through the hardware pins and converted into a count from which the next duty cycle value shall be calculated

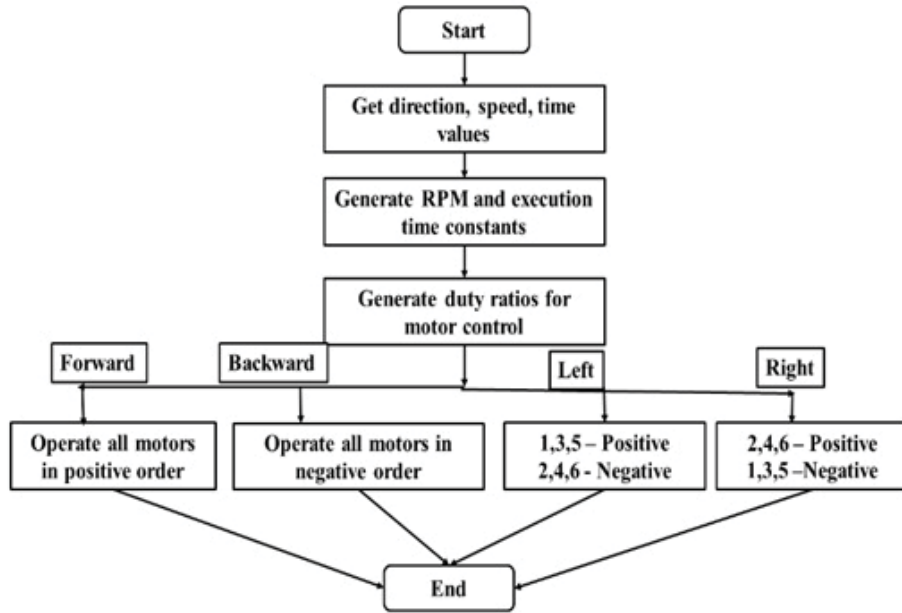


Figure 5.8: Medium level abstraction

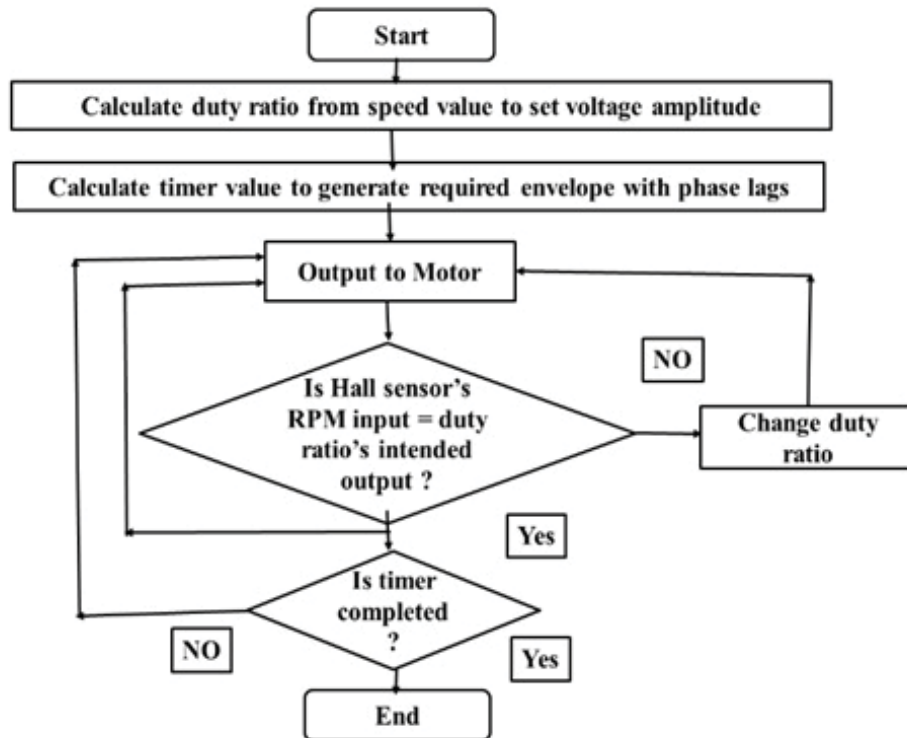


Figure 5.9: Low level abstraction

5.7.3 Operating sequence of the software

1. Outer Counter takes command/autonomy to decide the distance or time to be moved.
2. The software starts a counter which indicates the fixed count value based on the distance or time.
3. This gets translated into number of rpm i.e. expected number of hall sensor pulses.
4. The motor starts moving together initially at a constant envelop. The rpm Mx counter counts the no. of hall pulses for each motor and correlates with the final expected count.
5. If all the 3 legs are moving in perfect synchronization, all hall effect sensors will arrive at the same count value.
6. Assuming, M1 is arriving on time, the envelope of M1 PWM remains constant.
7. Assuming M3 is arriving late, the PWM envelope gets extended, i.e. more voltage is applied to speed up M3.
8. Assuming M5 is arriving early, the PWM envelope gets shortened, i.e. less voltage is applied to slow down M5.
9. Every time, the hall effect output is sensed, the number or rpm counter is incremented. When the terminal count is reached, it is understood that the intended distance has been traveled. The timing engine gets disabled waiting for the next command to initiate locomotion again.

5.8 Software modules

The software modules are as follows.

5.8.1 Main module

The software runs an initialization routine to bring all the legs to a predetermined position. Then it derives the speed and the execution time values either from the ground command or autonomous program execution. An outer counter is loaded with a fixed count value based on the distance or time. Based on the speed and time the required number of rpm is computed and accordingly PWM envelope is generated to control the speed of motors. The locomotion algorithm dynamically controls the PWM envelope and phase lags to ensure stability of the rover on different types of moon terrains.

5.8.2 Initialization module

The main purpose of initialization algorithm is to bring all the legs initially to a pre-determined position. The legs carry a powerful magnet which develops a digital signal when they come to the vicinity of the hall sensor. On the receipt of the first pulse from the hall sensor a timer which is loaded with a count corresponding to the desired initial position is triggered. On completion of this timer the leg movement is stopped thereby ensuring that the leg is at the pre-determined position. This exercise is repeated for all the legs.

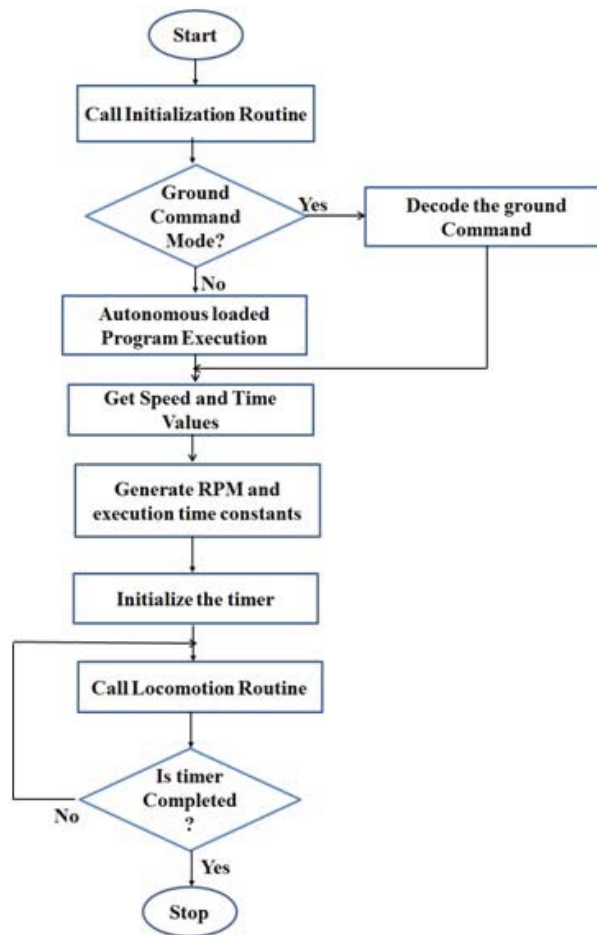


Figure 5.10: Main module

5.8.3 Linear motion (forward and reverse) module

Locomotion algorithm of the rover software ensures proper pulse shaping of the waveform which is fed to the motors. Switching on and off of the motors and synchronization among all the legs is done by referring to a hall effect sensor feedback mechanism. The duty ratio of the PWM waveform determines the speed of the motor. Higher duty ratio ensures higher rpm of the corresponding motor. For maintaining balance of the rover and stability, legs 1,3,5 and 2,4,6 and operated using two identical PWM waveforms with a predetermined phase difference as shown in the Figure ??.

The value $T_{on}/(T_{on} + T_{off})$ gives the duty ratio and sets the speed of the rover. The phase difference between the motors is generated by the delay values which are stored in the timer registers

5.8.4 PWM generator module

The motors are operated over repetitive cycles until the master timer which controls the execution time goes off. Within each cycle the two sets of motors are operated in a sequential manner consisting of four states as follows.

- S1 : PWM output only to Motors 1,3,5
- S2 : PWM output to Motors 1,3,5 and 2,4,6
- S3 : PWM output only to Motors 2,4,6

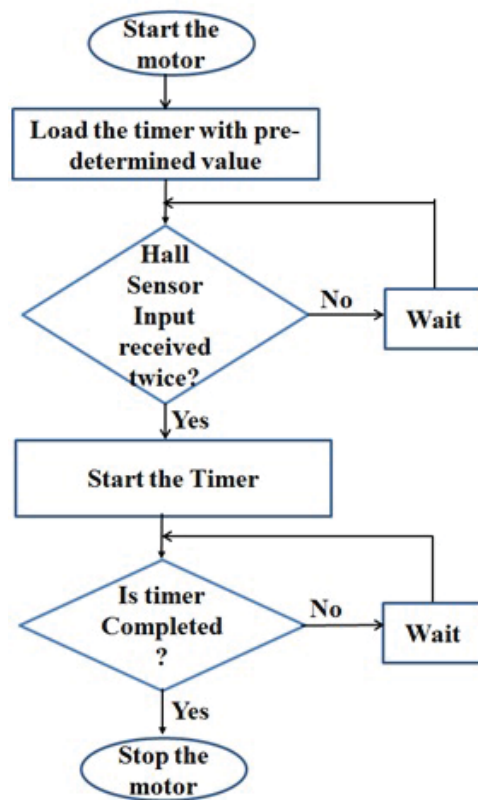


Figure 5.11: Initialization routine

- S4 : No PWM to any motor

During S2 when all the motors receive the PWM output the rover moves forward.

5.8.5 Synchronization module

To ensure the stability of the rover it is necessary that all the legs move in synchronization and hence all motors are fed with the same PWM output initially. However, depending on the surface properties encountered by a particular leg its speed might increase or decrease for the same PWM input. For example, a slope might accelerate the leg movement whereas loose soil might retard the movement. To compensate for this, the speed of the motors is monitored continuously with the help of hall sensor pulses and accordingly the duty ratio of the PWM output to different legs are dynamically adjusted to bring in the synchronization among all the legs. Figure 5.13 shows how the synchronization is achieved by changing the duty ratio of the PWM output with respect to the speed measured by hall sensor pulses.

5.8.6 Switching between forward and reverse motion

The motor driver circuit comprises of an H-bridge inverter which controls the direction of current flow through the motor. The OBC design gives a provision to pass current in either forward or reverse direction via an alternate set of GPOs which invert the bridges resulting in motors rotating in the opposite direction. Thus, in order to move the rover front or back, two sets of GPOs are used, one for forward movement and the other one for backward movement. The algorithms and state diagrams remain exactly same in both these cases in the case of DC motors. With BLDC motors, as explained in Section 4.6, the sequence of pulses given to 6 switches per motor has to be reversed in order to

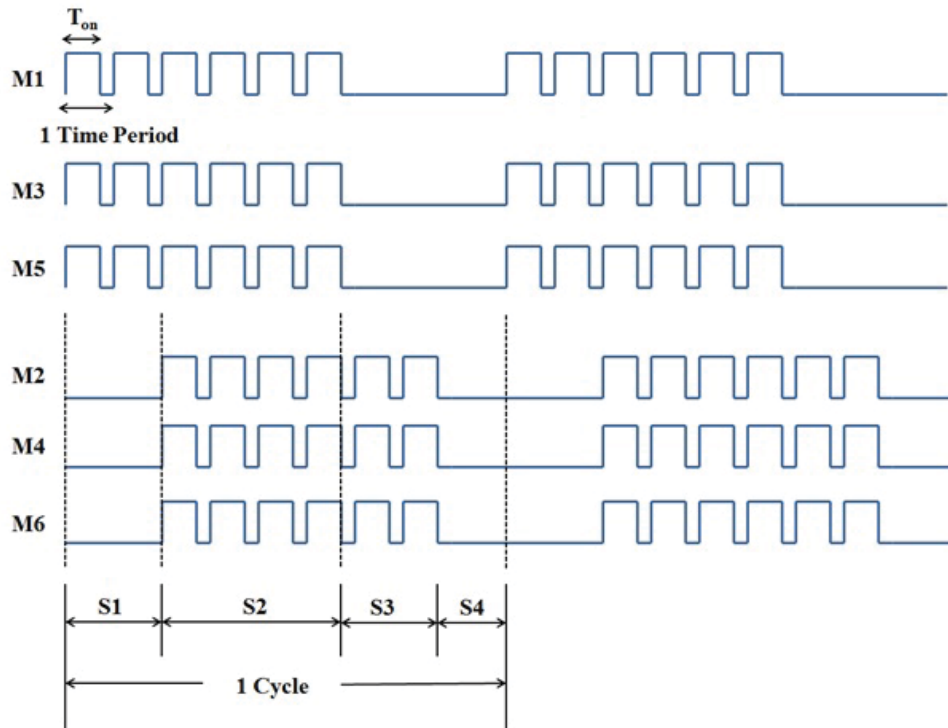
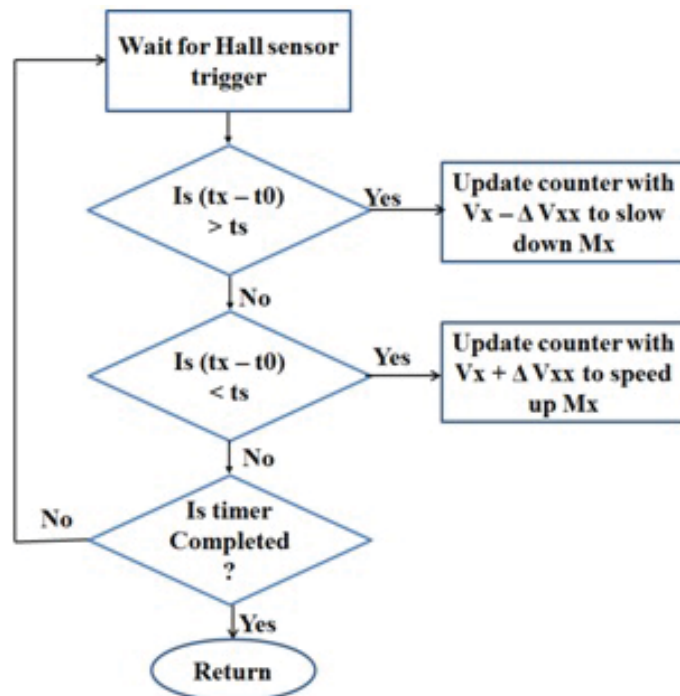


Figure 5.12: PWM waveforms



t_x : Time corresponding to the present speed of the motor X.
 t_0 : Time when motor X started rotating.
 t_s : Time corresponding to the set speed of the motor X.

Figure 5.13: Synchronization

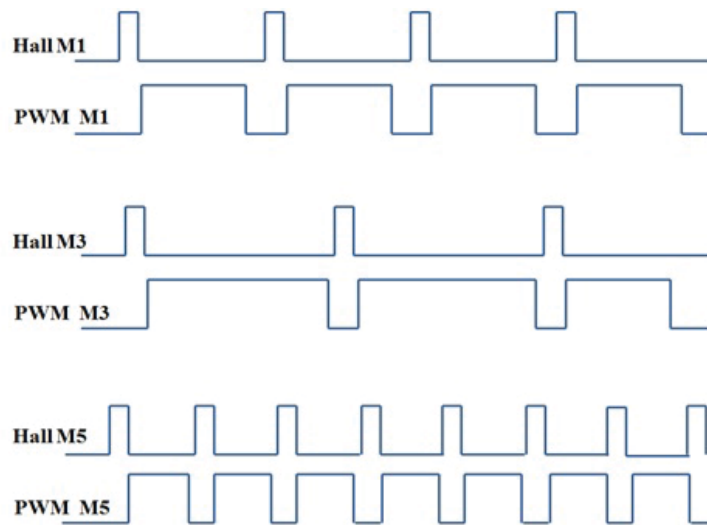


Figure 5.14: PWM Synchronization

rotate the motor in opposite direction. The logic flow and state diagrams still remain identical as that for forward motion.

5.8.7 Left rotation

The rover on lunar surface is expected to turn left or right as necessary to avoid collisions or unwanted mishaps from happening. The flowchart shown in Figure 5.15 summarizes the algorithm used to accomplish left rotational motion in the rover.

5.8.8 Right rotation

The flowchart shown in Figure 5.16 summarizes the algorithm used to accomplish right rotational motion in the rover.

5.9 Design Calculation for the Locomotion Algorithm

Movement of the rover can be broadly classified into two types: linear motion and turning motion. The locomotion algorithms and state diagrams described so far apply strictly to linear motions. The analysis and algorithms needed for the turning motion are described in this section.

For any body to rotate about an axis, a coupling force or torque has to be applied around the corresponding axis so that the net translational force is 0 and a turning tendency is generated for the body to turn. The only force available on lunar surface which can be manipulated to generate a turning moment for the rover is friction. Also, ways in which friction can be generated are:

5.9.1 Friction analysis

Rotating the motors in either the forward or reverse direction increases the friction and produces sufficient force depending on the coefficient of friction between the leg coating and the lunar dust. This friction acts along the axis of rover body as shown in Figure 5.17. The figure shows the direction of friction force on the rover when legs 2 and 6 are rotated in the forward direction.

By virtue of dragging a body on a surface: When a partial set of legs is rotated by turning on the corresponding motors, the body of the rover tends to drag the other set of legs on the lunar surface

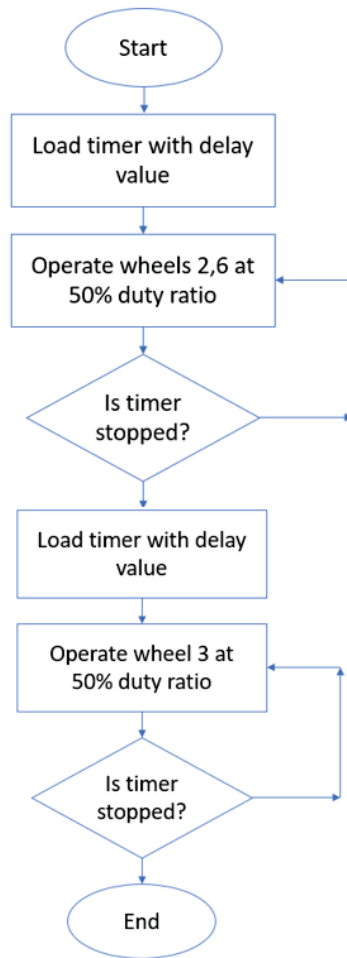


Figure 5.15: Left rotation

which in turn generates a 2 dimensional friction force acting on the point of contact of the legs being dragged. Assuming that the legs two and four are operated with a certain duty ratio, a free body diagram of the rover can be drawn as shown in Figure 5.18.

The darker arrows in the figure show the friction generated in the driven legs and lighter arrows show the friction generated at the points of contact of the dragged legs. It is to be noted that the generated friction at this moment is along the line of rover's central axis.

5.9.2 Calculations for PWM generation

This section describes the mathematical formulations used in the code to derive the PWM (duty cycle ratio) and timing parameters which drive the motors. The BLDC motors work over a voltage range of 6 to 36 V. The rpm of the motor depends on the applied voltage (in our case it is 12 V). The duty cycle ratio is calculated based on the effective voltage. Layer 5 of the code receives commands in the following manner:

- Distance to be moved = x m.
- Linear speed of movement = y m/s.

These parameters are either commanded from ground or derived from automation. The motor parameters are as follows.

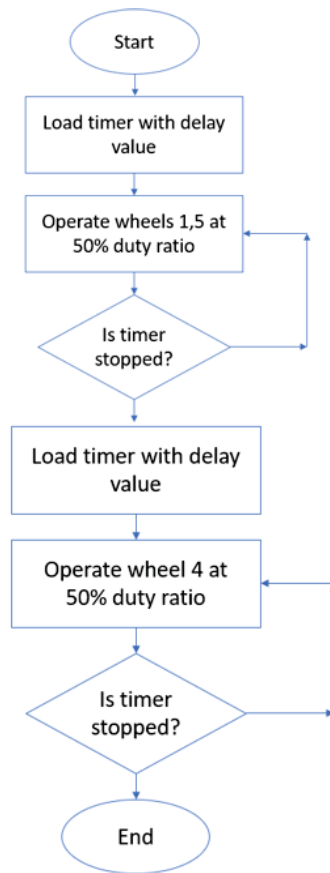


Figure 5.16: Right rotation

- The rpm of motor (Motor specification) at 12 V is given by R .
- Arc angle of the ground contact per revolution (derived from observation) is given by θ degrees.
- Gear reduction ratio is given by G . Based on the current motor selection, the gear ratio, G , is 256.
- Number of pulses received from the hall sensors per minute per motor at 12 V is given by $H = R \times 6 \times 3$.

Every rotation of the rover leg corresponds to 256 rotations of the motor's internal rotor. Every rotor rotation corresponds to 6 sets of 3 pulses from hall sensors within each motor. Therefore, the number of hall sensor inputs per second is equal $H/60$. Let the leg diameter be D m. We can calculate the distance moved between 2 hall pulses by one leg $= \pi D \theta / 360$.

The rover movement gives one pulse from each of the hall sensors mounted on the legs for each rotation of the leg. Thus, the distance covered between 2 hall pulses is same as the distance covered in one rotation of the legs. Therefore, the total number of rotations to be made $= x / (\text{distance moved in one rotation}) = (360x) / \pi D \theta$.

This implies that over the entire duration of locomotion a total of $(360x) / \pi D \theta$ pulses are expected from each leg. Now, the distance moved in 1 rotation of the legs $= 360 / \pi D \theta$ m.

Given that the rotation in 1 m $= \pi D \theta / 360$, the rotations in 1 second for speed y m/s $= y \pi D \theta / 360$. Therefore, the rotations in 1 minute $= y \pi D \theta / 60$. The rpm needed from the leg $= y D \theta / 60 x$.

The effective voltage $= (\text{Effective rpm}) / (\text{rpm at 12V})$, which is given by $y \pi D \theta / (5 R x)$.

Finally, the duty cycle ratio $(d) = (\text{Effective voltage}) / (12 \text{ V}) = y \pi D \theta / (60 R x)$.

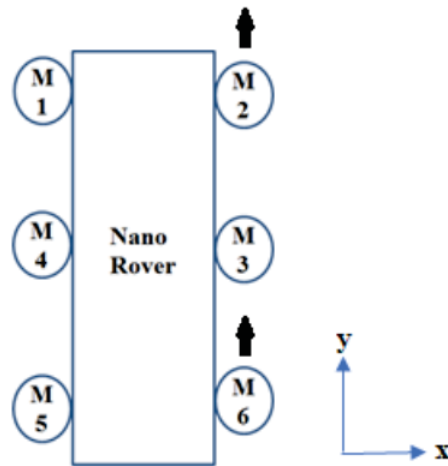


Figure 5.17: Left rotation

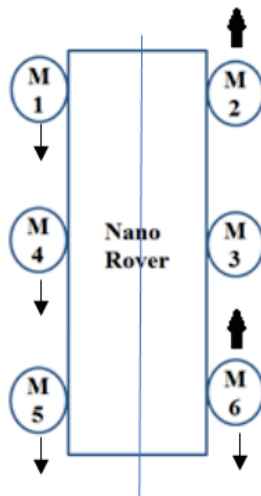


Figure 5.18: Right rotation

5.9.3 Calculations for PWM width adjustment of layer3 (Ring counter based lookup table)

In order to calculate the change in duty cycle ratio as mentioned in layer 3 (see Section 5.6.4 and Figure 5.9), we present a method to calculate the change in PWM width in this section.

Assuming the polling interval for hall sensor input is z seconds, the expected number of pulses in z seconds from one leg = $dHz/60$.

Let the received number of pulses be r . The difference in the number of pulses detected and the number of pulses expected can be calculated by $\Delta e = r - dHz/60$.

A lookup table based ring counter has been implemented to compensate for the mismatch in the hall sensor count. Based on the difference in expected and observed number of hall pulses, a change in duty ratio is calculated which is fed to the motors to bring all the motors in sync. A representation of the lookup table is shown in Figure 5.19.

Based on the error value Δe , a pointer address is selected to adjust the PWM. This corresponding corrective PWM is given to the respective motor. As there are six motors, six such pointers are used.

Pointer Address	PWM
0x64	100%
0x63	99%
0x62	98%
.	.
.	.
.	.
0x33	51%
0x32	50%
0x31	49%
.	.
.	.
.	.
0x03	3%
0x02	2%
0x01	1%
0x00	0

Default value →

Figure 5.19: Lookup table

The previous calculation were for each motor's synchronization. Now, we will calculate the synchronization of the legs and correspondingly take corrective actions if the legs are unsynchronized.

From the previous calculations, the number of hall pulses missed from one leg = $dHz/60 - r$. As the number of pulses received in one rotation of a leg is 6, the angle between the magnetic poles are 60° . Therefore, the angle of rotation missed for a particular leg (A) = $(dHz - 60r)$ degrees.

Therefore, the extra angle needed to be covered = $A\%360$ degrees.

This angle has to be covered up before the next set of legs start rotating. The same lookup table gives the corrective duty ratio as its output which is applied to the legs in order to correct the accumulated error. Values in the lookup table are calculated based on experiments.

Also, in order to prevent erroneous data from coming up due to single event upsets and bit flips, triple modular redundancy is implemented by making three ideally identical versions of the lookup tables and storing them in different locations in the memory. Whenever a value is to be updated, the variables with minimum two identical entries are accepted and all the entries in all three locations are rewritten with the accepted value. This practice is followed for all the variables in the program. Also, periodic memory marching is practiced in which variable values are read, stored in a buffer and rewritten back in order to ensure proper health and functioning of the memory locations.

5.9.4 Calculations for PWM frequency for the motors

This section deals with the design of the PWM frequency selection for each motor. This frequency determines how precisely the locomotion algorithm can control the movement of the rover. Higher the frequency, better is the resolution of the PWM based movement. The OBC card must be capable of generating this frequency, which can be done by our OBC card.

The number of pulses received per minute from each motor = $R \times 3 \times 6$. The pulses per second = $(3R)/(10)$. The minimum frequency of polling must be at least half of the number of pulses = $(3R)/(5)$. The PWM frequency is approximately chosen to be 100 times the polling frequency = $60R$.

For example, let the BLDC maximum rpm be 2500 rpm, then rps = $2500 / 60 = 416$ rps. Therefore it takes 2.6 ms per revolution. To have fine control, the PWM period has been fixed at $10 \mu s$. This permits a accuracy of 1%. Hence in one revolution, the number of PWM pulses that can be output are 250. Hence a very precise control of synchronization can be achieved among the motors.

However, the choice of the motor and the number of hall sensor can be fine tuned more accurately ONLY with experiments and the behavior of the motor on various terrains.

5.10 Summary

In this chapter, we first argued that an operating system is not required for achieving locomotion in Nano Rover. We analyzed the existing Zebro locomotion algorithm and concluded that this algorithm tends to have a jerky movement due to lack of synchronization. Therefore, we proposed a novel, ring-counter based algorithm for locomotion. Furthermore, we implemented a Triple Modular Redundancy based database for all the variables in order to take care of the data corruption due to single-event defects in space applications. The algorithm is modular and meets the software requirements, and the complexity of the algorithm is low. Moreover, the algorithm is tightly-coupled with the hardware, therefore, we achieve good synchronization leading to smoother movement of the rover.

The software written in VHDL and C are integrated into the OBC and the motor controller cards. They are tested in several conditions that are presented in the next chapter.

Evaluation, Experimentation, and Demonstration of Locomotion

In this chapter, we present the test and evaluation results for the designed OBC hardware and the motor driver card. We also assess the locomotion algorithm and its performance, and the demonstration of the locomotion on the simulated lunar terrain. We evaluated the system and its behavior for different locomotion scenarios such as forward, backward, left and right movement with different types of leg of varying length (L) and width (W).

6.1 Experimental Setup

In this section, we describe the experimental setup for demonstrating the locomotion of the Nano Rover both on the flat surface (lab) and simulated lunar terrain. The supporting subsystems and modules included in the setup for testing and demonstration are as follows.

6.1.1 Structure

A simple 3D printed structure made of Ultem has been designed for the Nano Rover prototype as shown in Figure 6.1. The dimension of the structure was set as 220mm x 180mm x 80mm which is the same as the final flight model. The overall weight of the rover was maintained to be 1.5 kgs. Provisions were made for fixing the motors and other electronic modules.

6.1.2 Motors

We test our proposed locomotion algorithm using single phase DC motors. The proposed locomotion algorithm performs its best when three phase BLDC motors with built in hall effect sensors are used. However when the feedback system(built in hall effect sensors) are not available, such as in the case of single phase DC motors, the algorithms' behaviour will be at its worst. Hence, we chose single phase DC motors for the evaluation - 12V, 60 rpm geared commercial grade motor from Vega because of its immediate availability. The final motor assembly on the structure is shown in the Figure 6.2.

The motors are individually tested by supplying 12 V. Motors are firmly assembled on to the bottom structure to provide access for easy assembly of legs. Legs are assembled on the sides of the bottom structure.



Figure 6.1: 3D structure

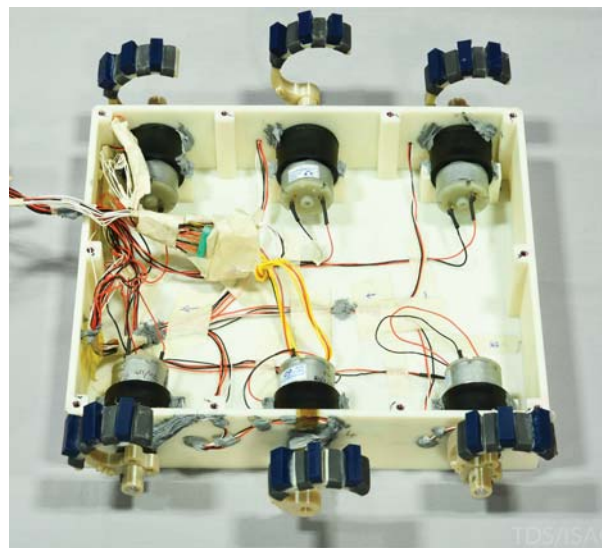


Figure 6.2: Motor assembly

6.1.3 Legs

The legs play an important role for locomotion on both flat surface, lunar terrain, obstacle negotiation and climbing slopes. Since there is an interdependency between the leg design and the locomotion algorithm, we test our algorithm with different types of legs. It can be seen from Figure 6.3 and Figure 6.4 that each leg has 3 holes at the end. This has been made to fix two magnets to trigger hall effect sensors (unipolar or bipolar). A single magnet at the appropriate hole is used for unipolar hall effect sensor and two for bipolar sensors which requires both north and south poles of the magnets. Two magnets are required since the Bipolar Hall sensor is used to get two pulse one at 0° and another at 180° for effective position control. The centre hole is attached to the motor shaft. Additional hole at 270° from the bottom is provided to mount a magnet in case more information about position is required.

Legs with different parameters were used to understand the behavior of the locomotion of the Nano Rover. The parameters considered are as follows.

1. length of the leg (distance from motor shaft hole to edge of the leg) 50mm and 80mm are used to understand rover behavior to crawl over larger obstacles.
2. leg width (width of landing surface of the leg) 10, 20, 40 and 55mm to vary contact area to the

terrain

3. leg surface (with and without teeth)-tests were conducted in anticipation that the teeth would provide better traction
4. leg surface material(rubberized teeth)- for better traction



Figure 6.3: Leg variants



Figure 6.4: Legs with different types and sizes

6.1.4 Hall effect sensor

We chose OMH090 commercial grade unipolar hall effect sensor due to its immediate availability. Six hall effect sensors are fixed appropriately on the structure for six motors.

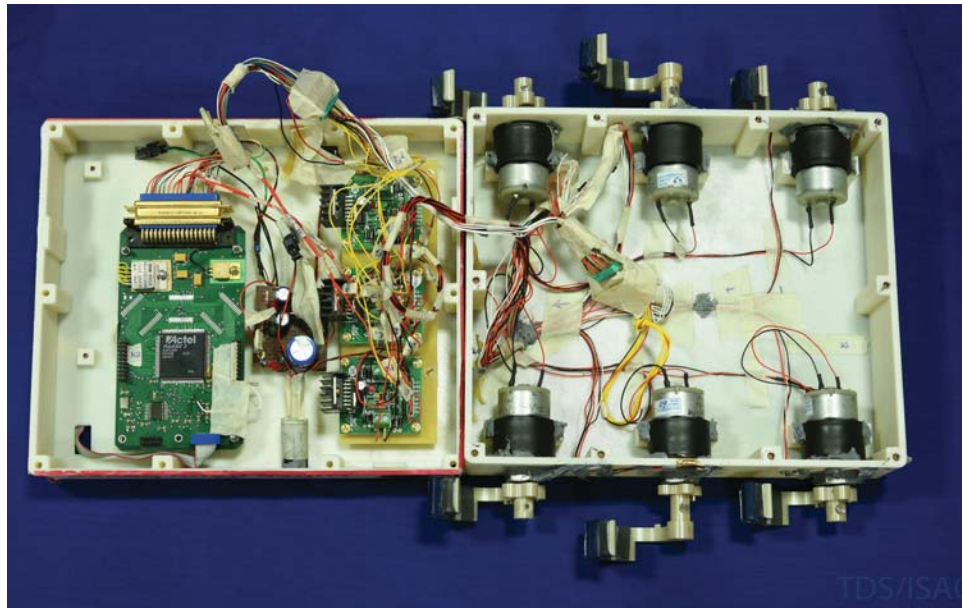


Figure 6.5: Hardware assembly

6.1.5 OBC card and motor drive card

The OBC and motor cards were tested for electrical isolation between live and return power lines after the completion of the assembly. The voltage regulator outputs were also verified. OBC and motor driver card were mounted and connected to the motors as shown in Figure 6.5.

6.1.6 Power module

We use external power supply to power up the electronic modules with 12 V DC. However, we also used battery as the power source in few cases.

6.1.7 1/6 Gravity emulation

To emulate the lunar gravity conditions ($1/6 g$) we used a spring balance to lift up the rover with $5/6$ th of its weight.

With this setup, the performance was evaluated in both the lab and the lunar terrain. The results are categorized for various test cases pertaining to different legs. In all the test cases, the performance of the locomotion algorithm was evaluated. In some cases, the movement was very smooth classified as satisfactory. In some cases, the movement ceased and is classified as unsatisfactory. In some cases, the movement was slippery and these are classified as partially satisfactory. These three categories/scenarios are defined as follows.

Unsatisfactory scenarios: In this scenario, the locomotion was good on the hard surface of the moon with specific leg types but they miserably fail to perform on the loose lunar soil and end up digging the soil. They are unable to climb/locomote the lunar loose soil surface both in lunar gravity and gravity on earth.

Partially satisfactory scenarios: In this case, the rover is able to locomote normally on the lunar hard surface and also on loose lunar soil approximately upto about 6 to 8° slope. However, there is a possibility of improving the friction during landing and locomotion.

Successful scenarios: The scenario is successful if the rover is able to move without any problem on flat, hard surface, or lunar terrain with or without slope, irrespective of the simulated gravity.

First we present the results for flat surface, followed by lunar terrain.

6.2 Locomotion Test on Flat Surface(Lab)

The rover was made to move on flat wooden surface with and without slopes under normal gravity ('g') as shown in Figure 6.6. The experimental results are tabulated in Table 6.1. The movement is satisfactory for all the types of legs except for 10mm width leg on the flat surface and slope up/down of 15°. The wheel of 10mm width collapsed while slope up.

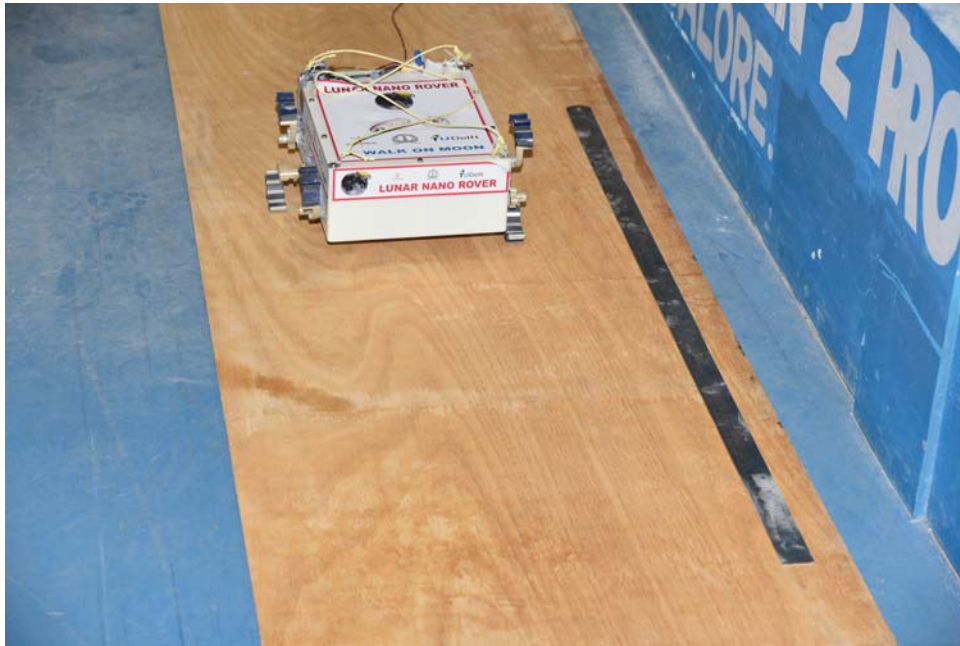


Figure 6.6: Wooden flat surface

The rover was made to move on flat wooden surface with and without slopes under 1/6th g as shown in Figure 6.7. The experimental results are tabulated in Figure 6.8. The movement is satisfactory for all the types of legs on the flat surface, but not satisfactory in slope up/down.

We also measured the time taken by the rover to cover a distance of 1 m to analyze the effect of change in leg sizer. All the legs included teeth and rubber. Figure 6.9 summarizes the results of successful experiments done on the selected legs on flat surface and normal g for a distance of 1 m. It is observed that: (i) leg type 2 takes an average of 28 seconds (ii) leg type 6 takes an average of 18 seconds (iii) leg type 10 takes an average of 29 seconds. Figure 6.10 summarizes the results of successful experiments done on the selected legs on flat surface with lunar g for a distance of 1 m. It is observed that: (i) leg type 2 takes an average of 28.6 seconds (ii) leg type 6 takes an average of 18.4 seconds (iii) leg type 10 takes an average of 27.4 seconds.

6.3 Locomotion Test on Lunar Terrain

The rover was made to move on simulated lunar surface with and without slopes as shown in Figure 6.11 and Figure 6.8 respectively. The movement is satisfactory for all the types of legs the flat lunar surface and teeth rubberised 20mm and 40mm width. For all other types of legs, slope up/down performance is not satisfactory. The experimental results are tabulated in Table 6.3.

The rover was made to move on simulated lunar terrain with and without slopes under lunar g (1/6th g) as shown in Figure 6.12. The experimental results are tabulated in Table 6.4. The movement

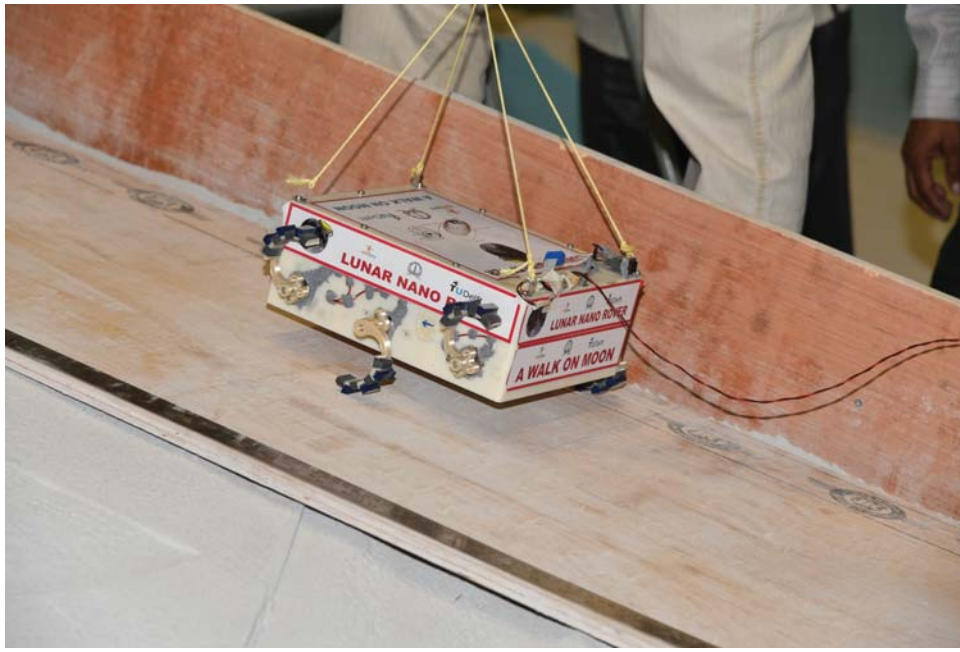


Figure 6.7: Locomotion on wooden flat surface at lunar g

is satisfactory for all the types of legs the flat lunar surface and teeth rubberized 20mm and 40mm width. For all other types of legs, slope up/down performance is not satisfactory.

Table 6.13 summarizes the results of successful experiments done on the selected legs on Lunar surface and Earth g for a distance of 1 meter. It is observed that: (i) leg type 2 takes an average of 25 seconds (ii) leg type 6 takes an average of 15 seconds (iii) leg type 10 takes an average of 27 seconds. Table 6.14 summarizes the results of successful experiments done on the selected legs on lunar surface and lunar g for a distance of 1 m. It is observed that: (i) leg type 2 takes an average of 26 seconds (ii) leg type 6 takes an average of 14 seconds (iii) leg type 10 takes an average of 25 seconds.

6.4 Inference

While designing of OBC, motor controller & power system cards are complaint to mission requirement, locomotion depends also on the legs design and its performance on the lunar surface. It depends on many factors, including the friction, mass and gravity. Nearly ten types of legs of varied dimensions with length, width and landing finish were 3D printed. Experiments were conducted on the normal earth conditions and all the types of legs function. However for the lunar surface experiments which has loose soil, boulders and 1/6th g of earth, the situation turned out to be different. With the experiments conducted, we observed that the wider wheels perform satisfactorily as the width has helped to get better friction both in normal and lunar g. Experiment was also conducted by having front and back legs 40mm and middle once 55mm. This provides excellent locomotion practically straight line as the forces on both sides are balanced. However actual mission has dimensional constraint. Therefore experiment with 20mm width teethed legs were continued. These legs were attached with 10mm thick Neoprene Rubber between the gaps of the teeth in a wheel. Each wheel had 4such rubbers attached. Nano rover was able to locomote both in normal g and lunar g and comfortably climb required slope of 15°. However our experiments showed that Nano Rover is able to climb up to 22°.

Further experiments were conducted for the successful combination of legs namely Type 2, Type 6 and Type10 to actually measure the time taken of locomotion for the various surface conditions. Experiments were also conducted for 80 slope as it is the most likely condition that the Nano rover might encounter. It is proved beyond doubt that the best suited legs for the Nano Rover are Types 2, 6 and 10. Given the constraint in space available on Lander, it is recommended to use Type

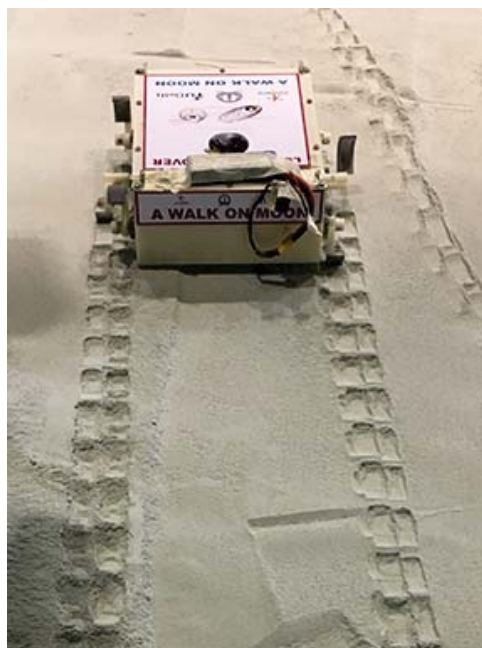


Figure 6.8: Locomotion on lunar terrain, flat surface

<u>SL.No</u>	Surface → Leg: Length/width Finish ↓	Earth Hard & Rough Surface	Earth Slope Up 8°	Earth Slope Down 8°	Earth Slope Up 15°	Earth Slope Down 15°	Average Time
1	Type 2: 50L/20W Teeth with Rubber	28Secs	29Secs	25Secs	31Secs	27Secs	28Secs
2	Type 6: 80L/20W Teeth with Rubber	19Secs	21Secs	17Secs	21Secs	15Secs	18Secs
3	Type 10: 50L/corner 20W and middle 40W Teeth with Rubber	29Secs	30Secs	27Secs	32Secs	27Secs	29Secs

Figure 6.9: Time taken by the rover to cover 1 m on flat surface with normal g

2. Also, based on the performance of BLDC motors, Type 10 legs could be used. Type 10 would also provide additional advantage of higher ground clearance, better obstacle climbing capability and faster locomotion. In all the above conditions the depth of impression on the lunar soil is about 11mm. Nano rover takes little higher time during slope up and takes lesser time due to the slip on a downward slope. This can be improved by using a set of motors with higher holding torque and improving ground friction by providing more rubberized contact area between the legs and surface.

Table 6.1: Results for flat surface with normal g

Surface Leg:Length/width/finish	Earth hard and rough surface	Earth slope up,15°	Earth,Slope Down,15°
Type 1: 50/20,Plain	Satisfactory	Satisfactory	Satisfactory
Type 2: 50/20,Teeth	Satisfactory	Satisfactory	Satisfactory
Type 3: 50/10,Plain	Satisfactory	Satisfactory	Unsatisfactory,Slips and runs down
Type 4: 50/10,Teeth	Satisfactory	Satisfactory	Unsatisfactory,Slips and runs down
Type 5: 80/20,Plain	Satisfactory	Satisfactory	Satisfactory
Type 6: 80/20,Teeth	Satisfactory	Satisfactory	Satisfactory
Type 7: 80/10,Plain	Satisfactory	Satisfactory	Unsatisfactory,Slips and runs down
Type 8: 80/10,Teeth	Satisfactory	Satisfactory	Unsatisfactory,Slips and runs down
Type 9: 50/40,Teeth	Satisfactory	Satisfactory	Satisfactory
Type 10: 50/corner 20,and middle 40,Teeth	Satisfactory	Satisfactory	Satisfactory
Type 11: 50/20,Teeth with Rubber	Satisfactory	Satisfactory	Satisfactory
Type 12: 80/20,Teeth with Rubber	Satisfactory	Satisfactory	Satisfactory

Table 6.2: Flat surface with lunar g

Surface Leg:Length/width/finish	Earth hard and rough surface 1/6g	Earth slope up 15°, 1/6g	Earth,Slope Down,15°, 1/6g
Type 1: 50/20,Plain	Satisfactory	Satisfactory	Partially satisfactory, Slips and stays
Type 2: 50/20,Teeth	Satisfactory	Satisfactory	Partially satisfactory, Slips and stays
Type 3: 50/10,Plain	Satisfactory	Partially satisfactory, Slips and stays	Unsatisfactory, Slips and runs down
Type 4: 50/10,Teeth	Satisfactory	Partially satisfactory, Slips and stays	Unsatisfactory, Slips and runs down
Type 5: 80/20,Plain	Satisfactory	Partially satisfactory, Slips and stays	Unsatisfactory, Slips and runs down
Type 6: 80/20,Teeth	Satisfactory	Partially satisfactory, Slips and stays	Unsatisfactory, Slips and runs down
Type 7: 80/10,Plain	Satisfactory	Partially satisfactory, Slips and stays	Unsatisfactory, Slips and runs down
Type 8: 80/10,Teeth	Satisfactory	Partially satisfactory, Slips and stays	Unsatisfactory, Slips and runs down
Type 9: 50/40,Teeth	Satisfactory	Satisfactory	Satisfactory
Type 10: 50/corner 20, and middle 40,Teeth	Satisfactory	Satisfactory	Satisfactory
Type 11: 50/20,Teeth with Rubber	Satisfactory	Satisfactory	Satisfactory
Type 12: 80/20,Teeth with Rubber	Satisfactory	Satisfactory	Satisfactory

Table 6.3: Lunar terrain with normal g

Surface Leg:Length/width/finish	Lunar hard and rough surface	Lunar slope up 15	Lunar,Slope Down,15
Type 1: 50/20,Plain	Satisfactory	Partially satisfactory slips and stays	Unsatisfactory, Slips and runs down
Type 2: 50/20,Teeth	Satisfactory	Partially satisfactory slips and stays	Unsatisfactory, Slips and runs down
Type 3: 50/10,Plain	Satisfactory	Partially satisfactory slips and stays	Unsatisfactory, Slips and runs down
Type 4: 50/10,Teeth	Satisfactory	Partially satisfactory slips and stays	Unsatisfactory, Slips and runs down
Type 5: 80/20,Plain	Satisfactory	Partially satisfactory slips and stays	Unsatisfactory, Slips and runs down
Type 6: 80/20,Teeth	Satisfactory	Partially satisfactory slips and stays	Unsatisfactory, Slips and runs down
Type 7: 80/10,Plain	Satisfactory	Partially satisfactory slips and stays	Unsatisfactory, Slips and runs down
Type 8: 80/10,Teeth	Satisfactory	Partially satisfactory slips and stays	Unsatisfactory, Slips and runs down
Type 9: 50/40,Teeth	Satisfactory	Satisfactory	Satisfactory
Type 10: 50/corner 20,and middle 40,Teeth	Satisfactory	Satisfactory	Satisfactory
Type 11: 50/20,Teeth with Rubber	Satisfactory	Satisfactory	Satisfactory
Type 12: 80/20,Teeth with Rubber	Satisfactory	Satisfactory	Satisfactory

Table 6.4: Lunar terrain with lunar g

Surface Leg:Length/width/finish	Lunar hard and rough surface 1/6 g	Lunar slope up 15,1/6 g	Lunar,Slope Down,15,1/6 g
Type 1: 50/20,Plain	Satisfactory	Unsatisfactory slips and digs into soil	Unsatisfactory Slips and runs down
Type 2: 50/20,Teeth	Satisfactory	Unsatisfactory slips and digs into soil	Unsatisfactory Slips and runs down
Type 3: 50/10,Plain	Satisfactory	Unsatisfactory slips and digs into soil	Unsatisfactory Slips and runs down
Type 4: 50/10,Teeth	Satisfactory	Unsatisfactory slips and digs into soil	Unsatisfactory Slips and runs down
Type 5: 80/20,Plain	Satisfactory	Unsatisfactory slips and digs into soil	Unsatisfactory Slips and runs down
Type 6: 80/20,Teeth	Satisfactory	Unsatisfactory slips and digs into soil	Unsatisfactory Slips and runs down
Type 7: 80/10,Plain	Satisfactory	Unsatisfactory slips and digs into soil	Unsatisfactory Slips and runs down
Type 8: 80/10,Teeth	Satisfactory	Unsatisfactory slips and digs into soil	Unsatisfactory Slips and runs down
Type 9: 50/40,Teeth	Satisfactory	Satisfactory	Satisfactory
Type 10: 50/corner 20,and middle 40,Teeth	Satisfactory	Satisfactory	Satisfactory
Type 11: 50/20,Teeth with Rubber	Satisfactory	Satisfactory	Satisfactory
Type 12: 80/20,Teeth with Rubber	Satisfactory	Satisfactory	Satisfactory

<u>SL.No</u>	Surface → Leg: Length/width Finish ↓	Earth Rough Surface 1/6 th g	Earth Slope Up 8° 1/6 th g	Earth Slope Down 8° 1/6 th g	Earth Slope Up 15° 1/6 th g	Earth Slope Down 15° 1/6 th g	Average Time
1	Type 2: 50L/20W Teeth with Rubber	29Secs	29Secs	26Secs	32Secs	27Secs	28.6Secs
2	Type 6: 80L/20W Teeth with Rubber	18Secs	21Secs	15Secs	23Secs	15Secs	18.4Secs
3	Type 10: 50L/corner 20W and middle 40W Teeth with Rubber	28Secs	28Secs	25Secs	30Secs	26Secs	27.4Secs

Figure 6.10: Time taken by the rover to cover 1 m on flat surface with 1/6th g



Figure 6.11: Locomotion on lunar terrain, normal g with slope

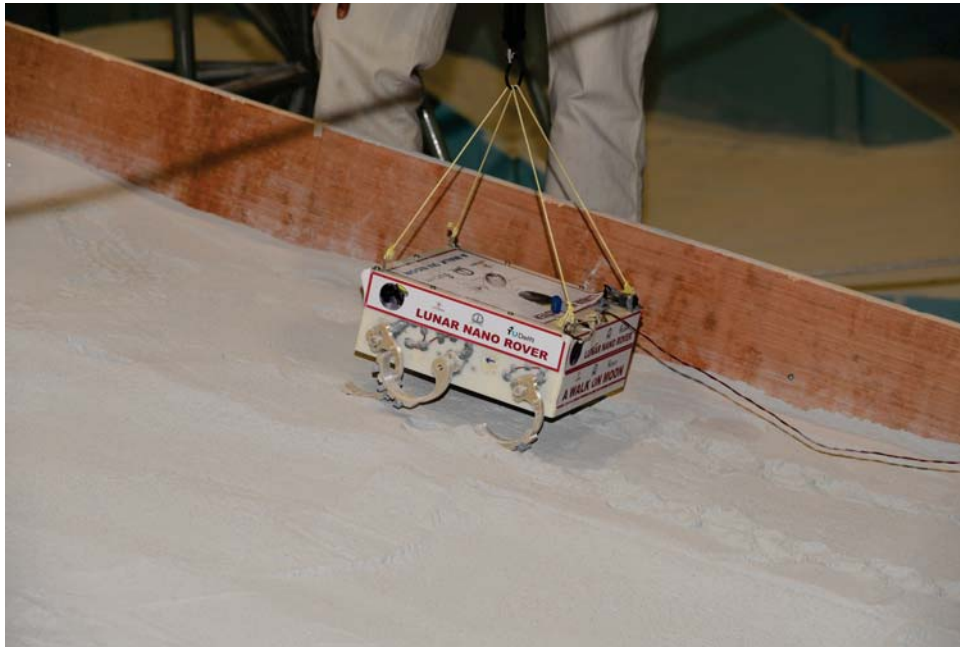


Figure 6.12: Locomotion on lunar terrain, $1/6$ g with slope

<u>SL.No</u>	Surface → Leg: Length/width Finish ↓	Lunar Hard & Rough Surface	Lunar Slope Up 8°	Lunar Slope Down 8°	Lunar Slope Up 15°	Lunar Slope Down 15°
1	Type 2: 50L/20W Teeth with Rubber	27Secs	29Secs	25Secs	32Secs	25Secs
2	Type 6: 80L/20W Teeth with Rubber	20Secs	21Secs	17Secs	21Secs	15Secs
3	Type 10: 50L/corner 20W and middle 40W Teeth with Rubber	29Secs	29Secs	26Secs	32Secs	27Secs

Figure 6.13: Time taken by the rover to cover 1 m on lunar surface with normal g

<u>SL.No</u>	Surface → Leg: Length/width Finish ↓	Lunar Rough Surface $1/6^{\text{th}}$ g	Lunar Slope Up 8° $1/6^{\text{th}}$ g	Lunar Slope Down 8° $1/6^{\text{th}}$ g	Lunar Slope Up 15° $1/6^{\text{th}}$ g	Lunar Slope Down 15° $1/6^{\text{th}}$ g
1	Type 2: 50L/20W Teeth with Rubber	26Secs	29Secs	24Secs	32Secs	26Secs
2	Type 6: 80L/20W Teeth with Rubber	18Secs	20Secs	16Secs	22Secs	14Secs
3	Type 10: 50L/corner 20W and middle 40W Teeth with Rubber	28Secs	29Secs	25Secs	32Secs	25Secs

Figure 6.14: Time taken by the rover to cover 1 m on lunar surface with $1/6^{\text{th}}$ g

Conclusion and Future work

This thesis provides a systematic description of the entire process of realisation of a space robotics mission to the Moon called Nano Rover. We covered the literature study extensively addressing lunar and interplanetary needs. Conceptualisation, design, and proof of concept realisation also considered the limits of most of the interplanetary missions as of today. Following goals have been reached in this thesis.

1. Study of the environmental conditions on the Moon and during Earth-Moon transit orbit were considered to arrive at specific environmental specifications for realizing the lunar compatible Nano Rover.
2. Analysis of the existing Zebro and sketching the requirements to adapt it to the lunar environment.
3. Conducting tests on Materials, Components and Elements (MCE) to use them for lunar and transit orbit environment we also tested some of the important and critical components at 186° C storage (worst case scenario).
4. Design, development, and testing of the on-board computer for lunar compatible Zebro in line with the literature studies.
5. Implementation of the TMR majority logic for mitigation of space radiation during earthbound, lunar bound and lunar landing phases of the Nano Rover.
6. Implementation and evaluation of specific algorithms and scheduling of activities of the Nano Rover.
7. Successful demonstration and testing of the locomotion of the rover on the simulated lunar terrain at ISRO.
8. Generation of important recommendations that are needed for the realisation of the flight grade Nano Rover.

The work was carried out in ISRO. First requirements for such a mission was studied. The important task was to propose an implementable plan to realise a Nano Rover. The task was also to bring the teams from three institutions together. The important step was to access the documents and the facility at ISRO which are confidential. As part of this work, there was some invaluable experience to learn how to work in the strategic space sector and in a multi-collaborative program.

Further, to realise a Nano Rover it was essential to study specific topics such as Chandrayaan-2 mission management, GSLV Launch vehicle dynamics during launch, Location of the Nano Rover in

Lander part of Chandrayaan 2 mission, design requirements for lunar mission, available space grade components and materials. Thus, in this thesis, we have recorded all the steps that were taken to design (including predesign tasks), implementation and testing of the moon rover.

7.1 Contributions of the thesis

In the sequel, we provide complete details of all the tasks, which were carried out in the sequel.

As part of the literature study, the thesis presents a study of the environmental conditions on the moon landing site and in earth-moon transit orbit. It is concluded that the Nano Rover has to meet storage temperature of -186°C and must operate between -20°C to $+70^{\circ}\text{C}$. Hence the designs of mechanical, electrical and electromechanical systems are to comply with this need. Literature survey also points to the fact that the legged robots are equally competent to be flown to Lunar Surface for locomotion and experimentation. Legged robots have a clear advantage over other types in terms of performance to climb obstacles, etc. Literature was studied extensively for components and material selection including experiments.

Hardware designs should have to comply with the specific mandatory requirements stipulated by ISRO for the interplanetary and lunar mission. As described in Chapter 2 & 3 all the elements used and the electronics should have to meet the radiation requirements of earth orbit, transit orbit, moon orbit and on the moon. Under these boundary conditions, ProASIC3 FPGA was selected which forms the nerve centre for the OBC design and rest of the peripherals are only for buffering and memory.

The battery is a crucial component of the mission as it is most vulnerable to low temperature. Custom built batteries meet harsh temperatures have been selected and tested to meet the lunar mission. Motors are BLDC type custom manufactured and tested to fit the Nano Rover. Solar panels and motor drive circuits are also of high reliability grade to suit this mission. The OBC hardware design fully complies with all the requirements and the PCB was fabricated and assembled to meet space standards. Fully assembled OBC was tested independently to function normally.

Motor drive card was designed to meet the BLDC motor. The MOSFETs and other related components were carefully selected. The card was fabricated and assembled as per ISRO guidelines including the grounding schemes. As the BLDC motors were not available BDC motors were used for making the prototype. This card is also tested independently before interfacing with OBC card.

We designed a modular and adaptive software. ProASIC3 is programmed in VHDL to configure the hardware. ARM Processor soft core is used for locomotion and other functions. Algorithms written in C language address synchronisation of legs, and movements. These softwares were extensively tested.

7.2 Assembly, Testing and Recommendations

A major part of the work in this thesis is building and testing of a prototype. Along with the electronics cards, the mechanical and structural assembly had to be designed. The mechanical assembly consists of bottom plate housing motors and the top cover housing OBC, Motor drive electronics and power system card. These mechanical structures were 3D printed at ISRO using a very special material UltemXX proprietary of ISRO which is as strong as aluminium and 1/3rd the weight of Aluminium.

Challenges were faced while interconnecting OBC running at 25Mhz and the motor drive card handling about 5A current which was causing spikes[VP9]. An add on the card was designed to solve this problem by properly terminating the ground connections of high frequency and that of the high current lines. The working model of the Nano Rover was then tested on ground and lunar terrain test facility.

Summary of observations: Experiments on 10 different combinations of legs have clearly indicated that the legs with 10mm width have very poor performance while loco motioning on the lunar surface. While teathed rubberised legs with width 20mm and 40mm performed very well in all the tested

conditions. The Teethed rubberised legs with width 20mm on four corners of nano Rover and width of 40mm performed The distance travelled with respect to time can be properly controlled to be same value for all the conditions including slope down of 80. However for 150 down word locomotion Nano Rover tends to move down faster due to slip. This needs to taken in to while realising Nano Rover using BLDC motor.

Looking back, the in-depth mathematical analysis could have been done with respect to the locomotion. However, given the limited availability of time, we had to make a decision whether to put more efforts into the implementation study or theoretical study of the algorithms for locomotion. Given the importance of this mission, we decided to put more efforts in the implementation of the engineering model with available resources and demonstrate on the lunar test terrain.

Based on the implementation, we provide a summary of the recommendations based on our experience below.

1. The technical aspects of the thesis have been generally accepted at ISRO. Therefore the current OBC and motor driver algorithm may be adopted as is.
2. Based on the experiments a 50mm/80mm rubberized teethed UltemXX legs can be used for qualification and flight models without any change.
3. An important recommendation is to go for 3D printed structure using Altem XX material.
4. Batteries play an important role. Generally, batteries are charged 50% in ISRO mission. A waiver to charge them 100% of its capacity will be an important step for the success of the mission.

7.3 Future Work

We provide some of the general recommendations first. Later based on the implementations of the prototype, we provide specific technical recommendations that need to be considered for the flight model.

General:

1. This activity is with strategic space organisation and the restrictions are too many. The procedures are time consuming. Therefore it is important to plan activities with sufficiently stricter time plan.
2. It is important to plan for multiple options for design and realisation including the multiple hardware and software ready for all options.
3. Performing experiments at cryogenic temperatures are a big challenge. The component selection needs to be tested well.
4. Availability of BLDC motor during realisation would have helped realise the flight model faster. Now it is important that BLDC motors need to be tested and used in the prototype immediately.

Technical:

1. The rover need to be built with BLDC motors and tested.
2. The algorithms have to be modified and tested for different terrain characteristics.
3. The locomotion algorithms have to be fine-tuned to dynamically adapt to the conditions.
4. The motors were tested at different speeds, however, more experiments need to be conducted with motor drives generating different torque.
5. A detailed analysis of failure cases need to be done so as to find the limiting cases of the rover locomotion.

7.4 Epilogue

It has been my dream to work in the area of space robotics. It was a great opportunity for me to work in Space robotics jointly with IISc and ISRO, Bangalore. It is a complex science problem but with an engineering approach!

Finally, With a high level of confidence, I can state that the Nano Rover project progress has been an excellent opportunity for me to have undertaken. I feel that a strong foundation is made through this thesis for the team at ISRO, IISc and TUDelft to continue and realise flight model of the Nano Rover.

Bibliography

- [1] A. S. Seeni, *Systems Study For Robotic Moon Missions*, Institute of Robotics and Mechatronics German Aerospace Center (DLR), August 2007.
- [2] *Landing Sites for Chandrayaan-2 Mission - A Study*, ISRO Satellite Centre, Indian Space Research Organisation, Bangalore, August 2014 - *Confidential Document*.
- [3] G. H. Heiken, D. T. Vaniman, B. M. French, *Lunar Sourcebook*, Cambridge University Press, 1991.
- [4] G. Lopes, *Zebro six legged robot*, [Online] - <http://robotics.tudelft.nl/?q=research/zebro-six-legged-robot>
- [5] M. Otten, *DeciZebro: the design of a modular bio-inspired robotic swarming platform*, TU Delft, Tech. Rep., 2017.
- [6] *SRO-ISAC-Chandrayaan-2-PR-2434*, ISRO Satellite Centre, Indian Space Research Organisation, Bangalore - *Confidential Document*.
- [7] *Chandrayaan-2 PDR Document - Rover Executive Summary*, ISRO Satellite Centre, Indian Space Research Organisation, Bangalore, Nov 2010 - *Confidential Document*.
- [8] *Radiation Specifications for Chandrayaan-2 Mission*, ISRO Satellite Centre, Indian Space Research Organisation, Bangalore, June 2014 - *Confidential Document*.
- [9] J. de Bruijkere, R. Smit, and L. R. Valk, *Zebro Light: Lightweight mobile hexapod robot*, Delft University of Technology, Tech. Rep., 2012.
- [10] *Chandrayaan-2 Ground Segment Design Review Mission And Flight Dynamics Volume-1*, ISRO Satellite Centre, Indian Space Research Organisation, Bangalore, June 2017 - *Confidential Document*.
- [11] *GSLV User manual*, Vikram Sarabhai Space Centre, Indian Space Research Organisation, Bangalore, 2014 - *Confidential Document*.
- [12] *Revision of GSLV MK II Dynamic environment*, Vikram Sarabhai Space Centre, Indian Space Research Organisation, Bangalore, June 2017 - *Confidential Document*.
- [13] *GSLV Mk 2 - CH2 II Mission Vehicle interface*, Vikram Sarabhai Space Centre, Indian Space Research Organisation, Bangalore, Oct 2013 - *Confidential Document*.
- [14] *Product Assurance Plan For Chandrayaan-2*, ISRO Satellite Centre, Indian Space Research Organisation, Bangalore, June 2017 - *Confidential Document*.

-
- [15] S. Nithin, *Modelling And Control Of A Six Wheeled Rocker-Bogie Rover For Planetary Exploration*, School Of Mechanical And Building Sciences, VIT, Chennai, in association with ISRO. April 2016.
- [16] J.Y.Wong, *Theory Of Ground Vehicles*, Johnwiley Sons, Inc.Third Edition.
- [17] J.Y.Wong, A.R. Reece, *Prediction of Rigid Wheel Performance Based on the Analysis of Soil-Wheel Stresses Part I. Performance of Driven Rigid Wheels*, Journal of Terramechanics, 4(1), pages 81-98, 1967.
- [18] J.Y.Wong, *Predicting the Performances of Rigid Rover Wheels on Extraterrestrial Surfaces Based on Test Results Obtained on Earth*, Journal of Terramechanics, 49(1), 49-61, 2012.
- [19] *Cortex M1 V3.1 Handbook*, Actel Corporation, Part No: 50200127-12, September 2010.
- [20] *Libero Soc V11.6 Users Guide*,MicroSemi Corporation,Part No:502912034, Release :July 2015.
- [21] *Core AHB2APB Direct Core*, Actel Corporation, Part No:51700074-2 Release: Januauary 2008.
- [22] *Core GPIO V3.1 Handbook*, MicroSemi Corporation, Part No:50200183-1 Release:March 2015.
- [23] *Core APB Direct Core*, Actel Corporation, Part No:51700073-2 Release:January 2008.
- [24] *Core AHBLite V5.2*, MicroSemi Corporation, Part No:50200144 Release:November 2014.
- [25] *Arm System-On-Chip Architecture*, 2nd Ed, Addison Wesley.
- [26] *ISRO Software Practices Document (ISRO-SES-PD-100) (Confidential)*, October 2006.
- [27] *Micro semi Data Sheet - Military ProASIC3/EL Low Power Flash FPGAs with Flash*Freeze Technology* Revision5.
- [28] Ward Brown, *Brushless DC Motor Control Made Easy*, Microchip Technology Inc., 2011.

Appendix A

A.1 Rovers for Interplanetary mission in the literature

For robotic exploration, locomotion plays a key role in achieving mobility. There are different kinds of locomotion configurations that could be conceived for a typical lunar exploration scenario. Most of it has already been developed or currently under development. These are wheels, tracks, legs, hybrids, hoppers, and ballistics. The first four locomotion concepts (wheels, tracks, legs, and hybrids) are considered in this work and discussed with a focus on survey and study of different robots.

Planetary Rover Variants: The various locomotion concepts (wheeled, tracked, legged, and hybrid) are assessed for different quantitative and qualitative parameters on a certain criteria specified in Table 2-14. The benchmark vehicle and grading scale

A benchmark vehicle with adequate capabilities is assumed. The capabilities of the vehicle in Table 2-15 are defined based on lunar terrain mobility requirements and assuming a worst-case scenario of unknown terrain case [Fuke et al., 1995]. Technology Readiness Levels The information contained in the table below is based on Technology Readiness Levels, A White Paper given by Mankins J.C., 1995 from the Advanced Concepts Office, Office of Space Access and Technology, NASA.

By default, the benchmark vehicles capabilities are assigned with rating 3. The benchmarked vehicle is thus assumed to have total points of 30, i.e. 3 (rating) x 10 (number of parameters).

Findings and summary of locomotion configuration The evaluation of the parameters for the concepts is difficult, and in some circumstances, non-comparable. It is important to note that the table does not contain broad parameters such as reliability, stability, etc. According to Table 2-17, wheeled locomotion concept and the legged locomotion has the highest ranking with 33 points and has more points than benchmark vehicle.

Table A.1: My caption

Quantitative Parameters	Description
Maximum speed capability	Capability to moving fast,on a flat surface
Obstacle traverse capability	Capability to move over obstacles/boulders; better to scale obstacles than avoiding them
Lunar soil sinkage	Ability to move on soft soil over flat surface by having the,least contact pressure without large slip, Nanomal sinkage, and mobility resistance (depends on vehicles mass)
Qualitative Parameters	Description
Mechanical simplicity	Less complexity of the locomotion subsystem with regard,to number of parts, linkages etc.; less moving parts
Level of redundancy	Capacity,of,the,vehicle,to,continue,on,the,mission,objective,in,case,of failure of,primary,mobility components (wheels, tracks, or legs)
Energy,efficiency	Ability to travel with low power, requirement/unit distance,when moving. In the,case of walkers, the power consumed while raising and lowering of legs is added along,with forward motion energy,rates
Onboard payload capacity	Capacity to carry a varied amount of instruments with more mass within a given body space
Lunar soil interaction	Capacity to carry a varied amount of instruments with more mass within a given body space
Technology readiness levels	Technology maturity and demonstration

Table A.2: Description of parameters of benchmark vehicle

Quantitative Parameters	Capabilities
Maximum speed capability	Capability to move on flat surface at a speed,of 30 cm/s
Obstacle traverse capability	Step climb ability of 25 mm height
Slope climb capability	Slope climb ability of 30 inclination
Lunar soil sinkage	Ability to move on soft soil over flat surface by having the,least contact pressure without large slip, Nanomal sinkage, and mobility resistance (depends on vehicles mass)
Qualitative Parameters	Capabilities
Mechanical simplicity	Moderately complex
Level of redundancy	Ability,to,continue,mission,even,after,permanent/temporary disablement or loss of two malfunctioned components (wheels, tracks, legs), assuming the vehicle having six components
Grades,Parameters	Capability to move with less battery power consumed per unit distance
Onboard payload capacity	Sufficient capacity of instruments,equivalent to MERs
Lunar soil interaction	Less interaction and more tolerance to lunar soil
Technology readiness levels	Breadboard validated in Moon-like terrain environment, i.e. TRL 5

Table A.3: NASA Technology Readiness Levels (TRL) classification

Level	Description
TRL 1	Basic principles observed and reported
TRL 2	Technology concept and/or,application formulated
TRL 3	Analytical,and,experimental,critical,function,and/or,characteristic,proof-of,concept
TRL 4	Component,and/or breadboard validation in laboratory environment
TRL 5	Component,and/or breadboard,validation in relevant environment
TRL 6	System/subsystem model or prototype demonstration in a relevant,environment (ground or space)
TRL 7	System prototype demonstration,in a space environment
TRL 8	Actual system completed,and flight qualified through test and demonstration (ground or space)
TRL 9	Actual system flight proven through successful mission,operations

Table A.4: ESA Strategic Readiness Levels classification

Level	Description
TRL 1	Technology concept and/or,application formulated
TRL 2	Analytical,and,experimental,critical,function,and/or,characteristic,proof-of,concept
TRL 3	Component,and/or breadboard validation in laboratory environment
TRL 4	Component,and/or breadboard,validation in relevant environment
TRL 5	Component,and/or breadboard,validation in relevant environment
TRL 6	System/subsystem model or prototype demonstration in a relevant,environment (ground or space)
TRL 7	System prototype demonstration,in a space environment
TRL 8	Actual system flight proven through successful mission,operations

Table A.5: Prime evaluation of locomotion concepts

Concept/Parameters	Wheeled	Tracked	Legged robot	Wheeled-leg	Legged
Maximum speed	3	2	3	3	2
Obstacle traverse	3	4	5	5	5
Slope climb,capability	2	3	3	5	3
Lunar soil,sinkage	3	4	2	3	3
Mechanical,simplicity	3	2	2	1	1
Level of,redundancy	4	1	4	5	4
Energy consumption rates	4	2	3	1	2
Onboard payload	3	3	2	3	3
Lunar soil,interaction	3	2	4	3	2
Technology,readiness levels	5	3	5	3	1
Total points	33	26	33	32	2

Table A.6: Advantages and disadvantages of locomotion systems

System	Advantages	Disadvantages
Wheels	<ol style="list-style-type: none"> 1. Better speed,in even terrain, 2. Simple and mature,technology, 3. Adequate redundancy (mobility), 4. Payload weight-to- mechanism weight ratio high, 5. Relatively low power,consumption rates and energy efficient 	<ol style="list-style-type: none"> 1. Relatively low slope, climb capacity due to wheel slippage, 2. Obstacle traverse relatively less compared to other,concepts
Tracks	<ol style="list-style-type: none"> 1. Good smooth terrain capability, 2. Technology well understood in terrestrial applications, 3. Better traction capability on loose soil, 4. Handles large hinders, small holes, ditches better, 5.Good payload capacity 	<ol style="list-style-type: none"> 1. Inefficient due to friction of tracks, 2.,Low speed operation, 3.,Slip turning and friction, 4.Low redundancy,,jamming of parts and prone to failure
Legs	<ol style="list-style-type: none"> 1.,Highly adapted to uneven terrain and hence better obstacle traverse capability, 2.Relatively less soil interaction 	<ol style="list-style-type: none"> 1. Large number of actuators. Control of walking,is complex. Slow mobility, 2. Impact,during each step, 3. Poor payload,weight-to- mechanism weight,ratio
Hybrids locomotion concept	<p>Shares the advantages of both</p> <ol style="list-style-type: none"> 1. More complexity, 2.Low technology maturity 	

